

**A SIMPLIFIED METHOD FOR COMPUTING PHASE BEHAVIOR
OF CRUDE OIL-CARBON DIOXIDE MIXTURES**

A Dissertation

by

SABRY ABDEL-ALIEM EL-SAYED MOHAMMED

**Submitted to the Graduate College of
Texas A&M University
in partial fulfillment of the requirements for the degree of
DOCTOR OF PHILOSOPHY**

May 1988

Major Subject: Petroleum Engineering

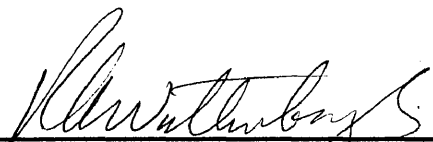
**A SIMPLIFIED METHOD FOR COMPUTING PHASE BEHAVIOR
OF CRUDE OIL-CARBON DIOXIDE MIXTURES**

A Dissertation

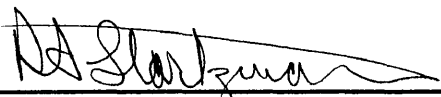
by

SABRY ABDEL-ALIEM EL-SAYED MOHAMMED

Approved as to style and content by:




R. A. Wattenbarger
(Chair of Committee)



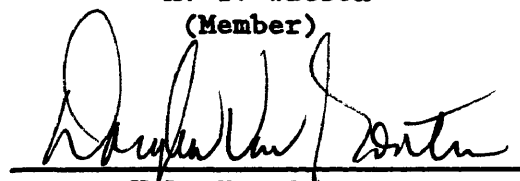
R. A. Startzman
(Member)



A. T. Watson
(Member)



L. D. Piper
(Member)



W. D. Von Gonten
(Head of Department)

May 1988

ABSTRACT**A Simplified Method for Computing Phase Behavior
of Crude Oil-Carbon Dioxide Mixtures. (May 1988)**

Sabry Abdel-Aliem El-Sayed Mohammed, B.S., Cairo University;

M.S., Cairo University, Egypt

Chairman of Advisory Committee: Dr. R. A. Wattenbarger

Phase behavior plays a fundamental role in oil recovery processes, ranging from the production of gas condensate and volatile oil reservoirs to the injection of CO₂ and N₂ for enhanced oil recovery processes. In phase behavior methods, equilibrium ratios are used to predict compositional changes in the reservoir fluids, particularly when using compositional simulators.

Literature search and experience in the phase behavior of CO₂-reservoir oil systems have shown that equations of state and available correlations give acceptable results in some areas, but in general, they are not satisfactory due to lack of accuracy, large computational time, or sometimes yielding trivial solutions. Therefore, accurate, faster and more reliable new methods are needed, particularly for actual compositional studies.

In this study, a K-value method is developed. This method, expressed in a simple mathematical form, relates the equilibrium ratios of each component with its boiling temperature, critical temperature and pressure, and the mixture's pressure, convergence pressure and overall compositional changes. This method uses some

experimental data for the mixture under study to adjust the form of the K-value expression. These experimental data are obtained from some the routine PVT laboratory tests. A least squares-linear programming optimization routine is adopted to adjust the correlation to match the actual behavior of the mixtures with the calculated.

Nine reservoir fluid samples were simulated, four retrograde gas condensate and five oil systems. The K-value method demonstrated good matches with the experimental data for all systems, including crude oil-carbon dioxide mixtures. This method worked well compared to Peng-Robinson and Soave-Redlich-Kwong equations of state for matching the saturation pressures and swollen volumes of four cases of CO₂ and N₂ injections into crude oil systems. The K-value method was faster than the equations of state by a factor of 7-20. In addition, the K-value method required less computer memory, less input data and fewer parameters to adjust than the equations of state. An approach for characterizing the heavy hydrocarbon fractions was developed as a combination of Ahmed's method, Whitson's method and Kay mixing rules. This approach was successfully used to split the heptanes-plus into pseudo components and estimate their properties.

DEDICATION

To
the soul of my mother,
to my father,
to my family,
to my sincere wife, Lobna
and
to my dear son, Ahmed

in appreciation for their love and support.

ACKNOWLEDGEMENT

I deeply thank God for granting me the guidance and the strength needed to accomplish this work.

I am grateful to all members of my Advisory Committee for their kind understanding, advise, and support. I would like to express my gratitude to Dr. R. A. Wattenbarger for the privilege of studying under his supervision. With his creative ideas, efficient directions, and generous encouragement, he enlightened the entire research process. Sincere thanks are due to Dr. R. A. Startzman, Dr. L. D. Piper, and Dr. A. T. Watson for their consent to serve on the Committee. I am indebted to Dr. G. R. Ferris for his service as Graduate Council Representative. I wish also to express my appreciation to Dr. W. D. Von Gonten, Dr. W. D. McCain, Jr., and Dr. W. J. Lee for their guidance during my graduate study.

This research has been possible through the sponsorship of the Egyptian Government. Computer facilities were generously provided by the Department of Petroleum Engineering, Texas A & M University.

Finally, I extend my deep and great appreciation to the soul of my mother, to my father, and to all members of my family for their support and encouragement throughout all phases of my study.

The encouragement, support, enduring love and understanding of my wife, Lobna El-Refaai, and my lovable son, Ahmed, through a journey of dedication and self-denial from their part are deeply acknowledged.

TABLE OF CONTENTS

| | Page |
|--|------|
| ABSTRACT | iii |
| DEDICATION | v |
| ACKNOWLEDGEMENT | vi |
| TABLE OF CONTENTS | vii |
| LIST OF TABLES | ix |
| LIST OF FIGURES | xi |
| INTRODUCTION | 1 |
| THEORY | 8 |
| Miscibility and Phase Behavior of | |
| Crude Oil-Carbon Dioxide Systems | 8 |
| Laboratory Tests | 15 |
| K-Value Methods | 21 |
| Equations of State | 30 |
| CHARACTERIZATION OF HYDROCARBONS HEAVY FRACTIONS | |
| AND PSEUDOIZATION, A NEW METHOD | 44 |
| A MODIFIED K-VALUE METHOD | 56 |
| RESULTS | 71 |
| DISCUSSION OF RESULTS | 113 |
| CONCLUSIONS | 142 |
| NOMENCLATURE | 144 |
| REFERENCES | 148 |
| APPENDIX A - FLASH CALCULATIONS | 157 |

| | Page |
|---|------|
| APPENDIX B - LEAST SQUARES LINEAR PROGRAMMING AS AN OPTIMIZATION TECHNIQUE | 173 |
| APPENDIX C - TEST CASES | 186 |
| APPENDIX D - COMPONENTS' PROPERTIES DATA | 216 |
| VITA | 218 |

LIST OF TABLES

| | Page |
|--|------|
| TABLE 1 - A Summary of Saturation Pressures for the Test Cases | 116 |
| TABLE 2 - A Summary of of The Parameters' Constraints of The K-value Method for The Test Cases | 117 |
| TABLE 3 - A Summary of The New K-value Method Parameters, and Convergence Pressures for the Test Cases .. | 119 |
| TABLE 4 - A Summary of Average Deviations, (%) | 120 |
| TABLE 5 - Composition of Brinkmann's Gas Condensate System | 122 |
| TABLE 6 - Composition of Brinkmann's Crude Oil System ... | 124 |
| TABLE 7 - A Summary of Speed Tests between The New Method and The Equations of State | 131 |
| TABLE C-1 - A Summary of Test Cases | 187 |
| TABLE C-2 - Fluid Composition (Case 1) | 188 |
| TABLE C-3 - Constant Composition Expansion Test (Case 1) .. | 189 |
| TABLE C-4 - Constant Volume Depletion Test (Case 1) | 190 |
| TABLE C-5 - Solubility and Swelling Test (Case 1) (Injection Gas = 95% Methane + 5% Ethane) | 191 |
| TABLE C-6 - Fluid Composition (Case 2) | 192 |
| TABLE C-7 - Constant Volume Depletion Test (Case 2) | 193 |
| TABLE C-8 - Fluid Composition (Case 3) | 194 |
| TABLE C-9 - Constant Composition Expansion Test (Case 3) .. | 195 |
| TABLE C-10 - Solubility and Swelling Test (Case 3) (Injection Gas = Pure Carbon Dioxide) | 196 |
| TABLE C-11 - Solubility and Swelling Test (Case 3) (Injection Gas = 50% CO ₂ + 50% N ₂) | 197 |

| | Page |
|---|------|
| TABLE C-12 - Fluid Composition (Case 4) | 198 |
| TABLE C-13 - Constant Composition Expansion Test (Case 4) .. | 199 |
| TABLE C-14 - Solubility and Swelling Test (Case 4) (Injection Gas = Pure Carbon Dioxide) | 200 |
| TABLE C-15 - Fluid Composition (Case 5) | 201 |
| TABLE C-16 - Constant Composition Expansion Test (Case 5) .. | 202 |
| TABLE C-17 - Solubility and Swelling Test (Case 5) (Injection Gas = Pure Carbon Dioxide) | 203 |
| TABLE C-18 - Fluid Composition (Case 6) | 204 |
| TABLE C-19 - Constant Composition Expansion Test (Case 6) .. | 205 |
| TABLE C-20 - Solubility and Swelling Test (Case 6) (Injection Gas = Pure Carbon Dioxide) | 206 |
| TABLE C-21 - Fluid Composition (Case 7) | 207 |
| TABLE C-22 - Constant Composition Expansion Test (Case 7) .. | 208 |
| TABLE C-23 - Constant Volume Depletion Test (Case 7) | 209 |
| TABLE C-24 - Fluid Composition (Case 8) | 210 |
| TABLE C-25 - Constant Composition Expansion Test (Case 8) .. | 211 |
| TABLE C-26 - Constant Volume Depletion Test (Case 8) | 212 |
| TABLE C-27 - Fluid Composition (Case 9) | 213 |
| TABLE C-28 - Constant Composition Expansion Test (Case 9) .. | 214 |
| TABLE C-29 - Constant Volume Depletion Test (Case 9) | 215 |
| TABLE D-1 - Pure Components' Properties | 216 |
| TABLE D-2 - Smoothed Heavy Fractions' Properties | 217 |

LIST OF FIGURES

| | Page |
|---|------|
| Fig. 1 - Conceptual Phase behavior for CO ₂ and Methane with Simple Hydrocarbons at Constant Pressure | 10 |
| Fig. 2 - Hypothetical Phase Behavior for Type I Systems | 12 |
| Fig. 3 - Constant Composition Expansion Test | 16 |
| Fig. 4 - Constant Volume Depletion Test | 18 |
| Fig. 5 - Solubility and Swelling Test | 20 |
| Fig. 6 - An Example of NGPSA K-values Charts, for Ethane with convergence pressure of 5000 psia | 22 |
| Fig. 7 - Hoffmann-Hocott-Crump Plot, Semi-log of K p vs. Characterization Factor | 27 |
| Fig. 8 - Typical K-values chart | 59 |
| Fig. 9 - Vapor pressure vs. Characterization Factor Plot .. | 62 |
| Fig. 10 - Change of K-values Slope with Pressure | 64 |
| Fig. 11 - Change of K-values Pivot with Composition | 69 |
| Fig. 12 - Constant Composition Expansion of Case 1: Relative Volume vs. Pressure, The K-value Method against Eqns. of State | 73 |
| Fig. 13 - Constant Volume Depletion of Case 1: Percent Liquid vs. Pressure, The K-value Method against Eqns. of State | 74 |
| Fig. 14 - Constant Volume Depletion of Case 1: Cum. Gas Produced vs. Pressure, The K-value Method against Eqns. of State | 75 |
| Fig. 15 - Constant Composition Expansion of Case 1: Relative Volume vs. Pressure, Nolen's against This Model's Eqns. of State | 76 |

| | Page |
|---|------|
| Fig. 16 - Constant Volume Depletion of Case 1: Percent Liquid vs. Pressure, Nolen's against This model's Eqns. of State | 77 |
| Fig. 17 - Constant Volume Depletion of Case 1: Cum. Gas Produced vs. Pressure, Nolen's against This Model's Eqns. of State | 78 |
| Fig. 18 - Constant Composition Expansion of Case 1: Relative Volume vs. Pressure, SPE 3rd Comparative Project | 79 |
| Fig. 19 - Constant Volume Depletion of Case 1: Percent Liquid vs. Pressure, SPE 3rd Comparative Project | 80 |
| Fig. 20 - Constant Volume Depletion of Case 2: Percent Liquid vs. Pressure, The K-value Method against Eqns. of State | 82 |
| Fig. 21 - Constant Volume Depletion of Case 2: Cum. Gas Produced vs. Pressure, The K-value Method against Eqns. of State | 83 |
| Fig. 22 - Constant Composition Expansion of Case 3: Relative Volume vs. Pressure, The K-value Method against Eqns. of State | 85 |
| Fig. 23 - Solubility and Swelling of Case 3: Relative Volume vs. Cum. CO ₂ Injected, The K-value Method against Eqns. of State | 86 |
| Fig. 24 - Solubility and Swelling of Case 3: Sat. Press. vs. Cum. CO ₂ Injected, The K-value Method against Eqns. of State | 87 |
| Fig. 25 - Solubility and Swelling of Case 3: Relative Volume vs. Cum. N ₂ +CO ₂ Injected, The K-value Method against Eqns. of State | 88 |
| Fig. 26 - Solubility and Swelling of Case 3: Sat. Press. vs. Cum. N ₂ +CO ₂ Injected, The K-value Method against Eqns. of State | 89 |
| Fig. 27 - Constant Composition Expansion of Case 4: Relative Volume vs. Pressure, The K-value Method against Eqns. of State | 91 |

| | Page |
|---|------|
| Fig. 28 - Solubility and Swelling of Case 4: Relative Volume vs. Cum. CO ₂ Injected, The K-value Method against Eqns. of State | 92 |
| Fig. 29 - Solubility and Swelling of Case 4: Sat. Press. vs. Cum. CO ₂ Injected, The K-value Method against Eqns. of State | 93 |
| Fig. 30 - Constant Composition Expansion of Case 5: Relative Volume vs. Pressure, The K-value Method against Eqns. of State | 95 |
| Fig. 31 - Solubility and Swelling of Case 5: Relative Volume vs. Cum. CO ₂ Injected, The K-value Method against Eqns. of State | 96 |
| Fig. 32 - Solubility and Swelling of Case 5: Sat. Press. vs. Cum. CO ₂ Injected, The K-value Method against Eqns. of State | 97 |
| Fig. 33 - Constant Composition Expansion of Case 6: Relative Volume vs. Pressure, The K-value Method against Eqns. of State | 99 |
| Fig. 34 - Solubility and Swelling of Case 6: Relative Volume vs. Cum. CO ₂ Injected, The K-value Method against Eqns. of State | 100 |
| Fig. 35 - Solubility and Swelling of Case 6: Sat. Press. vs. Cum. CO ₂ Injected, The K-value Method against Eqns. of State | 101 |
| Fig. 36 - Constant Composition Expansion of Case 7: Relative Volume vs. Pressure, The K-value Method against Eqns. of State | 103 |
| Fig. 37 - Constant Volume Depletion of Case 7: Percent Liquid vs. Pressure, The K-value Method against Eqns. of State | 104 |
| Fig. 38 - Constant Volume Depletion of Case 7: Cum. Gas Produced vs. Pressure, The K-value Method against Eqns. of State | 105 |
| Fig. 39 - Constant Composition Expansion of Case 8: Relative Volume vs. Pressure, The K-value Method against Eqns. of State | 107 |

| | Page |
|---|------|
| Fig. 40 - Constant Volume Depletion of Case 8: Percent Liquid vs. Pressure, The K-value Method against Eqns. of State | 108 |
| Fig. 41 - Constant Volume Depletion of Case 8: Cum. Gas Produced vs. Pressure, The K-value Method against Eqns. of State | 109 |
| Fig. 42 - Constant Composition Expansion of Case 9: Relative Volume vs. Pressure, The K-value Method against Eqns. of State | 111 |
| Fig. 43 - Constant Volume Depletion of Case 9: Cum. Gas Produced vs. Pressure, The K-value Method against Eqns. of State | 112 |
| Fig. 44 - Comparison of Calculated and Experimental K-values of Brinkmann's Gas Condensate System | 123 |
| Fig. 45 - Comparison of Calculated and Experimental K-values of Brinkmann's Crude Oil System | 125 |
| Fig. 46 - K-values of Case 1 at Different P_k | 126 |
| Fig. 47 - K-values of Case 2 at Different P_k | 127 |

INTRODUCTION

Phase behavior plays a fundamental role in oil recovery processes, ranging from the production of gas condensate reservoirs to the injection of CO₂ and N₂ for enhanced oil recovery processes. As more volatile oil and condensate reservoirs are found, the use of phase behavior techniques to predict their performance is increasing in importance, particularly when using compositional simulators. In the phase behavior methods, equilibrium ratios are used to predict compositional changes in the reservoir fluids.¹⁻¹²

Equilibrium ratios are also known as equilibrium constants, or simply, K-values. The K-values of any system are functions of pressure, temperature and composition of that system. However, at constant temperature, it was found that the K-values of simple mixtures could be expressed as functions of pressure only. K-values can be evaluated by three basic methods:(1) Raoult's and Dalton's laws, assuming ideal solutions, (2) using fugacities of pure components calculated from equations of state, and (3) by direct analysis of vapor and liquid in equilibrium at any pressure and temperature, based on the knowledge of some experimental data.¹³

In spite of the development of more sophisticated, theoretically based predictive techniques, notably the equations of

This dissertation follows the style of the Journal of Petroleum Technology.

state methods, K-values' correlations are still implemented into compositional reservoir simulators and other applications where efficiency and ease of adjustment to experimental data are essential.

One of the earliest attempts at a general correlation of K-values was made in 1952 by Rzasa et al.¹⁴ Based primarily on binary and ternary systems data, they correlated K-values in a graphical form for methane through decane, as functions of temperature, pressure, and convergence pressure. A major graphical correlation was presented in the 1957 *NGPSA Engineering Data Book*¹⁵, based on tabulations prepared in 1947 by G.G. Brown. Norman and Williams¹⁶ fitted polynomial functions to 65,000 data points taken from these charts, but the functions had two drawbacks. Continuity with respect to convergence pressure did not exist due to fitting the data at each convergence pressure separately; in addition, the functions were not constrained to converge to K-values equal to unity at the convergence pressure which resulted in limiting the use of the function to pressures below 80% of the convergence pressure. Although many of K-value charts were revised, in the 1966 *Engineering Data Book*¹⁷, and curve fits were prepared for these new charts, the functions suffered from the same drawbacks as the previous functions.

Cajander et al¹⁸, presented nomograms to be used for the K-values of a wide variety of hydrocarbons. Woertz¹⁹ graphically correlated methane K-values from the literature. He also correlated

K-values for ethane through mixed hexanes, but reported no correlation with convergence pressure was observed.

Canfield²⁰ proposed an equation relating K-values to the convergence pressure and the critical temperature, and compressibility factor of the component. Comparisons of the predicted K-values with the 1966 NGPSA charts for methane, n-pentane, n-decane at some temperatures and pressures revealed very large deviations. He recommended the use of his correlation to predict K-values for components not in the charts and for initial guesses for more complicated data systems.

McDonald²¹ fitted a portion of data points taken from the 1957 NGPSA charts with continuous functions of temperature, pressure, and convergence pressure designed to converge to K-values equal to unity at the convergence pressure. For ethane and heavier paraffins, regionally fitted functions were splined to be continuous, and were additionally constrained so that the slope of the graph equals to -1 at a pressure of 1 psia. For nitrogen, methane, carbon dioxide, and hydrogen sulfide, simple functions were employed.

Vadie²² fitted functions of temperature, pressure, and convergence pressure to the K-values of methane, ethane, propane, n-butane, and n-pentane derived from data in the literature on binary, ternary, and multicomponent systems and a few complex mixtures. Data below the critical temperature of the component were fitted with two functions constrained to be continuous through K-values equal to unity at the convergence pressure. A third function was used above the critical temperature. Although agreement between the two

regional fits was reasonably good at the critical temperature, continuity with respect to temperature was not preserved. The functions were also constrained so that K-values equal to unity at the convergence pressure and that they have infinite derivatives with respect to pressure at convergence.

Lawal et al²³ correlated the K-values as functions of pressure, temperature, and convergence pressure for the normal paraffin hydrocarbons from methane through decane, isobutane, isopentane, nitrogen, and carbon dioxide. The functions were designed to yield K-values equal to unity at the convergence pressure, but for the sake of generality, they were not subject to the other constraints associated with binary systems. They used least-squares fitting to correlate the K-values to some published experimental equilibrium states in binary, ternary, multicomponent, and complex systems. Galimberti and Campbell²⁴ correlated the experimentally determined K-values, as a linear function with the logarithm of squares of the critical temperature of each component .

One of the most widely used empirical correlations for approximate K-values estimation is Wilson's correlation²⁵. This equation correlates pressure, temperature, critical properties and acentric factors of the system into a simple expression for K-values. It is commonly used as a good estimator of initial K-values in equations of state calculations. This correlation was modified by Whitson²⁶ to consider the convergence pressure, to properly estimate K-values at high pressures and near the critical region.

Hoffmann *et al*²⁷ introduced an approach for graphically correlating the experimentally determined K-values as functions of pressure, temperature, characterization factor, and convergence pressure. Brinkmann and Sicking²⁸ introduced an iterative method for correlating the K-values based on some experimental data. Dykstra and Mueller²⁹ expressed the logarithm of K-values as a linear function of the characterization factor of each component. The constants of the linear relationship vary with a composition parameter and are determined from the data by an iterative process.

Besserer *et al*⁶ implemented a new procedure which involved developing a set of phase behavior correlations for the pressure and compositional ranges of interest. Their correlations were either table look-ups or analytical expressions, and were suitable for use in compositional simulators. Using their correlations, they reported that an acceptable match with the experimental data was obtained. This allowed the simulator to run several times faster than simulators with a standard equations of state package.

Equations of state have also been used to calculate K-values for hydrocarbon systems. In spite of their accuracy in phase behavior calculations, equations of state usually suffer from either slow convergence, or lack of convergence to the correct solution. Based on modifications of van der Waals' equation, they relate the system pressure, temperature, volume, and satisfy thermodynamic stability criteria at the critical point. Several equations of state were developed and are available in the literature, some of them are

implemented in the current study, namely, Soave-Redlich-Kwong³⁰, Peng-Robinson³¹, and Schmidt-Wenzel³² equations.

Literature review^{3,5,6} and experience in the phase behavior of CO₂-reservoir oil systems have shown that equations of state and available correlations give acceptable results in some areas, but in general, they are not satisfactory due to: (1) lack of accuracy, (2) large computational time, or (3) sometimes yielding trivial solutions. Therefore, accurate, faster and more reliable methods are needed, in particular for actual compositional studies.

The main objective of the current work is to devise a new technique for calculating the K-values of crude oil-carbon dioxide mixtures to be used in compositional simulation studies. The main advantage of K-value methods compared to equations of state is to increase the computational speed and accuracy. The new K-value method increases the computational speed by a simulation factor of 10 compared to equations of state.

This study entailed the following tasks:

- 1- Developing a phase behavior (PVT) computer program to simulate the standard PVT laboratory tests of reservoir fluids under different conditions, employing various methods for estimating the fluid properties and calculating the phase behavior of hydrocarbons^{1,30-39}.
- 2- Developing an automatic matching program using least squares-linear programming as an optimization technique⁴⁰, which was used as a tool for:

- (a) tuning the binary interaction coefficients of the mixtures.
 - (b) adjusting the critical properties of the heavy fractions of the hydrocarbon systems.
 - (c) correlating the slope of the new K-value equation such that a match is obtained with the experimental data.
- 3- Applying the developed program, including the new K-value method, to actual laboratory data of some crude oil-carbon dioxide mixtures, and matching the behavior of these mixtures under different conditions, and comparing the results with those obtained by some equations of state.
- 4- Investigating the speed and the accuracy of some of the methods commonly used for phase equilibria calculations, in particular for CO₂-crude oil mixtures, and comparing them with the new method.

THEORY

MISCIBILITY AND PHASE BEHAVIOR OF CRUDE OIL-CARBON DIOXIDE SYSTEMS

When two fluids are mixed in all proportions and remain as a single phase at all mixtures, they are called miscible fluids. Miscibility of fluids with reservoir oils can be divided into different types of miscible processes⁷, as follows:

First Contact Miscibility: In this process, miscibility takes place when fluids mix directly, in all proportions, with reservoir oils, and they always form a single phase. Examples of the first contact miscible injection fluids are the intermediate molecular weight hydrocarbons, such as ethane, propane, . . . , hexanes and LPG, which are first contact miscible with most reservoir oils.

Multiple Contact (Dynamic) Miscibility: In this type of miscibility, fluids are not miscible at first contact with reservoir oil. To achieve miscibility, in-situ mass transfer of intermediate molecular weight components takes place between reservoir oil and injection fluids. By so doing, a transition zone is formed of fluids with compositions that range from oil to injection fluid compositions. Therefore, miscibility results from the repeated contact of the injection fluids with the

reservoir oil. Examples of the multiple contact miscible injection fluids are: methane, nitrogen, flue gas and carbon-dioxide.

Carbon Dioxide Miscible Process

Although first contact miscibility of carbon dioxide with reservoir oils is not attainable at realistic reservoir pressures; dynamic miscibility is possible above a minimum miscibility pressure (MMP).²⁻⁷ One of the major advantages of carbon dioxide miscible processes is that their MMP is substantially lower than that of dry gas, flue gas or nitrogen. Accordingly, dynamic miscibility can be achieved at attainable pressures in a broad spectrum of reservoirs.

For more understanding of the miscibility of carbon dioxide with oils, we consider Fig.1. This figure depicts the conceptual phase behavior of CO₂ and methane with simple hydrocarbons by two groups of ternary diagrams. From these ternary diagrams, we note that dynamic miscibility with CO₂ is achieved at a lower pressure than with dry gas (methane). CO₂ extracts hydrocarbons of higher molecular weight from the oil than the predominantly C₂-through-C₅ hydrocarbons which methane vaporizes to achieve vaporizing-gas drive miscibility. This means that there is a restriction on the miscibility of methane with reservoir fluids, and these fluids must be rich in the intermediate-molecular-weight hydrocarbons (C₂...C₅). This restriction severely limits the applications of this process. On the other hand, this is an advantage for CO₂ process, since CO₂ achieves its dynamic miscibility by extracting high-molecular-weight

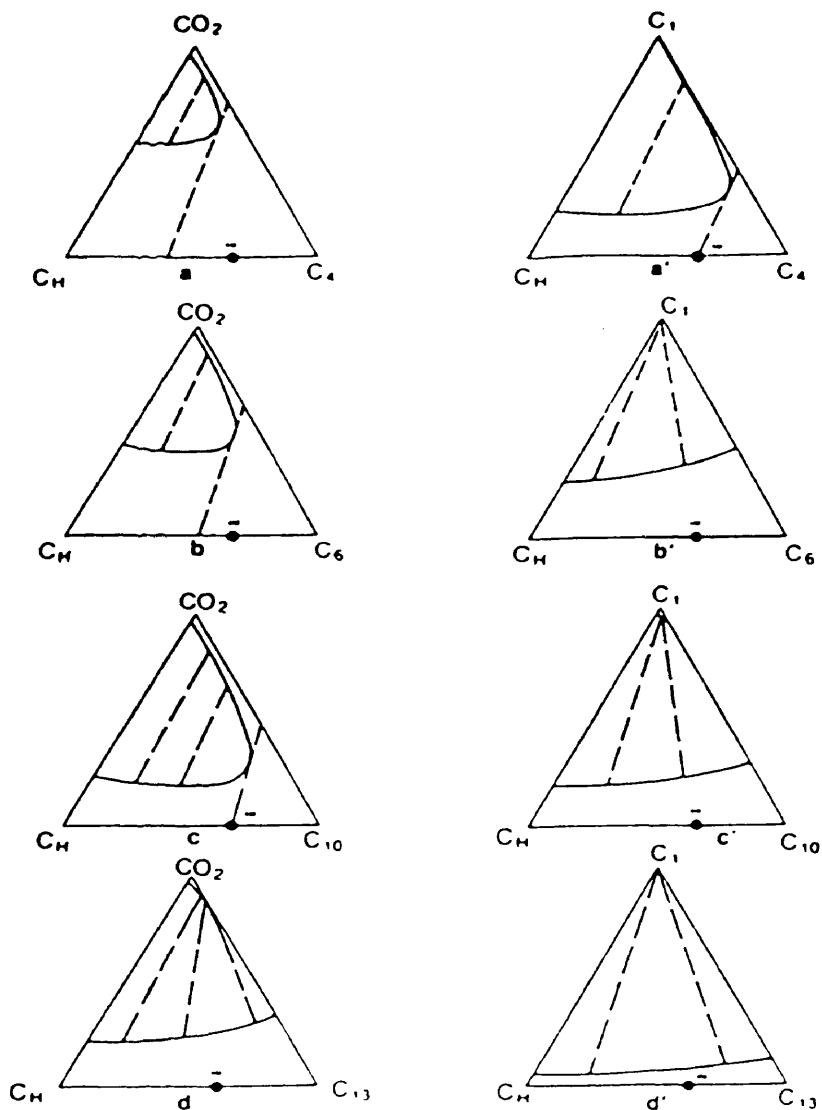


Fig. 1 - Conceptual Phase behavior for CO_2 and Methane with Simple Hydrocarbons at Constant Pressure. (after Ref. 7)

as well as intermediate-molecular-weight hydrocarbons.

Carbon Dioxide Phase Behavior

Metcalfe and Yarborough⁴¹ classify CO₂ - reservoir fluid phase behavior into two broad types according to the characteristics of the pressure - composition phase diagrams. In type I, only vapor and liquid coexist in the multiphase region of the P-X diagram, shown in Fig. 2-a. This type usually takes place at temperatures higher than about 120 °F. Type II phase behavior occurs relatively closer to the critical temperature of CO₂, generally at temperatures below about 115-120 °F. In this type, some mixtures may separate into two, three or maybe four different phases. Some mixtures may separate into liquid and vapor phases, some others separate into two coexisting liquid phases, in some cases a small region of the P-X diagram may have two liquids and gas, and in rare occasions with some oils solid precipitates of solid asphaltenes may form. Since the main objectives of this study is to simulate the phase behavior of volatile oils and gas condensates which are normally encountered in reservoirs of temperatures above 120 °F. Therefore, the focus here will be on the phase behavior of volatile oil-carbon dioxide mixtures where type I prevails.

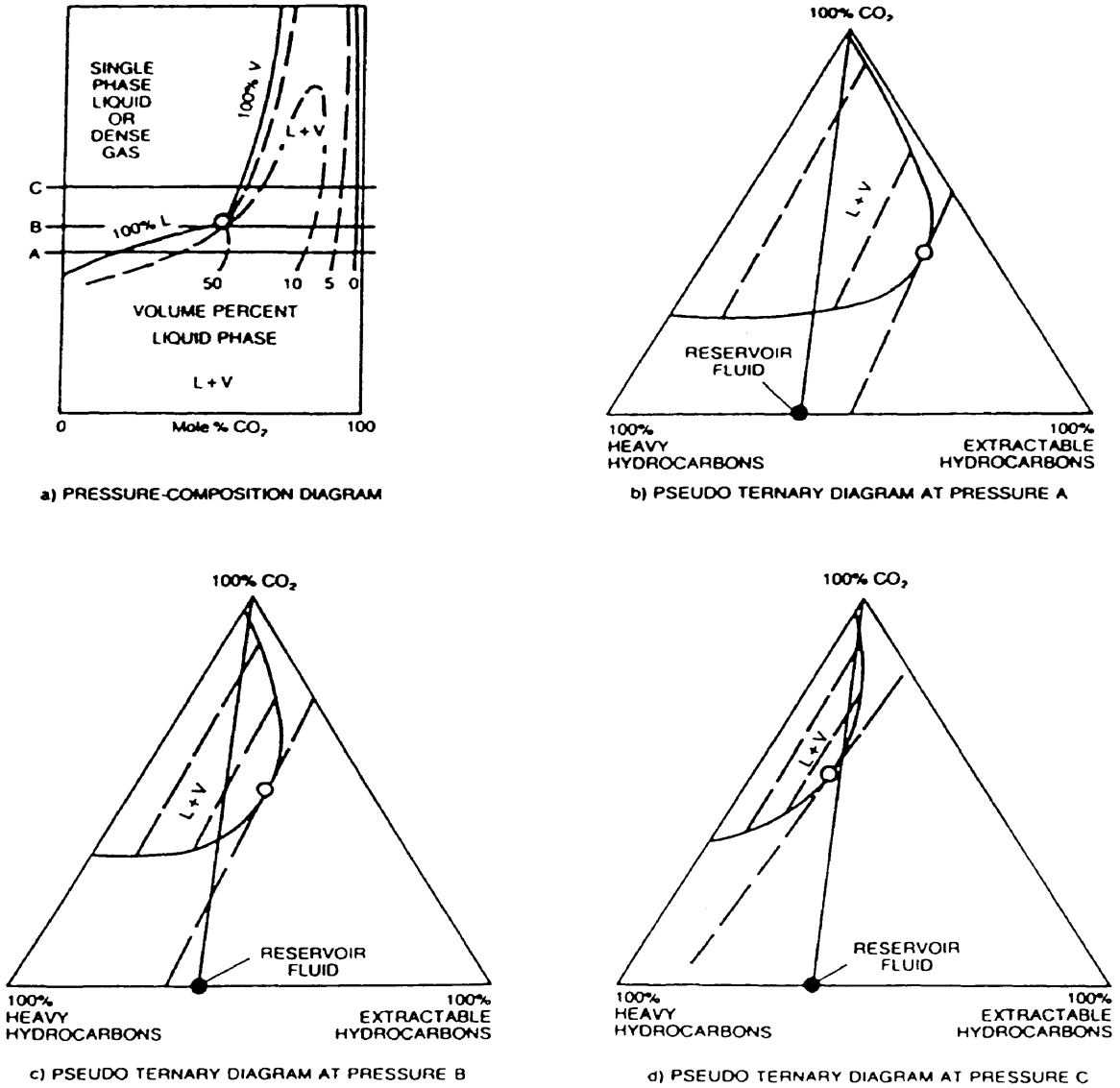


Fig. 2 - Hypothetical Phase Behavior for Type I Systems.
(after Ref. 7)

Type I Phase behavior

In this type two phases, equilibrium liquid and vapor, coexist in the multiphase region. Considering the ternary diagrams of Fig. 2, the pseudocomponents are CO₂, extractable hydrocarbons by CO₂, and high-molecular-weight (heavy/non-extractable) hydrocarbons.⁷ In this system, dynamic miscibility can be achieved by the vaporizing-gas drive mechanism. At sufficiently high pressures, CO₂ extracts some hydrocarbons from the oil until it is enriched to the degree that the CO₂ gas phase composition at the displacing front becomes miscible with reservoir oil. Three cases (A, B, and C) are considered at different pressures. In case A, the pressure is much lower than the MMP of this system and the reservoir fluid lies to the left of the limiting tie line through the plait point. Injecting or adding CO₂ to the reservoir oil will follow the line connecting the reservoir oil composition point and the 100 % CO₂ point. As CO₂ is added to the system, the mixture compositions changes from the single phase region to the two phase region by crossing the bubble point line. At higher pressures, cases B and C, the reservoir fluid composition lies to the right of the limiting tie line, which means dynamic miscibility is achievable in these cases. In case B, by adding CO₂ to the system, CO₂-oil mixtures moves from the single-phase region into the two-phase region by crossing the bubble point line. But, in case C, as CO₂ is added to the system, the mixtures enters the two-phase region by crossing the dew point line, and mixes directly with oil.

This suggests that, for type I, the MMP should be lower than the pressure at which the plait point takes place on the pressure-composition diagram.

LABORATORY TESTS

Routine laboratory tests are usually performed on reservoir fluid samples to measure their properties and phase behavior under different conditions. Fluid samples used for these laboratory tests are normally either volatile oil or gas condensate.

Constant Composition Expansion Test

In this test, a reservoir fluid sample is expanded in a series of discrete pressure increments, as shown in Fig. 3, starting at a pressure above the initial reservoir pressure to some pressure usually much lower than the saturation pressure. The test is conducted at a constant temperature equal to the reservoir temperature. The volumes of the cell, the gas phase and the liquid phase are measured when equilibrium is reached at each pressure level. This test is important for providing the following data:

- (1) The saturation pressure of the sample.
- (2) Liquid phase compressibility.
- (3) The compressibility factor of the gas phase.
- (4) The saturated fluids densities.

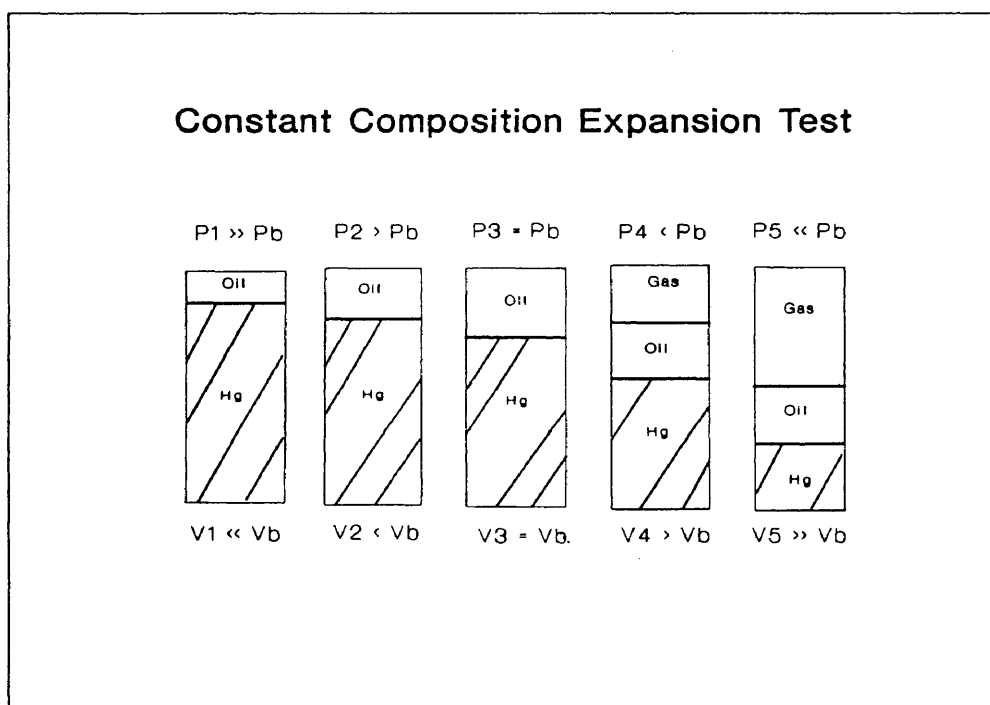


Fig. 3 - Constant Composition Expansion Test.

Constant Volume Depletion Test

This test involves also expansion of the fluid sample during step-wise pressure reductions in the cell, as shown in Fig. 4. The test starts at the saturation pressure of the sample and progresses through five or six pressure levels. At each pressure level, when the system reaches equilibrium, some volume of gas is withdrawn from the cell at constant pressure to restore it to its initial volume. The data which can be obtained from this test are:

- (1) The saturation pressure of the sample.
- (2) The compressibility factor of the gas produced at each step.
- (3) The composition of the gas produced at each step.
- (4) The cumulative gas produced as a percentage of the initial volume.
- (5) The liquid volume as a percent of the cell volume.
- (6) The composition of the liquid at the final pressure.

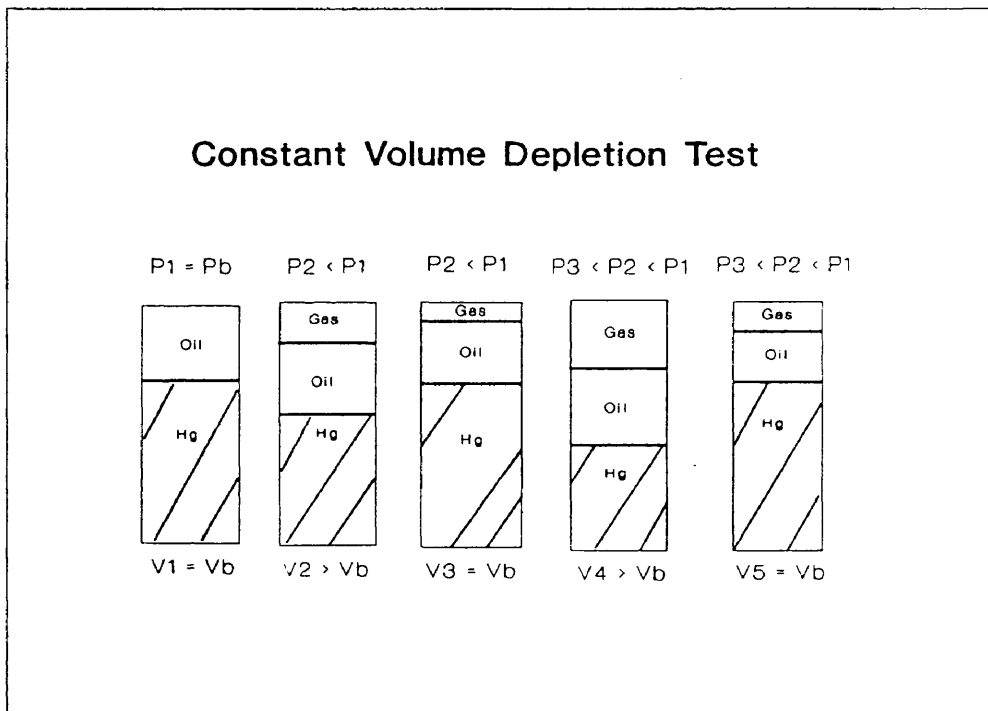


Fig. 4 - Constant Volume Depletion Test.

Solubility And Swelling Test

This test is usually conducted for reservoirs to be depleted under gas injection, miscible type displacement or dry gas cycling. In this test, a gas of known composition, usually similar to the proposed injection gas, is injected in a series of slugs into a reservoir oil sample, as shown in Fig. 5. The injection of the first gas slug starts at the bubble point pressure of the reservoir fluid sample and continues until a considerable amount of gas, normally about 70-80 mole percent of the sample volume, is injected. After each gas addition, the cell is pressured up until only one phase is present. This test provides the following data:

- (1) The relationship between the saturation pressure and the cumulative volume of the gas injected.
- (2) The volume of the saturated fluid mixture in relation to the volume of the original saturated reservoir oil as a function of the cumulative volume of the gas injected.

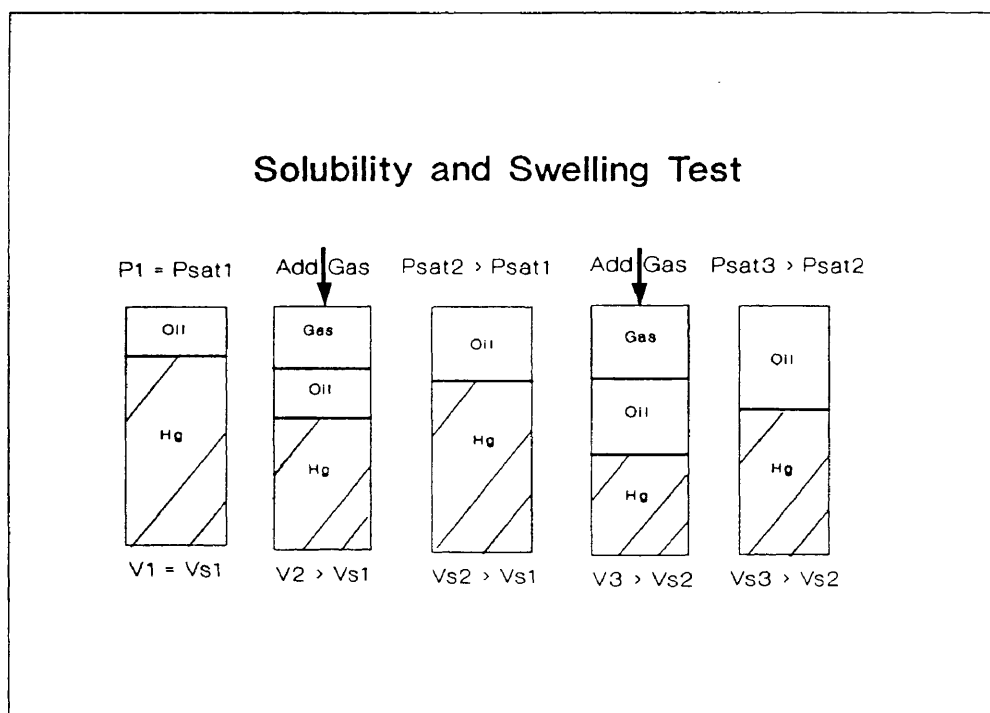


Fig. 5 - Solubility and Swelling Test.

K-VALUE METHODS

The equilibrium ratios are sometimes known as equilibrium constants or, simply, K-values. The K-values of any system are functions of pressure, temperature and composition of that system. However, at constant temperature, it has been found that the K-values of simple mixtures could be expressed as functions of pressure only. Different methods have been developed and used for K-value estimations. Some of these methods are implemented in this study to compare the accuracy and speed of each of them in the phase behavior calculations of the carbon dioxide-hydrocarbon systems. These methods and their theoretical backgrounds are covered in the following sections

NGPSA K-Value Charts

When plotted against pressure, at constant temperature, the K-values show that they converge almost to a common point at which the K-values equal unity and the pressure at that point is then called the convergence pressure. This expresses the K-values as a simple function of temperature, pressure and convergence pressure. These functions are correlated, for pure components, in the NGPSA charts^{15,17,42} in terms of the convergence pressure of the system. An example of the K-values for ethane with a convergence pressure of 5000 psia is shown in Fig. 6. Some techniques are available in the

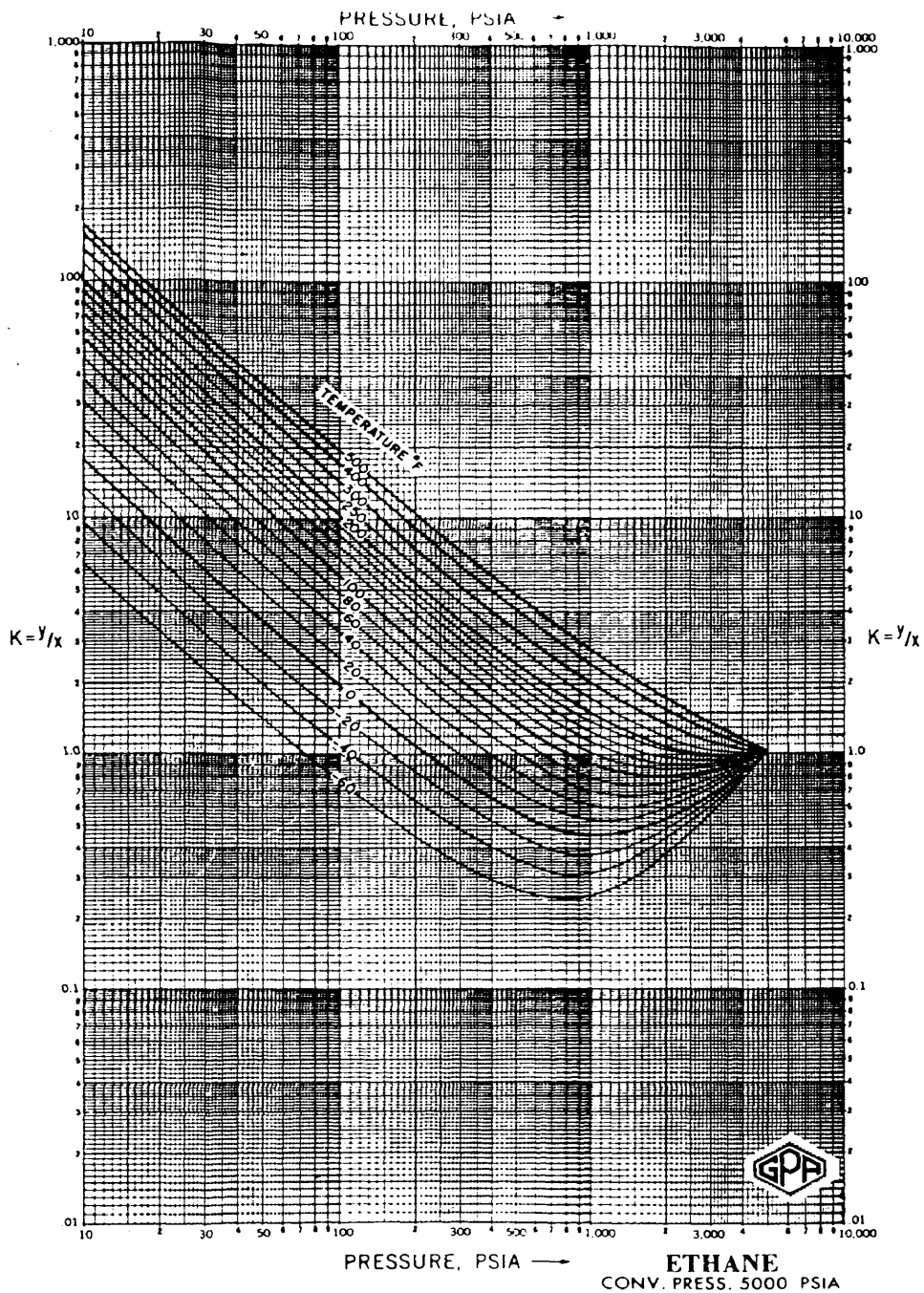


Fig. 6 - An Example of NGPSA K-values Charts, for Ethane with a convergence pressure of 5000 psia. (after Ref. 42)

literature for convergence pressure calculations such as Hadden's method⁴³, Kesler's method⁴⁴, and Rowe's method⁴⁵.

Two direct convergence pressure correlations are used throughout this work:

(1) For Oil Systems (Standing's equation⁴⁶):

$$P_k = 60.0 * MW_{C7+} - 4200.0$$

.....(1)

(2) For Gas Condensate Systems (Besserer's equation⁶):

$$P_k = \exp\{ 10.540064 - [1.475 + 6.15 (Z_{C6+} / Z_{C1})] * (1.0 - Z_{N2}) \}$$

.....(2)

Equations of State

Equations of state have been used to calculate the K-values of hydrocarbon systems. Based on modifications of van der Waals' equation, they relate the system's pressure, temperature, volume, and satisfy the thermodynamic stability criteria at the critical point. Several equations of state were developed and are available in the literature, some of them are implemented in this study; namely, Soave-Redlich-Kwong³⁰, Peng-Robinson³¹, and Schmidt-Wenzel³² equations. The details of K-values calculations, based on the

fugacities of each phase using each of these equations, are covered in the flash calculation section, in Appendix A .

Empirical Correlations

One of the most widely used empirical correlation for approximate K-values estimation is Wilson's correlation.²⁵ This correlation is based on correlating the pressure, temperature, critical properties and the acentric factors of the system into a simple expression for K-values. This correlation is commonly used as a good and approximate estimator of initial K-values in equation of state calculations. This equation is expressed as:

$$k_i = (1.0 / P_{ri}) \exp[5.3727 (1.0 + \omega_i) (1.0 - 1.0 / T_{ri})] \dots\dots\dots(3)$$

This expression was modified by Whitson²⁶ to consider the convergence pressure in the equation to properly estimate k-values near the critical region. The new form of this correlation is:

$$k_i = (P_{ci}/P_k)^{(A-1)} (1/P_{ri}) \exp[5.3727 (1 + \omega_i) (1 - 1/T_{ri})] \dots\dots\dots(4)$$

where:

A : slope of log(k p) vs. log(Fi)

According to Whitson and some experience with Eq. 2, this equation is valid only at low pressures (below 500 psia), and Eq. 4 can be used for high pressures.

Galimberti-Campbell Method

Galimberti and Campbell²⁴ correlated the experimentally determined K-values with critical temperature of each component. Their method is of immediate value in estimating K-values for the heaviest fractions from those of pure components. For a mixture, at a specified pressure and temperature, the logarithms of K-values of the various components will form a straight line when plotted against the squares of their absolute critical temperatures. Therefore, the correlation takes the simple linear form:

$$\text{Log}(K_i) = a (T_{ci})^2 + b \dots\dots\dots(5)$$

The constants a and b depend on pressure, temperature and the overall composition of the mixture, but they are the same for each constituent in a particular mixture.

Hoffmann-Grump-Hocott Method

Hoffmann *et al*²⁷ introduced one of the first techniques for correlating the experimentally determined K-values as a function of

pressure, temperature, characterization factor, and convergence pressure. In their approach, the product of K-value and system pressure (K_p) is plotted on a semilog plot against the characterization factor (F), for each component, which is defined as:

$$F = b \left(\frac{1}{T_B} - \frac{1}{T} \right) \dots\dots\dots(6)$$

where:

$$\begin{aligned} b &= (\Delta H_m / R) \log(e) \\ &= \log(p_c / 14.7) / \left(\frac{1}{T_B} - \frac{1}{T_c} \right) \end{aligned} \dots\dots\dots(7)$$

Then, the plot is smoothed yielding a group of straight lines at different pressures over an acceptable range of temperatures, as shown in Fig. 7. This relation will be useful to evaluate the K-values at different pressures and temperatures for each hydrocarbon component in terms of its characterization factor.

Brinkmann-Sicking Method

This method was called a combination mathematical-experimental method.²⁸ In order to use this method, the following experimental data should be available:

- (1) Reservoir temperature.
- (2) Overall composition of the system.

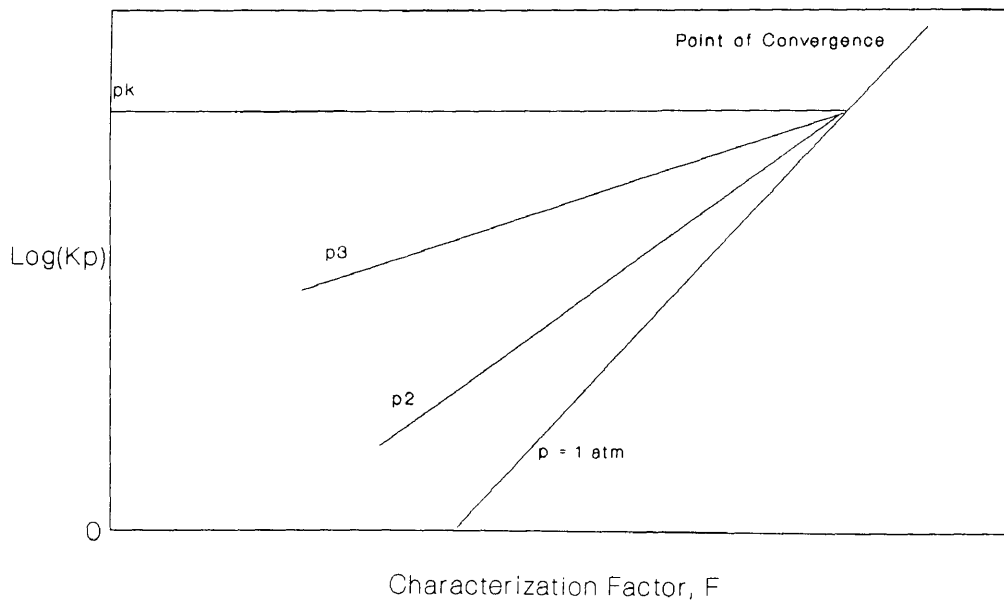


Fig. 7 - Hoffmann-Hocott-Crump Plot,
Semi-log of $K p$ vs. Characterization Factor.

- (3) Saturation pressure (bubble point or dew point pressure).
- (4) Relative vapor-liquid volumes at different pressures.
- (5) Relative densities of vapor-liquid as a function of pressure.

In their method, Brinkmann and Sicking used a correlation of the form:

$$K_i = (p_k / p) \exp(\text{slope} (F_i - F_k)) \dots\dots\dots(8)$$

to represent the family of straight lines of the plot $\log(K_i p)$ vs. F_i . Also the vapor mole fraction was expressed as:

$$V = \sum_{i=1}^{N_c} (Z_i V K_i / (L + V K_i)) \dots\dots\dots(9)$$

When combining Eqs. 8 and 9, we get:

$$V = \sum_{i=1}^{N_c} (Z_i / [(1 - V) (p / p_k) \exp(\text{slope} (F_i - F_k)) + V]) \dots\dots\dots(10)$$

The approach for solving this equation is to assume a value for V and then iterate on the slope until the calculated quantity of V using Eq. 10 equals the assumed value. Then, the vapor-liquid

volumes are calculated and compared with the experimentally determined values; if the two are not equal, a new value for V is assumed and the entire iterative procedure is repeated until agreement is obtained. The K -values are then obtained from Eq. 8.

Dykstra-Mueller Method

Dykstra and Mueller²⁹ described a method for obtaining compositions of gas and oil phases in equilibrium as lean or enriched gas is injected into a reservoir oil not in equilibrium with the gas. They expressed the logarithm of K -values as a linear function of the characterization factor of each component. The constants of the linear relationship vary with a composition parameter and are determined from the data by an iterative process. The method consists of calculating the K -values as a function of the liquid composition and then using these K -values to calculate the changes in composition of gas as it successively contacts original reservoir oil.

Abel, Jackson, and Wattenbarger⁴⁷ used this method in a gas recycling compositional simulation study. They varied the slope of $\log(K_p)$ vs. F as a function of pressure, and the convergence pressure as a function of the compositional changes. They matched the experimental data by trial and error, keeping the characterization factors and the fluid properties of the components constant.

EQUATIONS OF STATE

An equation of state is a relationship between pressure, temperature, composition and volume. A cubic equation of state is cubic either in volume or in compressibility factor Z . There may be one, two (seldom) or three real roots which satisfy the specified conditions. In practice, the largest root of the cubic equation is defined as for vapor phase and the smallest root as for liquid phase. If a third root exists, it is merely ignored. In the case of having only one root to satisfy the equation, then there is no problem in choosing the correct solution.

Cubic Equations of State

In 1873, van der Waals⁴⁸ proposed the first cubic equation of state. Since then, the evolution of cubic equations has resulted in new and different forms such as those introduced by Redlich-Kwong (RK)⁴⁹, Martin(M)⁵⁰, Soave-Redlich-Kwong (SRK)³⁰, Usdin-McAuliffe (UM)⁵¹, Peng-Robinson(PR)³¹, Schmidt-Wenzel (SW)³², and many others. Several alternate forms of these equations have been suggested, but the RK equation has been certainly the most popular, and widely used, basis for modifications. A recent trend has been to propose generalized cubic equations which can be simplified to more popular and familiar forms. Most investigators agree that no single equation, no matter how complicated (two, three, four or even five

constants), can accurately predict volumetric and phase behavior of pure compounds or mixtures over a large range of conditions and compositions.

Most petroleum engineering applications of cubic equations depend on a modification of RK or PR equations of state. Although several variants of the RK equation are acceptable, Soave's modification (SRK) is the simplest and most widely used. Unfortunately it yields poor liquid densities. The PR equation is comparable to the SRK in simplicity and form. Peng and Robinson report that their equation predicts liquid densities better than the SRK. A distinct advantage of PR and SRK equations is their reproducibility, and also the simple temperature-dependent expressions which are used to express the correlation of the equation of state constant A . Schmidt and Wenzel equation of state exhibits a superior predictive capability for volumetric properties of gas condensate systems. A three constant equation of state was proposed almost simultaneously by Usdin-McAliffe (UM)⁵¹ and Fuller. Although it has not received wide acceptance, their equation exhibits several qualities which make it an attractive alternative.

In this study, three equations of state are considered. These equations are two-parameter, cubic equations. These equations are:

- (1) Soave-Redlich-Kwong equation of state.
- (2) Peng-Robinson equation of state.
- (3) Schmidt-Wenzel equation of state.

These equations are characterized by sharing the general form:

$$p = R T / (V - b) - a / [(V + \alpha_1 b) (V + \alpha_2 b)] \quad \dots\dots\dots(11)$$

where:

$$a = \sum_{j=1}^{Nc} \sum_{i=1}^{Nc} y_i y_j a_{ij} \quad \dots\dots\dots(12)$$

$$b = \sum_{j=1}^{Nc} \sum_{i=1}^{Nc} y_i y_j b_{ij} \quad \dots\dots\dots(13)$$

$$a_{ij} = (a_i a_j)^{1/2} (1.0 - \delta_{ij}) \quad \dots\dots\dots(14)$$

$$b_{ij} = (1.0 - \xi_{ij})(b_i + b_j) / 2 \quad \dots\dots\dots(15)$$

$$a_i = (\Omega_a R^2 T_{ci}^2 / P_{ci}) [1.0 + m_i (1.0 - T_{ri}^{1/2})] \quad \dots\dots\dots(16)$$

$$m_i = m(\omega_i) \quad \dots\dots\dots(17)$$

$$b_i = (\Omega_b R T_{ci} / P_{ci}) \quad \dots\dots\dots(18)$$

δ_{ij} = binary interaction parameter for hydrocarbons.

ξ_{ij} = binary interaction parameter for hydrocarbon-carbon-dioxide system.

Soave-Redlich-Kwong Equation of State: Soave's equation³⁰ is a modification of the original Redlich-Kwong equation. The RK equation has an excellent predictive capability of the second virial coefficient, which secures good performance at low densities and

reliable predictions at high densities in the super-critical region. All pure components are required to have a critical compressibility factor of 1/3, which is reasonable for lighter hydrocarbons but is less satisfactory for heavier compounds.

In an attempt to improve the vapor-pressure predictions, i.e. the vapor-liquid equilibrium, by introducing a correction term for the equation of state constant A, Soave used vapor pressures directly to determine the functional relation of the correction factor. Although the SRK is the most accepted modification to date, it still underestimates liquid densities of petroleum mixtures.

The SRK offers a good predictive tool for systems requiring accurate predictions of vapor-liquid equilibrium and vapor properties, but should be used with good caution, however, when liquid volumes are important for the engineering applications.

The generalized form of the equation of state can be adapted for the SRK by using:

$$\alpha_1 = 1.0 \quad \dots\dots\dots(19)$$

$$\alpha_2 = 0.0 \quad \dots\dots\dots(20)$$

$$\Omega_a = 0.42747 \quad \dots\dots\dots(21)$$

$$\Omega_b = 0.08664 \quad \dots\dots\dots(22)$$

So, the equation could be expressed as:

$$p = R T / (V - b) - a / [V (V + b)] \dots\dots\dots(23)$$

Soave correlated the slope m , of Eq. 17, against the acentric factor ω by the generalized relationship:

$$m(\omega_i) = 0.480 + 1.574 \omega_i - 0.176 \omega_i^2 \dots\dots\dots(24)$$

The SRK equation can be written in terms of the compressibility factor Z as:

$$Z^3 - Z^2 + (A - B - B^2) Z - A B = 0 \dots\dots\dots(25)$$

where:

$$A = a p / (R^2 T^2) \dots\dots\dots(26)$$

$$B = b p / (R T) \dots\dots\dots(27)$$

The correct root, for liquid is Z_L , or for vapor Z_V , is always selected based on the minimum Gibbs free energy criteria for a phase rather than the generally accepted heuristic of maximum root for vapor phase and minimum root for liquid phase.

The Gibbs free energy for a phase is defined as:⁵²

$$\begin{aligned}
 G = & \sum_{i=1}^{Nc} x_i G_i^\circ + R T \sum_{i=1}^{Nc} x_i \ln(x_i) \\
 & + R T \ln(p) + R T \ln(f/p) \\
 & \dots\dots\dots(28)
 \end{aligned}$$

From Eq. 28, it is suggested that only phase fugacity need to be evaluated to calculate the Gibbs free energy, in order to select the appropriate root, rather than evaluating all the individual component fugacities.

Since the state of equilibrium is frequently expressed in terms of fugacity of present components in each phase, the component fugacity is defined as:

$$\begin{aligned}
 \ln[f_i/(x_i p)] = & \ln \Phi_i \\
 = & - \ln(Z - B) \\
 & + [2 \sum_{j=1}^{Nc} x_i b_{ij} / b - 1.0] (Z - 1.0) \\
 & - [A / (\alpha_1 - \alpha_2) B] \\
 & * \ln\{(Z + \alpha_1 B) / (Z + \alpha_2 B)\} \\
 & * \{(2 \sum_{j=1}^{Nc} x_j a_{ij} / a) - (2 \sum_{j=1}^{Nc} x_j b_{ij} / b) \\
 & + 1.0 \} \dots\dots\dots(29)
 \end{aligned}$$

Peng-Robinson Equation of State: In 1975, Peng and Robinson³¹ proposed a new two-constant equation which is also a modification of the RK equation. The advantage of this equation over SRK is its

capability of predicting the liquid density as well as the vapor pressure in order to further improve vapor-liquid equilibrium predictions. The equation does not produce inferior vapor-liquid equilibria compared with the RK equation.

The largest improvement offered by the PR equation is a universal critical compressibility factor of 0.307401, which is somewhat lower than the SRK value of 1/3 and is closer to the experimental values of heavier hydrocarbons.

The generalized form of the equations of state can be adapted for the PR equation by using:

$$\alpha_1 = 2.41421 \dots\dots\dots(30)$$

$$\alpha_2 = -0.41421 \dots\dots\dots(31)$$

$$\Omega_a = 0.45724 \dots\dots\dots(32)$$

$$\Omega_b = 0.07780 \dots\dots\dots(33)$$

So that the PR equation could be written as:

$$p = R T / (V - b) - a / [(V + 2.4142 b)(V - 0.4142 b)] \dots\dots\dots(34)$$

and the slope $m(\omega_i)$ was used as:

$$m(\omega_i) = 0.37464 + 1.54226 \omega_i - 0.26992 \omega_i^2 \dots\dots\dots(35)$$

This expression was later expanded by the investigators to give the relationship:

$$\begin{aligned}
 m(\omega_i) = & 0.3796 + 1.485 \omega_i - 0.1644 \omega_i^2 \\
 & + 0.01667 \omega_i^3 \\
 & \dots\dots\dots(36)
 \end{aligned}$$

Rearranging the generalized equation into the compressibility factor Z form, we get:

$$\begin{aligned}
 Z^3 + (B - 1.0) Z^2 + (A - 3 B^2 - 2 B) Z \\
 - (A B - B^2 - B^3) = 0.0 \\
 \dots\dots\dots(37)
 \end{aligned}$$

where:

$$A = a p / (R^2 T^2) \quad \dots\dots\dots(38)$$

$$B = b p / (R T) \quad \dots\dots\dots(39)$$

Similar to the SRK approach, the correct root, for liquid is Z_L , or for vapor Z_V , is always selected based on the minimum Gibbs free energy criterion for a phase rather than the maximum root for the vapor phase and the minimum root for the liquid phase. On the same basis, we use Eq. 28 to calculate the Gibbs free energy and Eq. 29 to calculate the fugacity of each component.

Schmidt-Wenzel Equation of state: Schmidt and Wenzel³²

proposed a generalized form of van der Waals' equation. They replaced the denominator V^2 in the attraction term of the original equation by an expression quadratic in volume, such that the equation has the form:

$$p = RT / (V - b) - a / (V^2 + U b V + W b^2) \quad \dots\dots\dots(40)$$

where:

$$a = a(T) \quad \dots\dots\dots(41)$$

$$U = 1 + 3 \omega \quad \dots\dots\dots(42)$$

$$W = - 3 \omega \quad \dots\dots\dots(43)$$

We note that the PR and SRK equations are special forms of the SW equation. For the PR equation, the parameters are:

$$U = 2 \quad W = -1 \quad (\text{i.e., } \omega = 1/3) \quad \dots\dots\dots(44)$$

For the SRK equation, the parameters are:

$$U = 1 \quad W = 0 \quad (\text{i.e., } \omega = 0) \quad \dots\dots\dots(45)$$

Rearranging Eq. 40 into the Z factor form, we get:

$$\begin{aligned}
 Z^3 - [B - UB + 1.0] Z^2 + [WB^2 - UB^2 - UB + A] Z \\
 - [WB^3 + WB^2 + AB] = 0 \\
 \dots\dots\dots(46)
 \end{aligned}$$

The constants of Eq. 40 and 46 are defined as:

$$A = a_p / R^2 T^2 \dots\dots\dots(47)$$

$$B = b_p / RT \dots\dots\dots(48)$$

$$a(T) = a_c \alpha(T_r, m(\omega_i)) \dots\dots\dots(49)$$

$$a_c = \Omega_a R^2 T_c^2 / p_c \dots\dots\dots(50)$$

$$b = \Omega_b R T_c / p_c \dots\dots\dots(51)$$

$$\begin{aligned}
 \Omega_a = (1.0 - \xi_c (1.0 - \beta_c))^3 \\
 \dots\dots\dots(52)
 \end{aligned}$$

$$\Omega_b = \beta_c \xi_c \dots\dots\dots(53)$$

$$\begin{aligned}
 \xi_c = 1.0 / (3 (1.0 + \beta_c \xi_c)) \\
 \dots\dots\dots(54)
 \end{aligned}$$

The parameter β_c is given by the smallest positive root of the equation:

$$\begin{aligned}
 (6\omega + 1.0) \beta_c^3 + 3\beta_c^2 + 3\beta_c - 1.0 = 0.0 \\
 \dots\dots\dots(55)
 \end{aligned}$$

An approximation (or initial guess) for β_c is provided by:

$$\beta_c = 0.25989 - 0.0217 \omega + 0.000375 \omega^2$$

.....(56)

The function $\alpha(T_r, m(\omega_i))$ can be calculated at different conditions as:

(1) at temperatures below the critical:

$$\alpha = [1.0 + m(1 - T_r^2)]^2$$

.....(57)

$$m = m_1 \quad \text{for } \omega \leq 0.40$$

.....(58)

$$m = m_2 \quad \text{for } \omega \geq 0.55$$

.....(59)

$$m = [(\omega - 0.4) / 0.15] m_2 + [(0.55 - \omega) / 0.15] m_1$$

for $0.40 < \omega < 0.55$
.....(60)

where:

$$m_1 = m_0 + (1 / 70) [5 T_r - 3 m_0 - 1.0]^2$$

.....(61)

$$m_2 = m_0 + 0.71 [T_r - 0.779]^2$$

.....(62)

$$m_o = 0.465 + 1.347 \omega - 0.528 \omega^2$$

for $\omega \leq 0.3671$

.....(63)

$$m_o = 0.5361 + 0.9593 \omega$$

for $\omega > 0.3671$

.....(64)

(2) at temperatures above the critical (super critical):

$$\alpha = 1.0 - [0.4774 + 1.328 \omega] \ln(T_r)$$

.....(65)

For mixtures, the following mixing rules are employed:

$$a = \sum_{i=1}^{Nc} \sum_{j=1}^{Nc} X_i X_j a_{ij}$$

.....(66)

$$b = \sum_{i=1}^{Nc} X_i b_i$$

.....(67)

$$a_{ij} = [a_i a_j]^{1/2} (1.0 - \delta_{ij})$$

.....(68)

$$\omega_{mix} = \left(\sum_{i=1}^{Nc} \omega_i Y_i b_i^{0.7} \right) / \left(\sum_{i=1}^{Nc} Y_i b_i^{0.7} \right)$$

.....(69)

ω_{mix} is used in evaluating the basic constants W and U.

To calculate the fugacity, the following expression is used:

$$\begin{aligned}
 \ln[f_i/(x_i p)] &= \ln \Phi_i \\
 &= - \ln(Z - B) + b_i (Z - 1.0) / b \\
 &* A / (B G) \ln\{ (Q + B G) / (Q - B G) \} \\
 &* \left(- 2 \sum_{j=1}^{Nc} Y_j a_{ij} / a + b_i / b \right. \\
 &\quad \left. + [S (U + 2)] \right) \\
 &- \left(S (1 - Z + B) / (Z - B) \right) \\
 &* \left(U Z + 2 Z + 2 W B + U B \right) \\
 &\dots\dots\dots(70)
 \end{aligned}$$

Where:

$$G = (U^2 - 4 W)^{1/2} \dots\dots\dots(71)$$

$$Q = 2 Z + U B \dots\dots\dots(72)$$

$$\begin{aligned}
 S &= 3 b_i^{0.7} (\omega_i - \omega) / \left[G^2 \left(\sum_{j=1}^{Nc} Y_j b_j^{0.7} \right) \right] \\
 &\dots\dots\dots(73)
 \end{aligned}$$

This fugacity equation is reduced to the PR and SRK fugacity equation form, when substituting by the term $(\omega_i - \omega_{mix}) = 0.0$.

Comments on The Equations of State

Some important observations on the performance of the two constant cubic equations of state are:

- 1 - The critical properties, acentric factors and molecular weights for each component in any mixture are not well defined properties for petroleum fractions. They are difficult to estimate; it could be found that different correlations give considerably different results.
- 2 - The constant "A" in any of the equations usually dictates vapor-liquid-equilibrium and vapor density predictions.
- 3 - The constant "B" in any of the equations usually dictates liquid density predictions.
- 4 - The critical temperature " T_c " has more influence on the vapor-liquid-equilibrium and vapor density predictions than the critical pressure " p_c ", for any mixture.
- 5 - The binary interaction parameters are often used to correct the vapor-liquid-equilibrium deficiencies for mixtures of compounds of unlike properties.
- 6 - The mixing rules, used for estimating the coefficients of mixtures, may have some effect on the performance of the equation of state used, in particular with PR equation.
- 7 - The PR equation underestimates liquid phase densities.

CHARACTERIZATION OF HYDROCARBONS

HEAVY FRACTIONS AND PSEUDOIZATION, A NEW METHOD

Equations of state have become an essential means of modeling the phase behavior of hydrocarbon systems. To model a hydrocarbon system accurately using an equation of state, a large number of components is usually used, which excessively increases the calculations. Also, an improper description of the physical properties of the heavy hydrocarbon fractions may result in erroneous predictions of the phase behavior of hydrocarbon system. Therefore, the problem is either one of lumping together the many experimentally determined fractions, or the converse of modeling the hydrocarbon system properly when the only experimental pieces of data available for the heptanes-plus fraction are the molecular weight and density. Several researchers have worked on the characterization of the hydrocarbon plus fractions and pseudoization.

Watson and Nelson⁵³ introduced two new concepts for the correlation of the physical properties of the heptanes-plus fraction. The molal average boiling point was used in all correlations involving the boiling point of the oil. They expressed, by the aid of a characterization factor, qualitative variations in physical properties with a change in the character of the oil. The characterization factor was defined as the ratio of the cubic root

of the molal average boiling point (in deg. R.) to the specific gravity. They conclude that this ratio changes from 12.5 for purely paraffinic fractions to 10.0 for highly cracked aromatic stocks. Later, Watson *et al*⁵⁴ extended that work to other hydrocarbon groups.

Edmister⁵⁵ introduced an improved integral technique for petroleum distillation calculations. Later, Taylor and Edmister⁵⁶ proposed a method by which it is possible to obtain rigorous solutions using a single set of equations which could be employed in a single computer program. In a more recent paper, Taylor and Edmister⁵⁷ demonstrated the capabilities and applications of their general solution in obtaining rigorous solutions for process handling of hydrocarbon fractions by means of the integral technique.

Lee *et al*⁵⁸ employed the physical reasoning that crude oil fractions, having relatively close physico-chemical properties, can accurately be represented by a single fraction. Having observed that the closeness of these properties are reflected by the slopes of curves when these properties are plotted against the weighted-averaged boiling point curve, they used the weighted sum of slopes of these curves as a criterion for lumping the crude oil fractions. Although this scheme results in a satisfactory lumping of some crude oil fractions, it lacks any theoretical basis. In addition, it requires large amounts of experimental data which normally are not available.

Whitson⁵⁹ developed some methods for characterizing the molar distribution and physical properties of petroleum fractions. The three parameter gamma probability function is used to characterize the molar distribution, as well as to fit experimental weight and molar distributions and to generate synthetic distributions of heptanes-plus fraction. Also, a regrouping scheme is introduced to reduce the extended analyses to only a few multiple carbon number groups.

Mehra *et al*⁶⁰ devised an algorithm which is based upon the minimization of the errors introduced in the predicted phase saturations. This algorithm requires the generation of a second derivative matrix of the phase saturation with respect to moles present at various expected reservoir conditions, which are then used to calculate the correlation coefficient matrix and to establish the criterion for combining reservoir constituents. Once that criterion is established, the properties of the pseudocomponents are determined by Kesler and Lee's mixing rule⁶¹. The efficiency of the proposed scheme is demonstrated through several examples.

Hong⁶² modified the method of Lee *et al*⁵⁸ for reducing the number of components without a significant loss of accuracy in describing the phase behavior. He suggested that the average carbon number could be used by itself as a lumping criterion, since most properties of a hydrocarbon fraction are related to the average molecular weight which in turn is related to the average carbon number. His trial and error procedure computes the phase diagram

using a small number of pseudocomponents. The number of components is systematically increased until a satisfactory match between predicted and experimental phase envelopes is achieved. This method could be quite time consuming depending upon the reservoir constituents and the prevailing operating conditions.

Schlijper⁶³ introduced a method which recognizes that a pseudo-component represents a mixture of components; and therefore has the thermodynamic behavior of a mixture rather than that of a single component. In this approach the standard expression for the potential is replaced by an adapted pseudo-potential.

Montel and Gouel⁶⁴ proposed an iterative clustering algorithm around mobile centers. Their algorithm classifies the given reservoir oil system into an optimum number of pseudo-components according to the equation of state considered. The procedure defines a mixed calculation of critical properties, and also suggests a criterion to choose between an accurate calculation of true critical properties and the classical mixing rules.

Ahmed *et al*⁶⁵ presented a generalized correlation for characterizing the hydrocarbon heavy fractions. Their method is based upon the detailed laboratory analysis of the thirty four hydrocarbon systems considered in their study. Their method is covered in detail in this work.

Beherns and Sandler⁶⁶ introduced a semicontinuous thermodynamic description to model heptanes-plus fraction for equation of state calculations. A semicontinuous fluid mixture consists of identifiable discrete components, include light hydrocarbons and

inorganic gases such as carbon dioxide and nitrogen, and a continuous distribution to represent all other components according to one of the properties such as boiling point. This is achieved by choosing an analytical distribution function, fitting the parameters of this to the oil fraction being modeled, and then assigning pseudocomponents corresponding to the Gaussian quadrature points (employed in their work). Later, the equation of state calculations are performed as if the system were composed of only discrete components.

Obut and Ertekin⁶⁷ introduced a method for splitting the heptanes-plus fractions and then evaluating their pseudocritical properties and interaction coefficients. First, the heavy fraction is split into a defined number of pseudocomponents, and starting values of binary interaction parameters and critical properties are obtained using available correlations and mixing rules. Then, a linear optimization technique is adopted for nonlinear applications by using iterative techniques considering the iterative variables being pseudocomponents properties and their binary interaction coefficients with butane. Tuned sets of these binary interaction parameters and critical properties are generated by using experimental depletion curve.

THE TECHNIQUE USED IN THIS WORK

Ahmed *et al's*⁶⁵ method for characterizing the hydrocarbon heavy fractions is employed in this work. By this method the heptanes-plus

fraction can be split into a predefined number of heavier hydrocarbon components. Then, Whitson's⁵⁹ approach is used for regrouping these components into groups of pseudocomponents. Kay's⁶⁸ mixing rules are then used to evaluate the properties of the pseudocomponents.

Background and Procedure

Lohrenz *et al*⁶⁹ proposed that the heptanes-plus fraction could be divided into a mixture of normal paraffin hydrocarbon from C₇ to C₄₀. The mole fraction of each hydrocarbon component is obtained as:

$$Z_n = Z_6 \exp\{ A (n - 6)^2 + B (n - 6) \}$$

$$n = 7, 8, \dots, N_c \quad \dots\dots\dots(74)$$

where:

$$N_c = 40$$

Considering the following two conditions:

$$Z_{7+} = \sum_{n=7}^{N_c} Z_n \quad \dots\dots\dots(75)$$

$$Z_{7+} * MW_{7+} = \sum_{n=7}^{N_c} (Z_n * MW_n) \quad \dots\dots\dots(76)$$

The constants A and B can be determined by substituting Eq. 74 into Eqs. 75 and 76, and then solving for A and B.

Pederson *et al*^{70,71} suggested that an exponential relationship exists between the mole fraction, Z_n , and the corresponding carbon number, C_n , of naturally occurring hydrocarbon mixtures for $C_n > 6$. That relationship is expressed as:

$$Z_n = (1 / B) \exp\{ C_n - A \} \dots\dots\dots(77)$$

The constants A and B of this equation are determined by the least squares fit to the experimental data.

Ahmed *et al*⁷² devised a method for splitting the C_{7+} of gas condensate systems into several pseudocomponents. They proposed a plot of the molecular weight ratios of (MW_{n+} / MW_{7+}) against the carbon number C_n , would produce a straight line for any condensate system. Each straight line would have a different slope according to the specific gravity of the heptanes-plus of that condensate system. That family of straight lines will meet at a common point at $(MW_{n+}/MW_{7+}, C_n) = (1,7)$. The slopes of these straight lines could be expressed as an exponential function of the specific gravity as:

$$\text{Slope} = 688.0563583 \exp\{ (- 11.46167654) (\gamma_{7+}) \} \dots\dots\dots(78)$$

Using this slope, the molecular weight of any plus fraction is calculated as:

$$MW_{n+} = MW_{7+} * (1 + slope (C_n - 7)) \dots\dots\dots(79)$$

From Eqs. 74 and 75, the mole fraction Z_n can be calculated at a progressively higher carbon number until the sum of the calculated mole fraction is equal to the mole fraction of the C_{7+} in the system.

Ahmed *et al*⁶⁵ proposed a new method to split the heavy fraction based on a generalized correlation which was developed using a data base consisted of 34 condensate and oil systems. In their approach, based on the laboratory data available, an average molecular weight of each plus fraction is calculated from the equation:

$$MW_{n+} = ((Z_{7+} - \sum_{i=7}^{n-2} Z_i) * MW_{(n-1)+} - Z_{n-1} * MW_{n-1}) / Z_{n+} \dots\dots\dots(80)$$

Then, the calculated average molecular weights of the plus fractions are plotted against the number of carbon atoms (C_n). Two distinct groups of smooth curves are obtained, each corresponding to a different hydrocarbon system. They approximated this family of curves by a series of two-segment straight lines having the generalized equation:

$$MW_{n+} = MW_{7+} + S * (C_n - 7) \dots\dots\dots(81)$$

where:

C_n = number of carbon atoms.

S = slope

From the plots, the values of the slope "S" for each segment of the straight lines are:

| C_n | <u>Condensate Systems</u> | <u>Crude Oil Systems</u> |
|-------|---------------------------|--------------------------|
| = 8 | 15.50 | 16.50 |
| > 8 | 17.00 | 20.10 |

Prediction of the Molar Distribution

In this approach the only input data required are the molecular weight and the total mole fraction of the heptanes-plus fraction. The mole fractions are progressively calculated for higher carbon numbers. This extraction process continues until the sum of the mole fractions of the pseudocomponents equals to the total mole fraction of the heptanes-plus. Considering the following equations:

$$Z_{n+} = Z_n + Z_{(n+1)+} \dots \dots \dots (82)$$

$$Z_{n+} * MW_{n+} = Z_n * MW_n + Z_{(n+1)+} * MW_{(n+1)+} \dots \dots \dots (83)$$

Solving Eqs. 82 and 83 for Z_n , yields the following final expression:

$$Z_n = Z_{n+1} * (MW_{(n+1)+} - MW_{n+}) / (MW_{(n+1)+} - MW_n)$$

.....(84)

REGROUPING SCHEME

Whitson⁵⁹ proposed a method for estimating the number of multiple carbon number (MCN) groups needed for adequate plus-fraction description as well as which single carbon number (SCN) groups belong to each of the MCN groups. The number of MCN groups, N_g , can be estimated by:

$$N_g = \text{Int}[1.0 + 3.3 \log(N - n)]$$

.....(85)

where:

n : first SCN.

N : last SCN.

For black oil systems, this number probably can be reduced by one.

The molecular weights separating each MCN group are estimated as:

$$MW_I = MW_n * \{ \exp[(1.0 / N_g) * \ln(MW_N / MW_n)] \}^I$$

$$I = 1, 2, \dots, N_g \quad \dots \dots \dots (86)$$

MW_N : Molecular weight of the last SCN group (may be of a plus-fraction).

MIXING RULES

Molar, volumetric, and critical properties as well as acentric factors of MCN groups are calculated using Kay's⁷² mixing rules, as follows:

$$MW_I = \sum^I (z_i / Z_I) MW_i \quad \dots \dots \dots (87)$$

$$\gamma_{pcI} = 1.0 / \{ \sum^I (fw_i / fw_I) \gamma_{ci} \}$$

$$\dots \dots \dots (88)$$

$$V_{pcI} = \sum^I (fw_i / fw_I) V_{ci} \quad \dots \dots \dots (89)$$

$$P_{pcI} = \sum^I (z_i / Z_I) T_{ci} \quad \dots \dots \dots (90)$$

$$T_{pcI} = \sum^I (z_i / Z_I) T_{ci} \quad \dots \dots \dots (91)$$

$$T_{bI} = \sum^I (z_i / Z_I) T_{bi} \dots\dots\dots(92)$$

$$\omega_I = \sum^I (z_i / Z_I) \omega_i \dots\dots\dots(93)$$

Where Z_I and fw_I are the summations of z_i and fw_i found in MCN group I.

A MODIFIED K-VALUE METHOD

The method developed in this study is basically aimed at calculating the K-values for carbon dioxide-hydrocarbon systems using a simplified correlation, provided that the correlation maintain these conditions:

- (1) yields accurate results,
- (2) has good and valid theoretical basis, and
- (3) takes less computer time than the equations of state.

Therefore, it was thought that modifying Hoffmann *et al's* approach could be potentially important in fulfilling the required conditions. The approach documented in SSC N-Comp documentations (1971)⁷³, which was based on the same concept of Hoffmann *et al's* approach, is followed in this study.

Theoretical Background of The Modified Approach

From the theory of ideal and non-ideal solutions, we can conclude the following analysis:

1 - For ideal solutions, we have:

1.1 - Raoult's law is expressed as:

$$P_i = x_i P_i^{\circ} \quad \dots\dots\dots(94)$$

$$\begin{aligned}
 P &= \sum_{i=1}^{Nc} P_i \\
 &= \sum_{i=1}^{Nc} x_i P_i^{\circ} \quad \dots\dots\dots(95)
 \end{aligned}$$

1.2 - Dalton's law of partial pressures is expressed as:

$$P_i = y_i P \quad \dots\dots\dots(96)$$

$$\begin{aligned}
 y_i &= P_i / P \\
 &= x_i P_i^{\circ} / \sum_{i=1}^{Nc} x_i P_i^{\circ} \\
 &= x_i (P_i^{\circ} / P) \quad \dots\dots\dots(97)
 \end{aligned}$$

2 - For any solution, we have:

$$y_i = K_i x_i \quad \dots\dots\dots(98)$$

By comparing Eqs. 97 and 98, we note that for hydrocarbon solutions at low pressures which are considered ideal, we have:

$$K_i = P_i^{\circ} / P$$

$$K_i p = p_i^\circ \quad \dots\dots\dots(99)$$

From the plot of $\log(K_i)$ vs. $\log(p)$, Fig. 8 as an example, we note that at low pressures (at pressures below 100 psia) the isotherm is linear, and that the slope of each isotherm is calculated as:

$$\begin{aligned} \text{Slope} &= [\log(K_1) - \log(K_2)] / [\log(p_1) - \log(p_2)] \\ &= \log(K_1 / K_2) / \log(p_1 / p_2) \\ &= \log[(p^\circ / p_1) / (p^\circ / p_2)] / \log(p_1 / p_2) \\ &= \log(p_2 / p_1) / \log(p_1 / p_2) \\ &= - 1.0 \quad \dots\dots\dots(100) \end{aligned}$$

From Eq. 100, we conclude that:

$$\begin{aligned} \log(K_i) &= - \log(p) + \text{constant} \\ \log(K_i p) &= \text{constant} \quad \dots\dots\dots(101) \end{aligned}$$

From Eqs. 99 and 101 we note the analogy between the product ($K p$) and the vapor pressure p° . Since the plot of $\log(p_i^\circ)$ vs. $(1/T)$ is almost a straight line over a reasonable range of temperatures (Cox chart)⁴⁶, and that for all hydrocarbons these straight lines converge to a common point of intersection which is known as the point of convergence, it was suggested that those lines be rotated into a single common line by appropriate changes in slope when employing a single constant for each line.

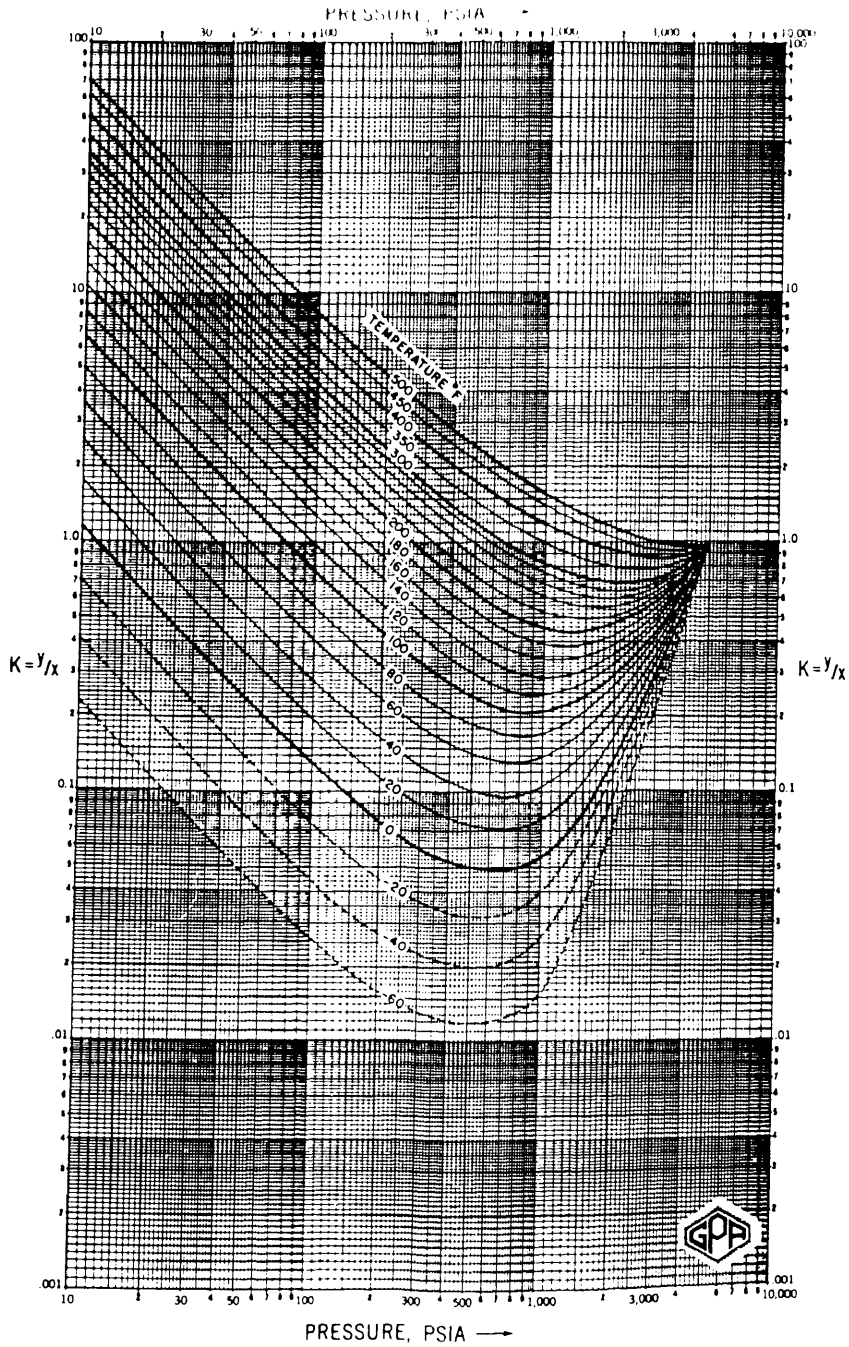


Fig. 8 - Typical K-value chart.
(after Ref. 17)

From the Clausius-Clapeyron equation:

$$\ln(p_2^\circ/p_1^\circ) = (\Delta H_m / R) (1 / T_1 - 1 / T_2)$$

.....(102)

Or,

$$(\Delta H_m / R) \log(e) = \log(p_2^\circ/p_1^\circ) / (1 / T_1 - 1 / T_2)$$

.....(103)

Since we have the two conditions:

$$(1) \quad T_1 = T_B$$

$$p_1 = 14.7 \text{ psia.} \quad \text{.....(104)}$$

$$(2) \quad T_2 = T_C$$

$$p_2 = p_c \quad \text{.....(105)}$$

and introducing the constant b for each hydrocarbon, we can get this expression:

$$b = (\Delta H_m / R) \log(e)$$

$$= \log(p_c / 14.7) / (1 / T_B - 1 / T_C)$$

.....(106)

Now, we can express the Clausius-Clapeyron equation as:

$$\text{Log}(p_2^\circ / p_1^\circ) = b (1 / T_1 - 1 / T_2) \dots\dots\dots(107)$$

If we apply again condition (1), $T_1 = T_B$ at $p_1 = 14.7$, then we get:

$$\text{Log}(p_2^\circ / 14.7) = b (1 / T_B - 1 / T_2) \dots\dots\dots(108)$$

Or simply as:

$$\text{Log}(p^\circ) = b (1 / T_B - 1 / T) + \text{log}(14.7) \dots\dots\dots(109)$$

Therefore, the approach is to construct a single vapor pressure curve for all hydrocarbons by plotting $\text{log}(p^\circ)$ vs. F , Fig. 9, where F is the characterization factor expressed by the equation:

$$F = b (1 / T_B - 1 / T) \dots\dots\dots(110)$$

and b is the factor required for each hydrocarbon to rotate its vapor pressure curve to the common line, which has been described by Eq. 106. We can simply express Eqs. 109 and 110 as:

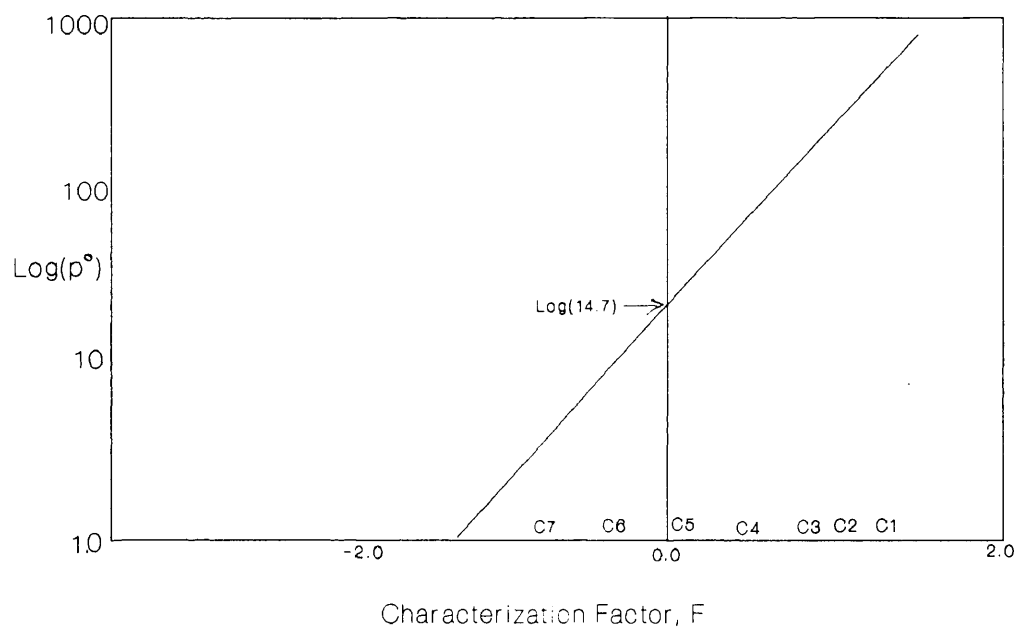


Fig. 9 - Vapor pressure vs. Characterization Factor Plot.

$$\text{Log}(p_i^\circ) = F_i + \log(14.7) \dots\dots\dots(111)$$

The slope of this line is equal to unity on the semi-log scale, and the intercept is equal to $\log(14.7)$ (see Fig. 9). It is worth mentioning that the linear relationship expressed by Eq. 111 applies for all hydrocarbons over wide ranges of temperatures.

Extension of This Approach For K-Value Predictions

Now, if we look at the plot of $\log(K p)$ vs. F , Fig. 10, the slope of any pressure line is calculated as:

$$\begin{aligned} \text{Slope} &= \log(K_i p / K_{i-1} p) / (F_i - F_{i-1}) \\ &= \log(K_i p / p_k) / (F_i - F_k) \\ &\dots\dots\dots(112) \end{aligned}$$

or the K-values are expressed as:

$$K_i = (p_k / p) 10^{(F_i - F_k) \text{ slope}} \dots\dots\dots(113)$$

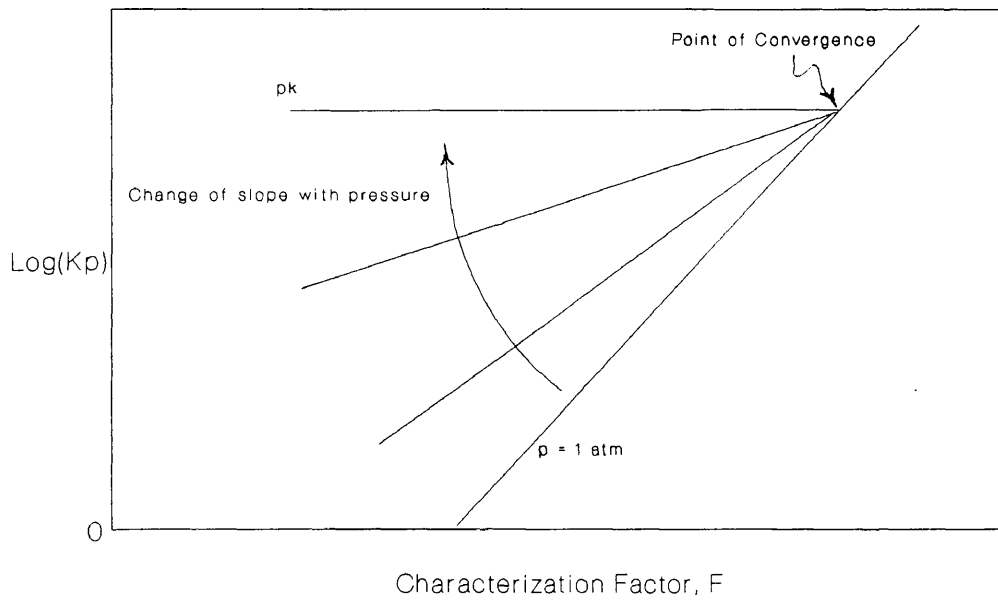


Fig. 10 - Change of K-value Slope with Pressure.

Theoretical Slope (Linear Form of The Slope): The slope in both Eqs. 112 and 113 could be expressed as a linear function of pressure as:

$$\text{Slope} = a_0 + a_1 p \quad \dots\dots\dots(114)$$

To calculate the coefficients a_0 and a_1 , we need two conditions which are:

$$(1) \text{ At } p = 0.0$$

$$\text{slope} = a_0$$

i.e.:

$$a_0 = 1.0 \quad \dots\dots\dots(115)$$

Since a_0 is calculated as the slope of $\log(p^\circ)$ vs. F which is equal to unity.

$$(2) \text{ At } p = p_k$$

$$\text{slope} = 0.0$$

i.e.:

$$\begin{aligned} a_1 &= - a_0 / p_k \\ &= - 1.0 / p_k \quad \dots\dots\dots(116) \end{aligned}$$

So, the slope of the K-value correlation can be expressed as:

$$\begin{aligned} \text{slope} &= a_0 (1.0 - p / P_k) \\ \text{slope} &= (1.0 - p / P_k) \dots\dots\dots(117) \end{aligned}$$

Therefore, we can use Eqs. 113 and 117 to calculate the equilibrium ratios (K-values) with good accuracy over a reasonable range of pressures and temperatures.

Polynomial Form of the Slope (Cubic Form): Another modification to Eq. 113 is to consider the slope as a polynomial function of (p / P_k) . If we consider a cubic form, then:

$$\begin{aligned} \text{slope} &= a_0 + a_1 (p / P_k) + a_2 (p / P_k)^2 + a_3 (p / P_k)^3 \\ &\dots\dots\dots(118) \end{aligned}$$

For Eq. 118, when the conditions 1 and 2 are applied, we get

$$\begin{aligned} (1) \text{ At } p &= 0.0 \\ \text{slope} &= a_0 \\ &= 1.0 \dots\dots\dots(116) \end{aligned}$$

$$\begin{aligned} (2) \text{ At } p &= P_k \\ \text{slope} &= 0.0 \end{aligned}$$

$$\begin{aligned}
 a_1 + a_2 + a_3 &= - a_0 \\
 &= - 1.0 \\
 &\dots\dots\dots(119)
 \end{aligned}$$

Now, to evaluate the coefficients a_1 , a_2 and a_3 , considering Eq. 119, by trial and error we run the PVT model using different values of these coefficients until an acceptable match with the PVT data is obtained. Then the slope is evaluated by substituting into Eq. 118 with the coefficients which produced the best match.

Another approach for estimating these coefficients is to use the Least Squares-Linear Programming model to automatically calculate the optimal coefficients that minimize the error between the experimental and calculated PVT data. The procedure is summarized as follows:

- (1) Run the PVT model several times, each time with different group of parameters which are randomly estimated, and then calculate the error norm between the experimental and calculated behavior for each run.
- (2) Calculate the optimal coefficients by using the optimization model (LSLP).
- (3) Substitute with these coefficients into Eq. 118 to compute the slope. Detailed formulation and documentation of the optimization approach is available in Appendix B.

Modification of the Approach for Compositional Changes

Normally in the phase behavior of the hydrocarbon systems with changes in temperature and pressure along with the injection of miscible gases, such as carbon dioxide or nitrogen, and the production of the reservoir fluid, major changes in the overall composition of the reservoir fluid constantly take place. As a result, the convergence pressure of the reservoir fluid system continuously changes, particularly with the changes of the mole fractions of the intermediate hydrocarbons in the system. On the semi-log plot of $(K p)$ vs. F , as shown in Fig. 11, the point of convergence (pivot) moves continuously as the composition of the fluid mixture changes. In order to account for these compositional changes and their effect on the system's convergence pressure, a new expression is introduced to relate the change in the convergence pressure with the change of the intermediate hydrocarbons overall mole fraction. That expression takes the form:

$$P_k - P_{kr} = b_0 + b_1 (\Delta C_I) + b_2 (\Delta C_I)^2 + b_3 (\Delta C_I)^3$$

.....(120)

where:

- P_{kr} : Convergence pressure at reference conditions.
- ΔC_I : Change in mole fraction of intermediate hydrocarbons (C_2-C_6), from reference conditions.
- $\Delta C_I = C_I - C_{Ir}$

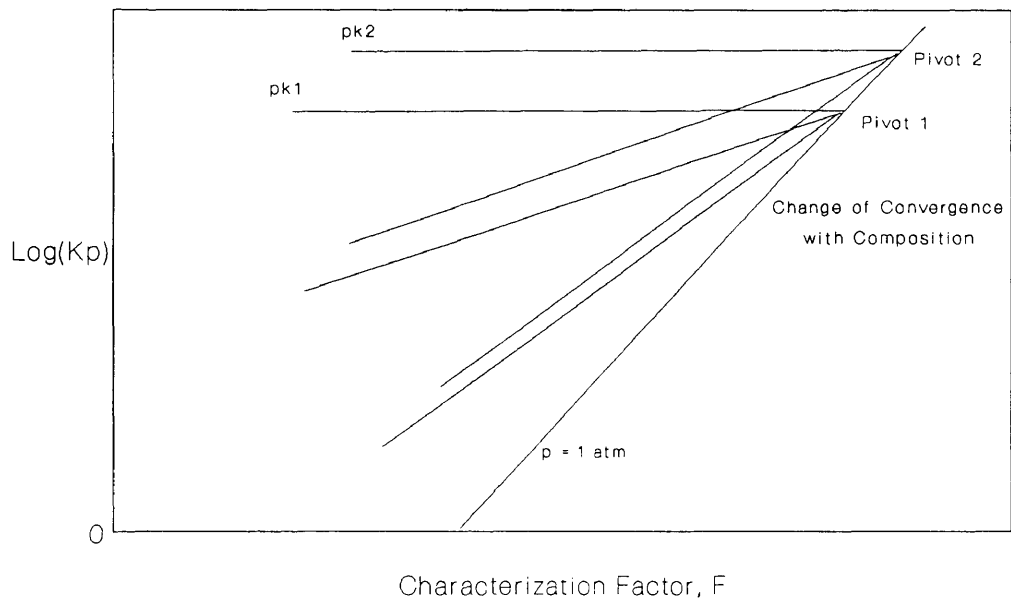


Fig. 11 - Change of K-values Pivot with Composition.

The coefficients b_0 , b_1 , b_2 and b_3 are calculated following either one of the approaches of calculating the slope coefficients.

Input Parameters for This Method: The input parameters for this method are:

- 1) Convergence pressure, p_k .
- 2) Characterization factors, $F_i = f(T_{bi}, T_{ci}, P_{ci})$.
- 3) Slope coefficients, a_0, a_1, a_2, a_3, a_4 .
- 4) Change in p_k function coefficients, b_0, b_1, b_2, b_3 .

RESULTS

The PVT program developed in this study was run using the K-value method and the three equations of state. Nine sets of hydrocarbon mixtures were used to test and validate the K-value method. Each fluid sample composition was represented in the PVT program by 12 components. The heptane plus of each sample was split into four pseudocomponents, using the new approach of characterization of heavy hydrocarbons "CPLUS model" developed in this work. Convergence pressures were computed by Standing's equation for oil samples or by Besserer's equation for gas condensates.

Nolen's commercial PVT package⁷⁴ was used to run the same test cases, to verify the developed model and validate the K-value method. The results obtained are graphically represented as comparisons between the K-value method and the equations of state.

Case No. 1

The first fluid sample is gas condensate. This sample has a convergence pressure of 5,500 psia, reservoir temperature of 200 °F and dew point pressure of 3,428 psig. Constant composition expansion and constant volume depletion tests were simulated. The data are available in Tables C-1 through C-5. The simulation study did not include the solubility and swelling test for this sample because of the injection of lean gas into a gas condensate system, which was not suitable to use in the model.

The simulation results obtained are graphically represented as comparisons between the K-value method and the equations of state in Figs. 12 through 19. The matching parameters are summarized in Table 3. The average deviations between the experimental and calculated results are summarized in Table 4 in next section.

Case 1

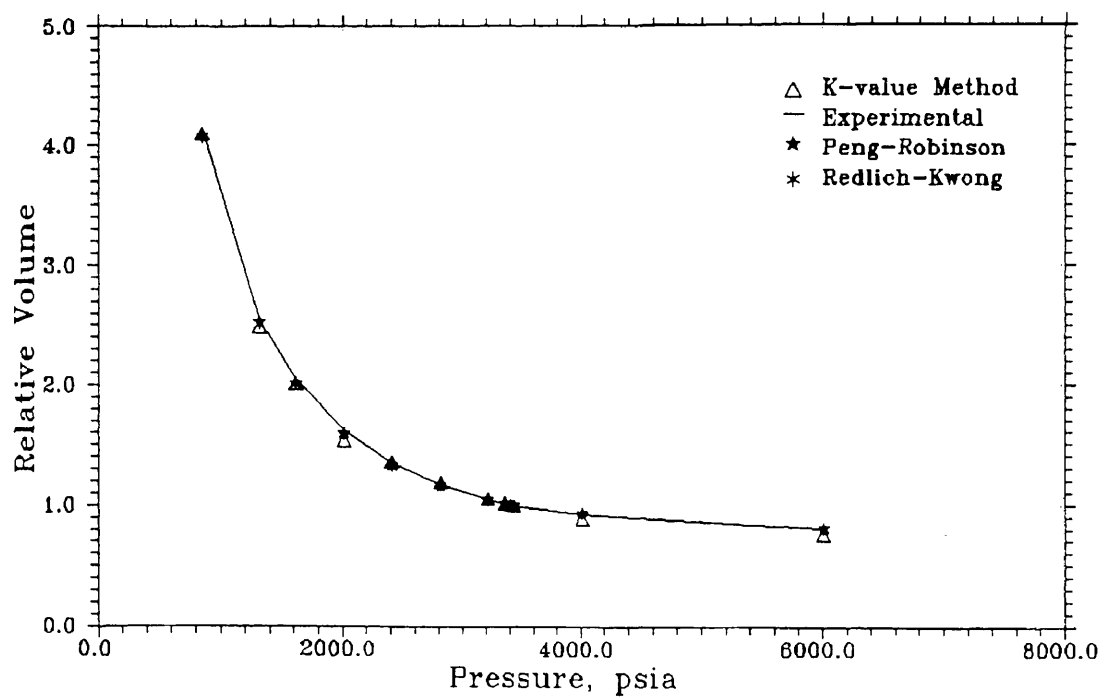


Fig. 12 - Constant Composition Expansion of Case 1:
Relative Volume vs. Pressure,
The K-value Method against Eqns. of State.

Case 1

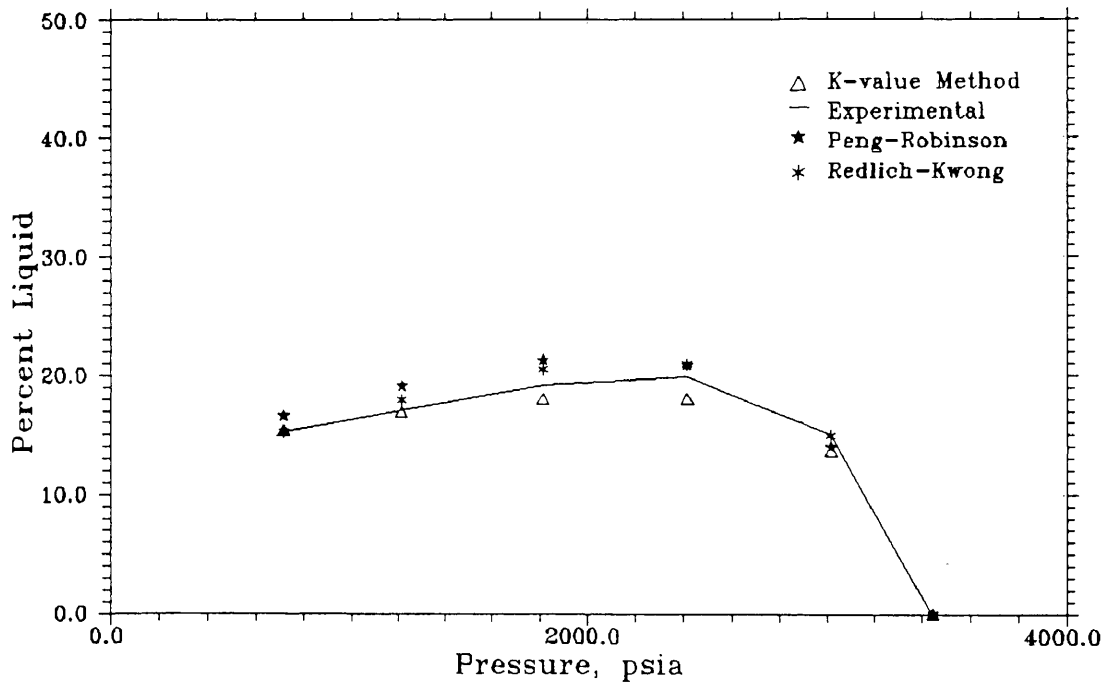


Fig. 13 - Constant Volume Depletion of Case 1:
Percent Liquid vs. Pressure,
The K-value Method against Eqns. of State.

Case 1

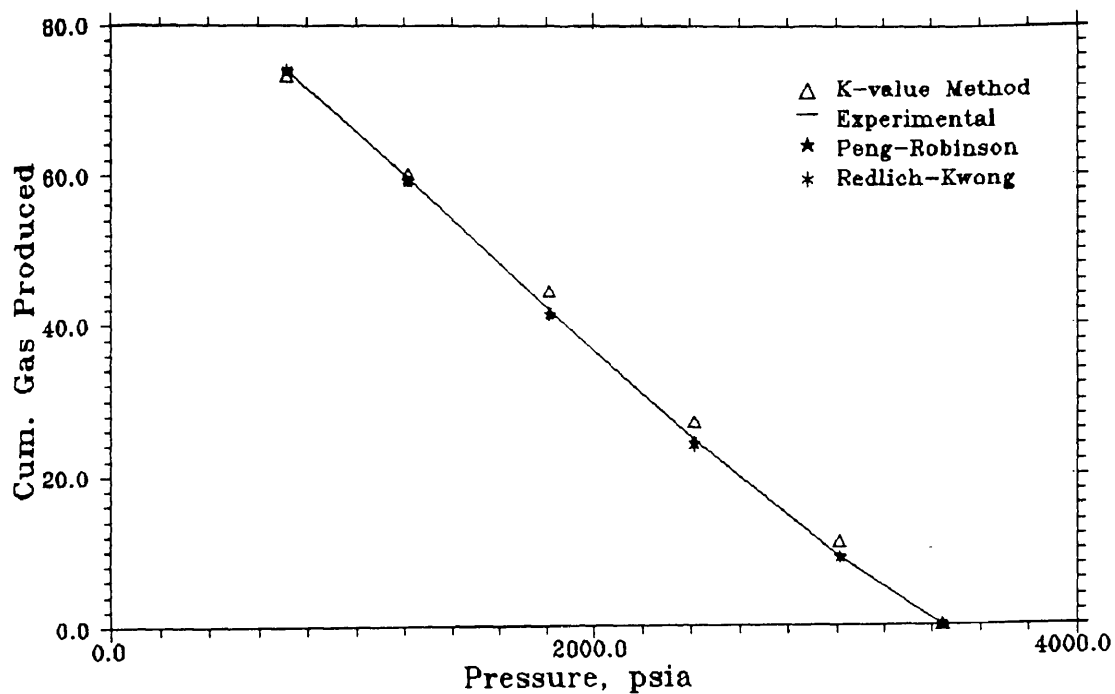


Fig. 14 - Constant Volume Depletion of Case 1:
Cum. Gas Produced vs. Pressure,
The K-value Method against Eqns. of State.

Case 1

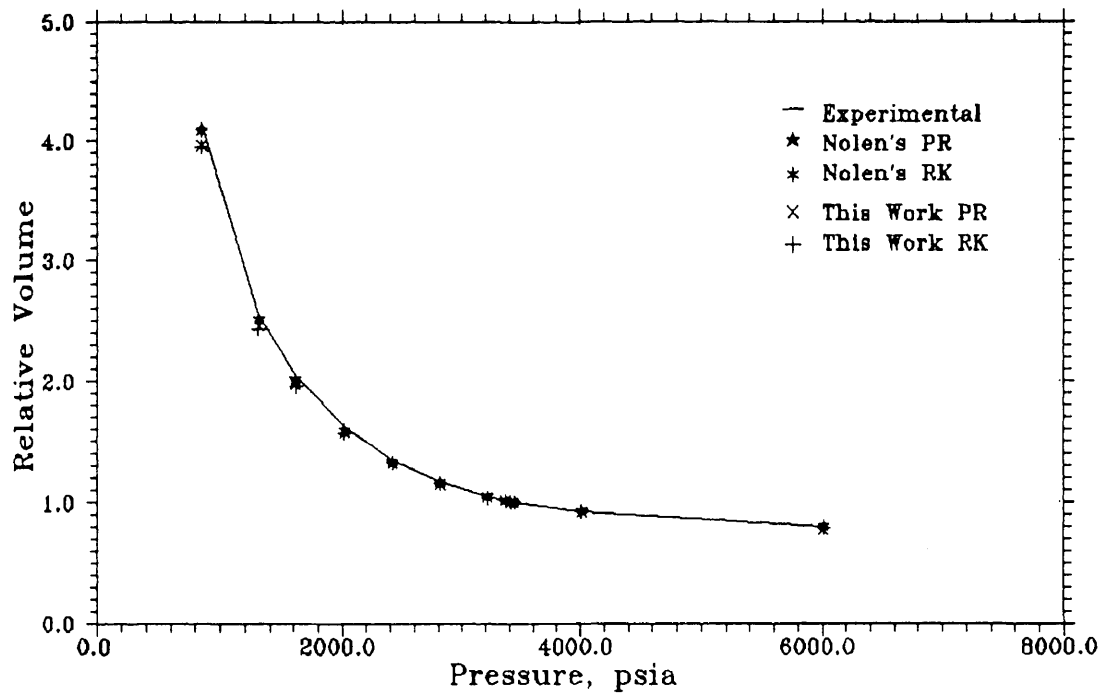


Fig. 15 - Constant Composition Expansion of Case 1:
Relative Volume vs. Pressure,
Nolen's against This Model's Eqns. of State.

Case 1

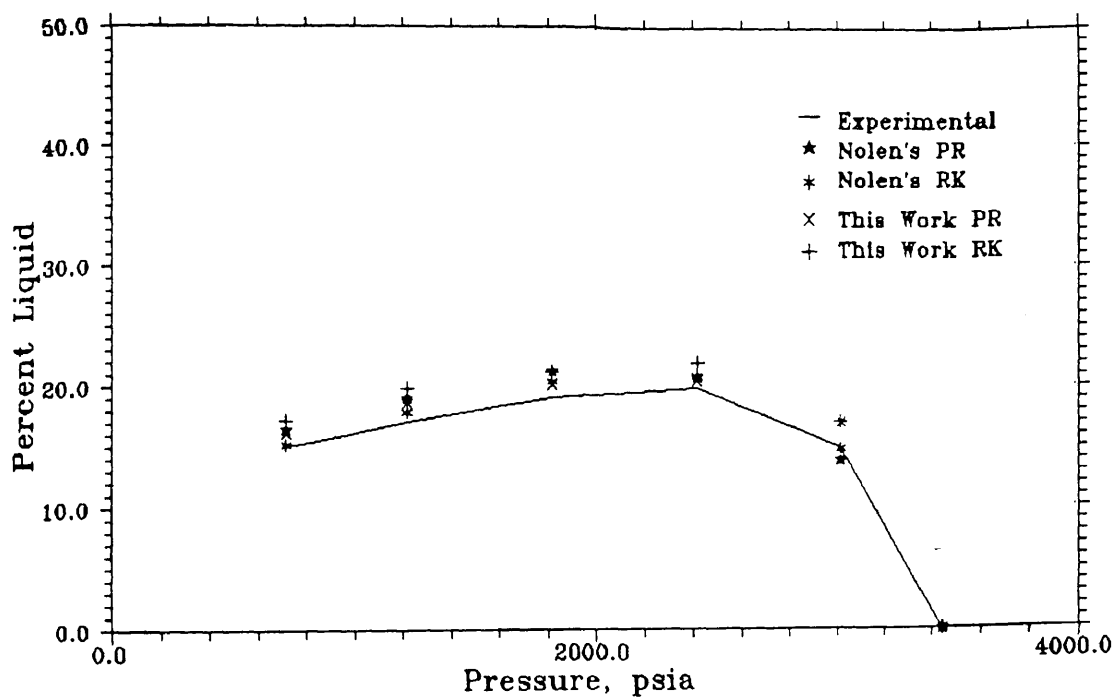


Fig. 16 - Constant Volume Depletion of Case 1:
Percent Liquid vs. Pressure,
Nolen's against This model's Eqns. of State.

Case 1

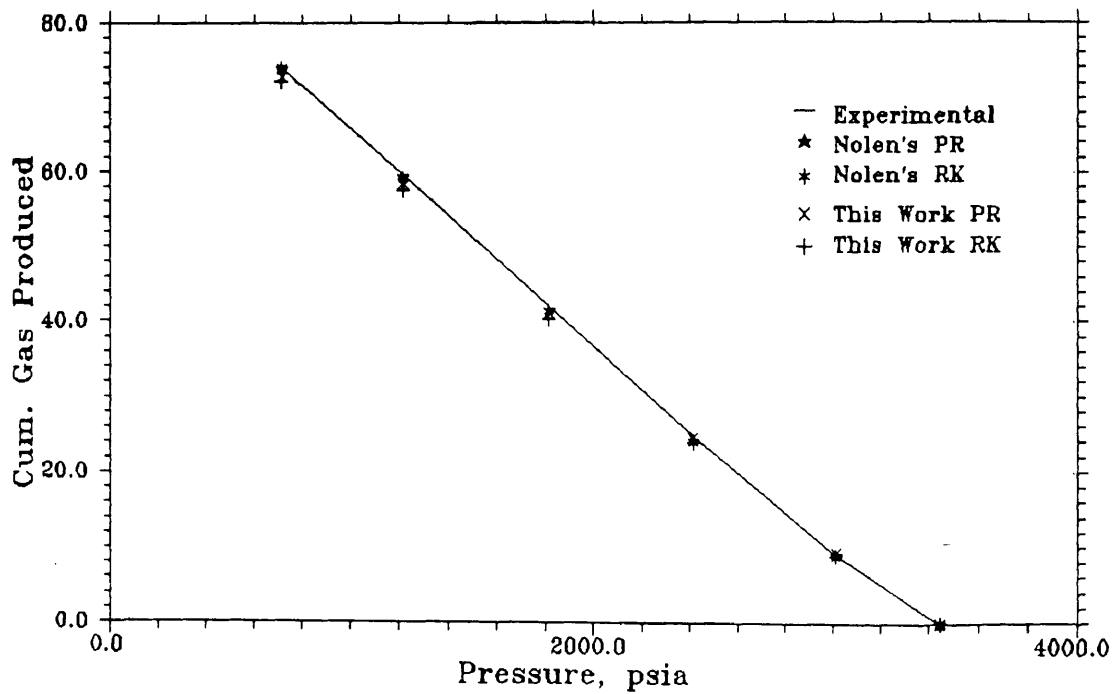


Fig. 17 - Constant Volume Depletion of Case 1:
Cum. Gas Produced vs. Pressure,
Nolen's against This Model's Eqns. of State.

Case 1

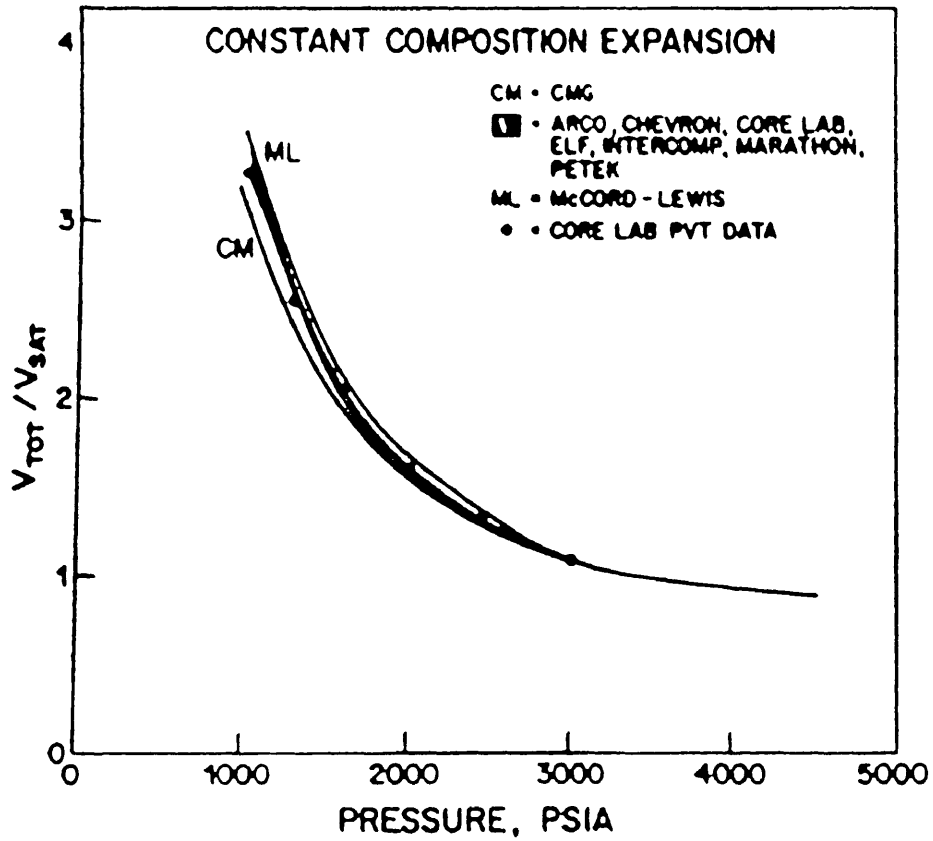


Fig. 18 - Constant Composition Expansion of Case 1:
 Relative Volume vs. Pressure,
 SPE 3rd Comparative Project.

Case 1

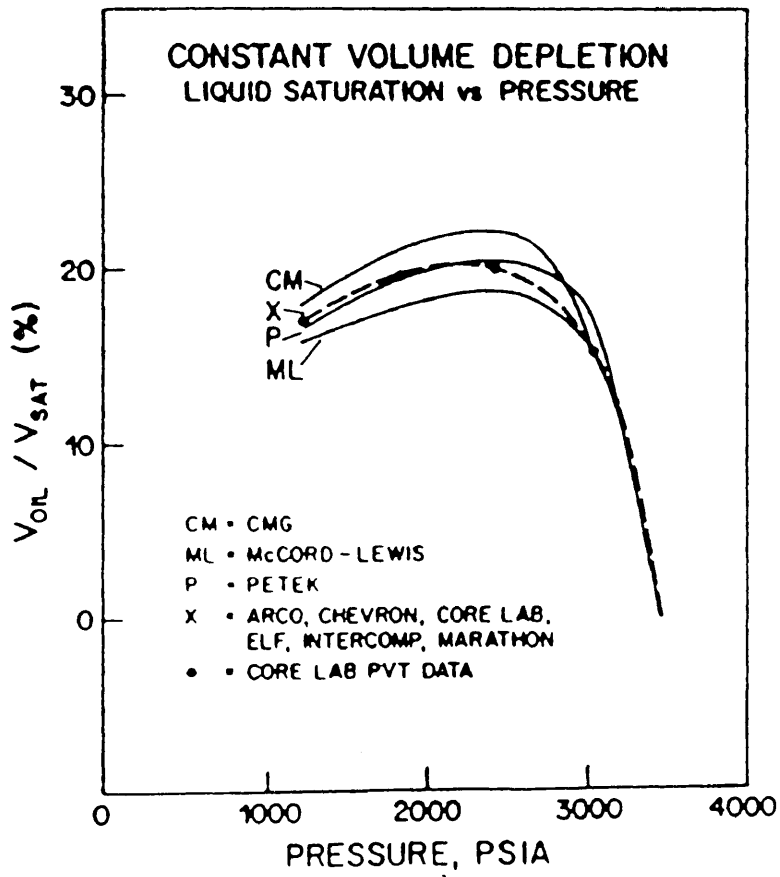


Fig. 19 - Constant Volume Depletion of Case 1:
Percent Liquid vs. Pressure,
SPE 3rd Comparative Project.

Case No. 2

The second fluid sample is rich gas condensate. This sample has a convergence pressure of 8,180 psia, reservoir temperature of 280 °F and dew point pressure of 6,750 psig. The data included only the constant volume depletion test. The data are available in Tables C-6 and C-7.

The simulation results obtained are graphically represented as comparisons between the K-value method and the equations of state in Figs. 20 and 21. The matching parameters are summarized in Table 3. The average deviations between the experimental and calculated results are summarized in Table 4 in next section.

Case 2

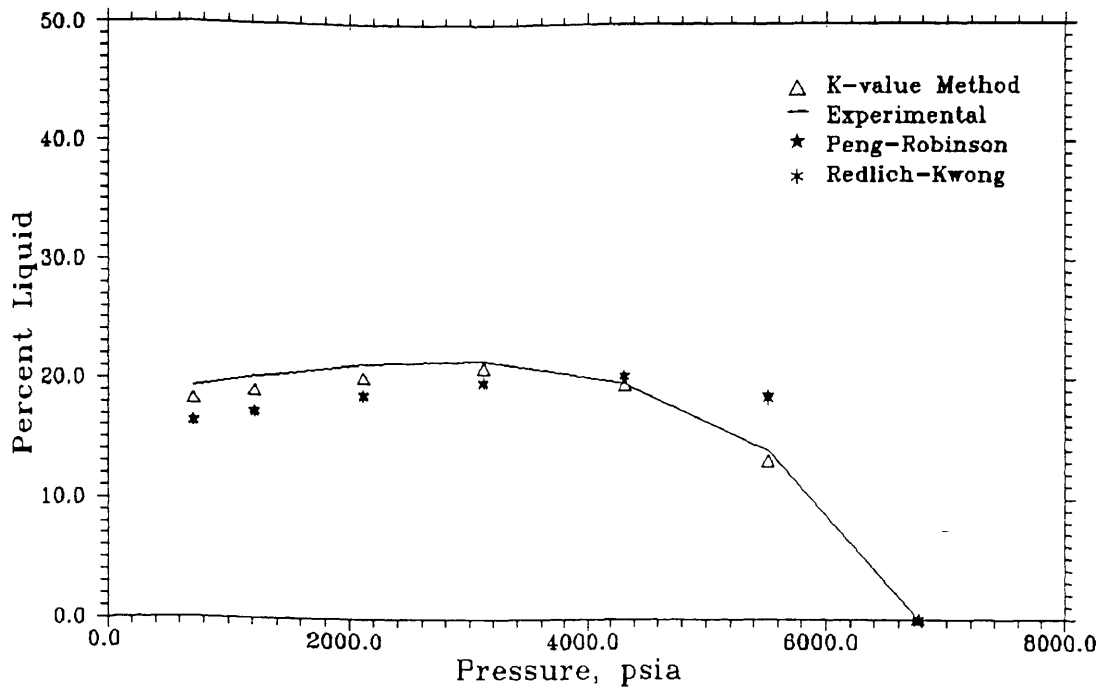


Fig. 20 - Constant Volume Depletion of Case 2:
 Percent Liquid vs. Pressure,
 The K-value Method against Eqns. of State.

Case 2

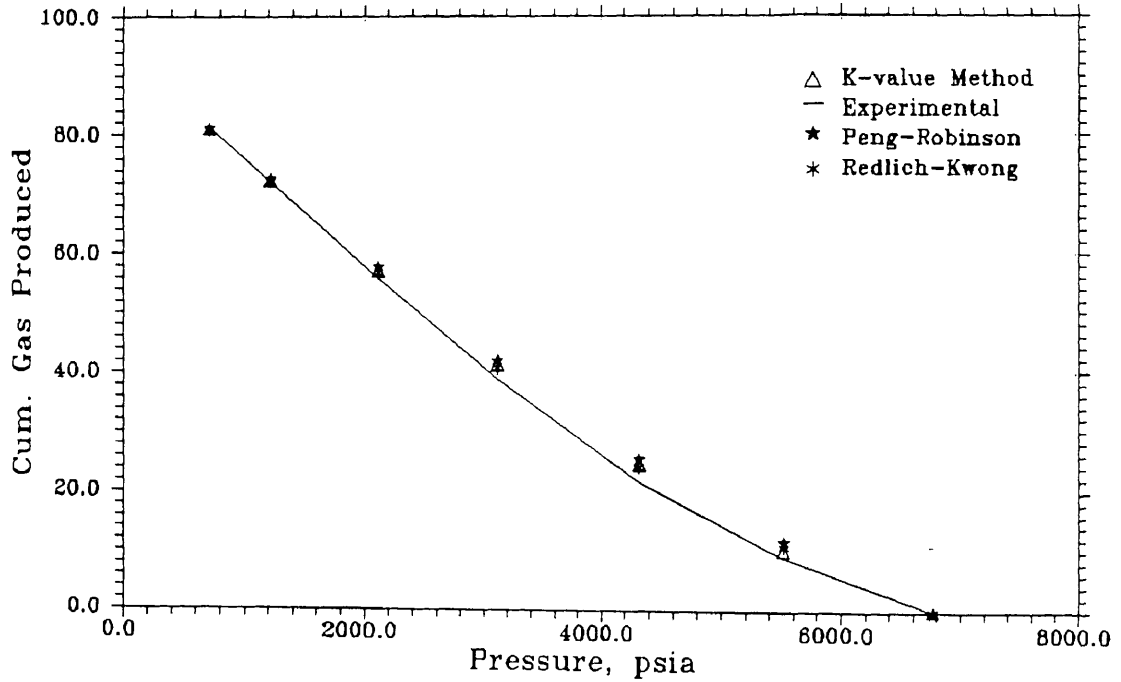


Fig. 21 - Constant Volume Depletion of Case 2:
Cum. Gas Produced vs. Pressure,
The K-value Method against Eqns. of State.

Case No. 3

The third fluid sample is oil. This sample has a convergence pressure of 9,500 psia, reservoir temperature of 225 °F and bubble point pressure of 1,500 psig. Constant composition expansion and solubility and swelling tests were simulated. The data are available in Tables C-8 through C-11. The simulation study included the solubility and swelling test for two types of injection gases. The first was pure carbon dioxide, and the second was a mixture of 50% carbon dioxide and 50% nitrogen.

The simulation results obtained are graphically represented as comparisons between the K-value method and the equations of state in Figs. 22 through 26. The matching parameters are summarized in Table 3. The average deviations between the experimental and calculated results are summarized in Table 4 in next section.

Case 3

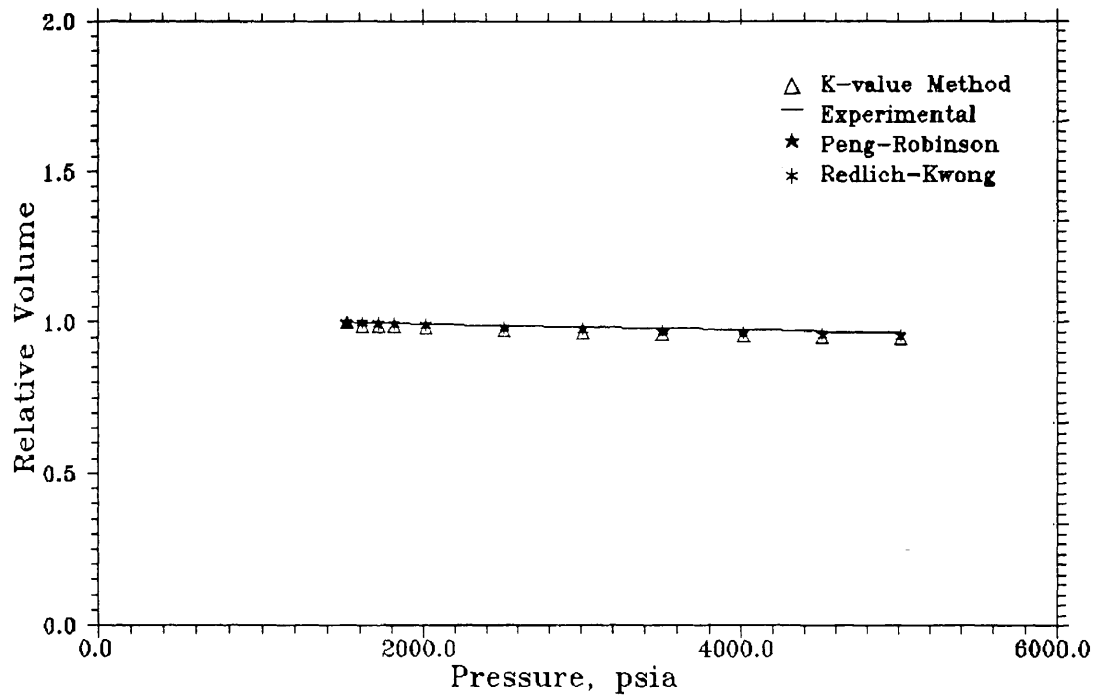


Fig. 22 - Constant Composition Expansion of Case 3:
Relative Volume vs. Pressure,
The K-value Method against Eqns. of State.

Case 3

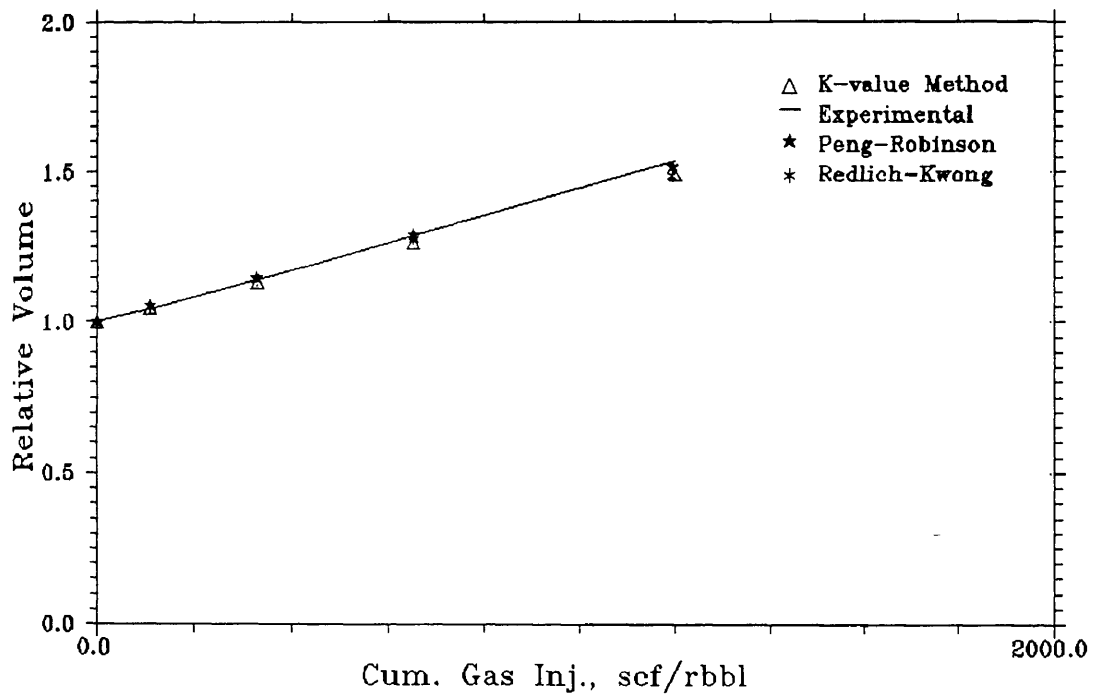


Fig. 23 - Solubility and Swelling of Case 3:
Relative Volume vs. Cum. CO₂ Injected,
The K-value Method against Eqns. of State.

Case 3

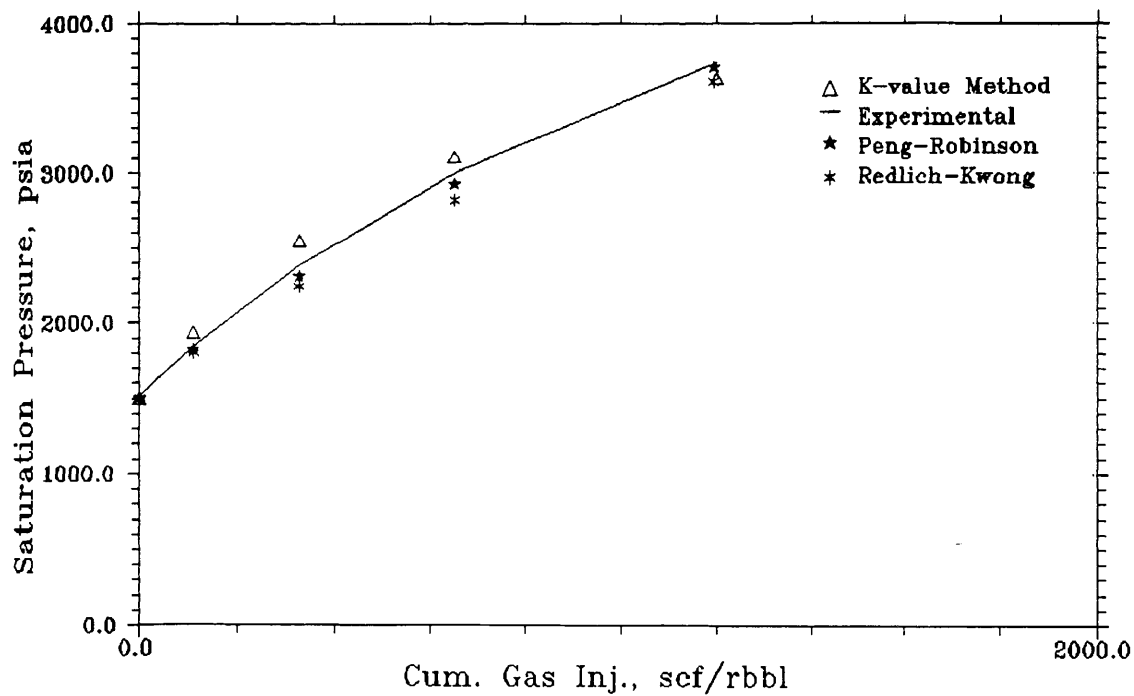


Fig. 24 - Solubility and Swelling of Case 3:
Sat. Press. vs. Cum. CO₂ Injected,
The K-value Method against Eqns. of State.

Case 3

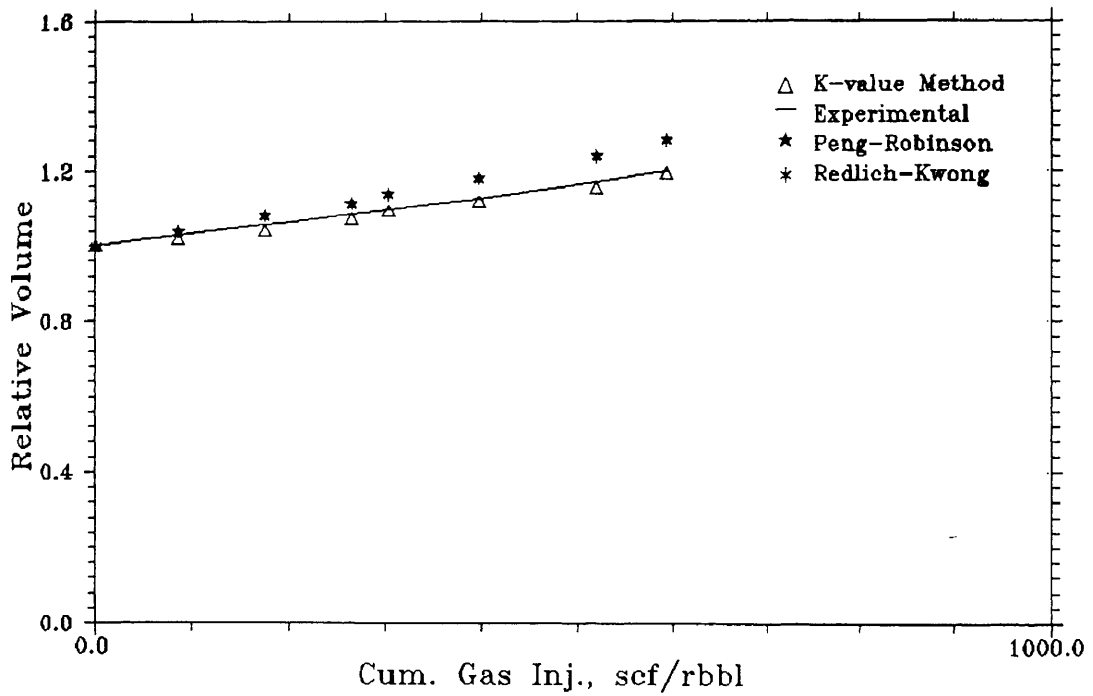


Fig. 25 - Solubility and Swelling of Case 3:
Relative Volume vs. Cum. N_2+CO_2 Injected,
The K-value Method against Eqns. of State.

Case 3

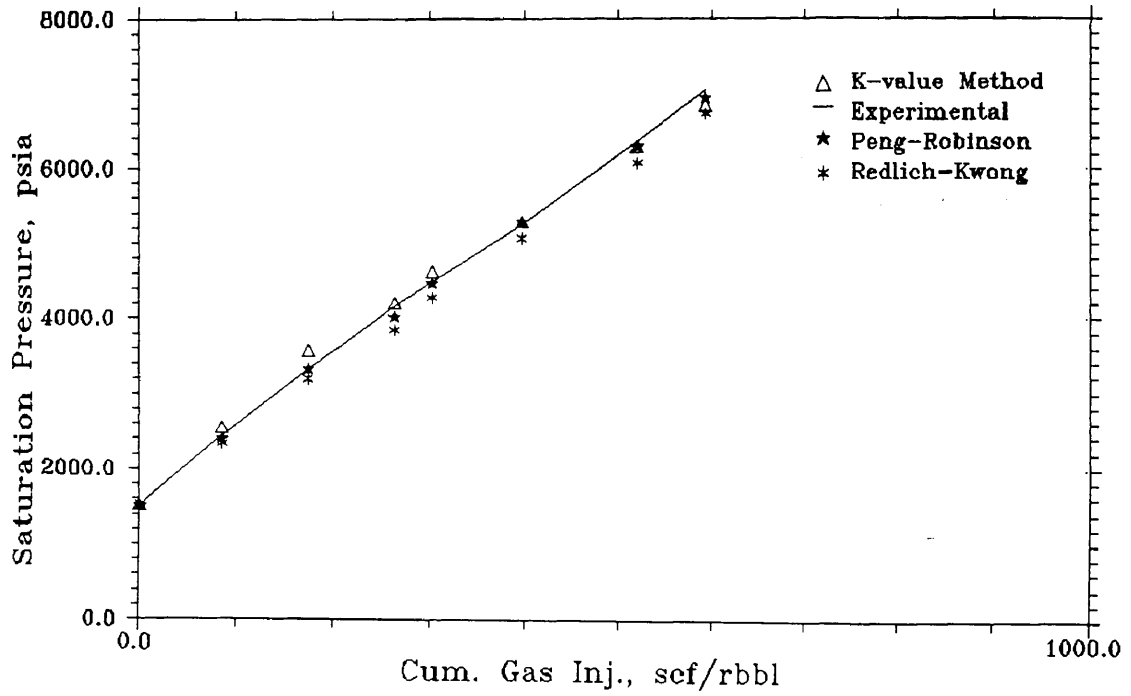


Fig. 26 - Solubility and Swelling of Case 3:
 Sat. Press. vs. Cum. N_2+CO_2 Injected,
 The K-value Method against Eqns. of State.

Case No. 4

The fourth fluid sample is oil. This sample has a convergence pressure of 13,560 psia, reservoir temperature of 110 °F and bubble point pressure of 215 psig. Constant composition expansion and solubility and swelling tests were simulated. The data are available in Tables C-12 through C-14. The simulation study included the solubility and swelling test for pure carbon dioxide.

The simulation results obtained are graphically represented as comparisons between the K-value method and the equations of state in Figs. 27 through 29. The matching parameters are summarized in Table 3. The average deviations between the experimental and calculated results are summarized in Table 4 in next section.

Case 4

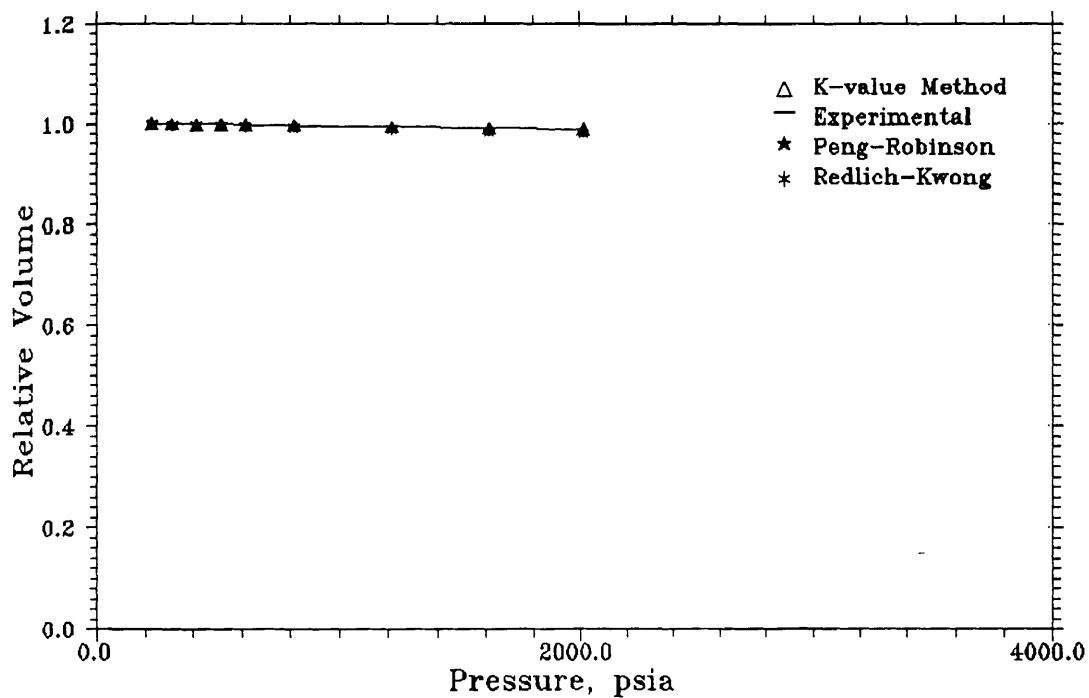


Fig. 27 - Constant Composition Expansion of Case 4:
Relative Volume vs. Pressure,
The K-value Method against Eqns. of State.

Case 4

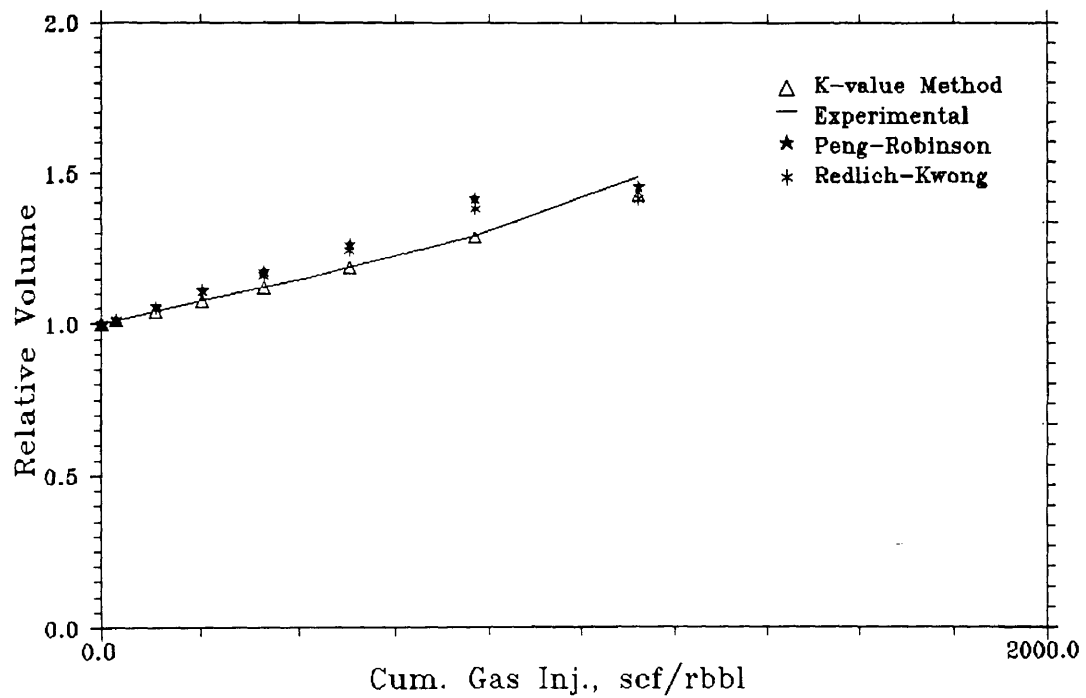


Fig. 28 - Solubility and Swelling of Case 4:
Relative Volume vs. Cum. CO₂ Injected,
The K-value Method against Eqns. of State.

Case 4

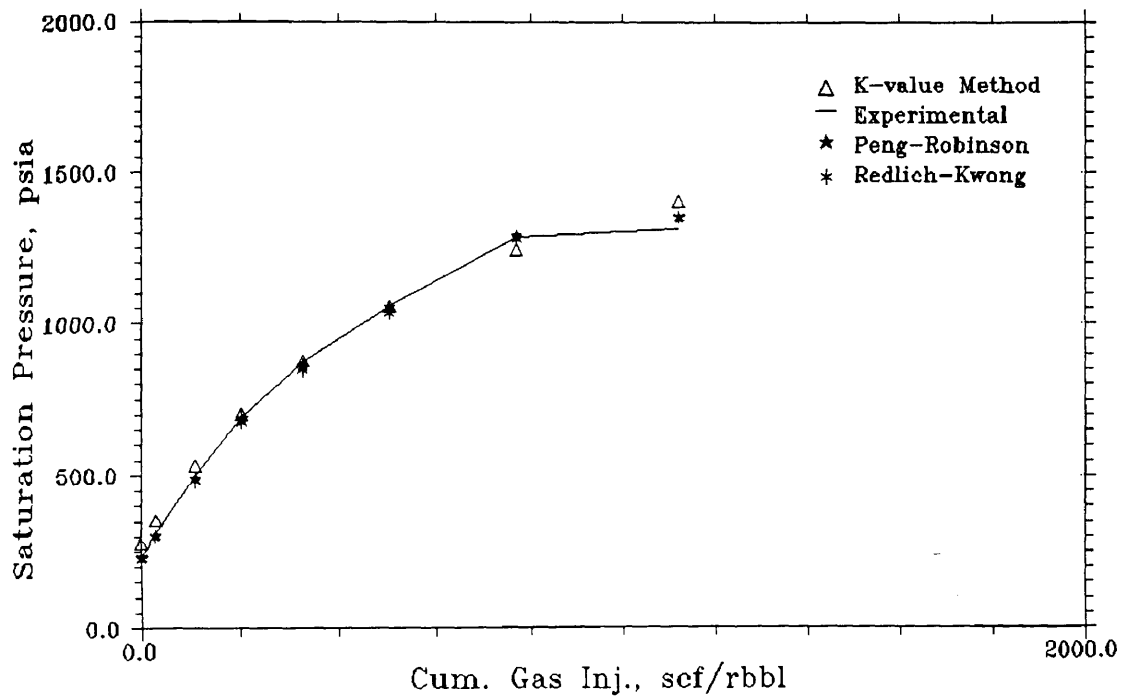


Fig. 29 - Solubility and Swelling of Case 4:
Sat. Press. vs. Cum. CO₂ Injected,
The K-value Method against Eqns. of State.

Case No. 5

The fifth fluid sample is oil. This sample has a convergence pressure of 11,820 psia, reservoir temperature of 155 °F and bubble point pressure of 249 psig. Constant composition expansion and solubility and swelling tests were simulated. The data are available in Tables C-15 through C-17. The simulation study included the solubility and swelling test for pure carbon dioxide.

The simulation results obtained are graphically represented as comparisons between the K-value method and the equations of state in Figs. 30 through 32. The matching parameters are summarized in Table 3. The average deviations between the experimental and calculated results are summarized in Table 4 in next section.

Case 5

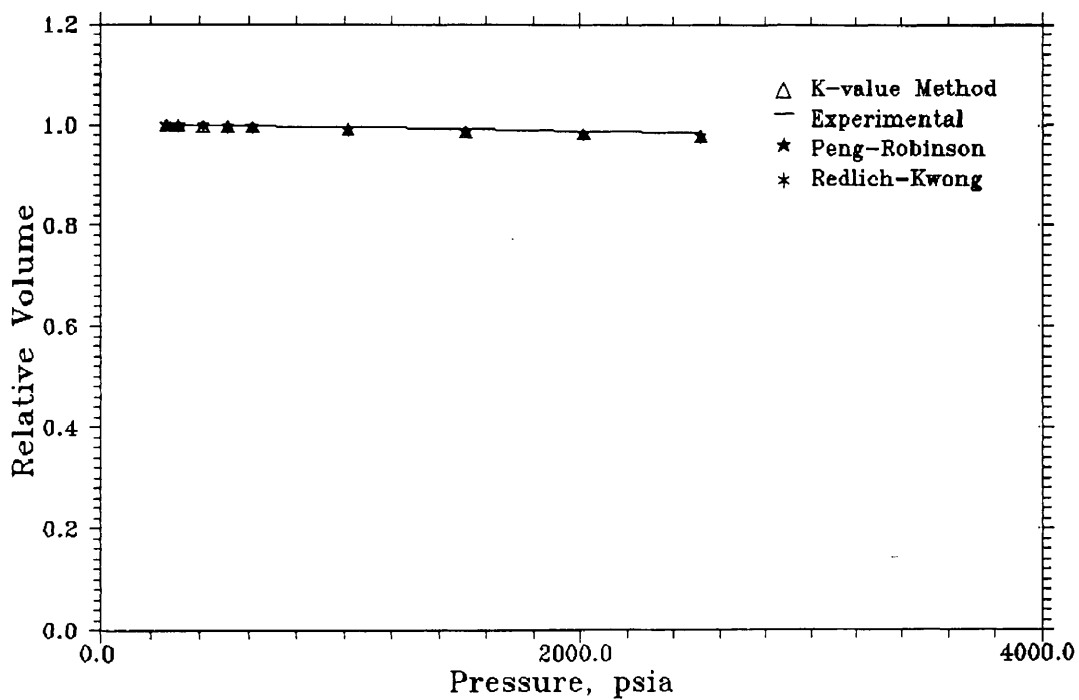


Fig. 30 - Constant Composition Expansion of Case 5:
Relative Volume vs. Pressure,
The K-value Method against Eqns. of State.

Case 5

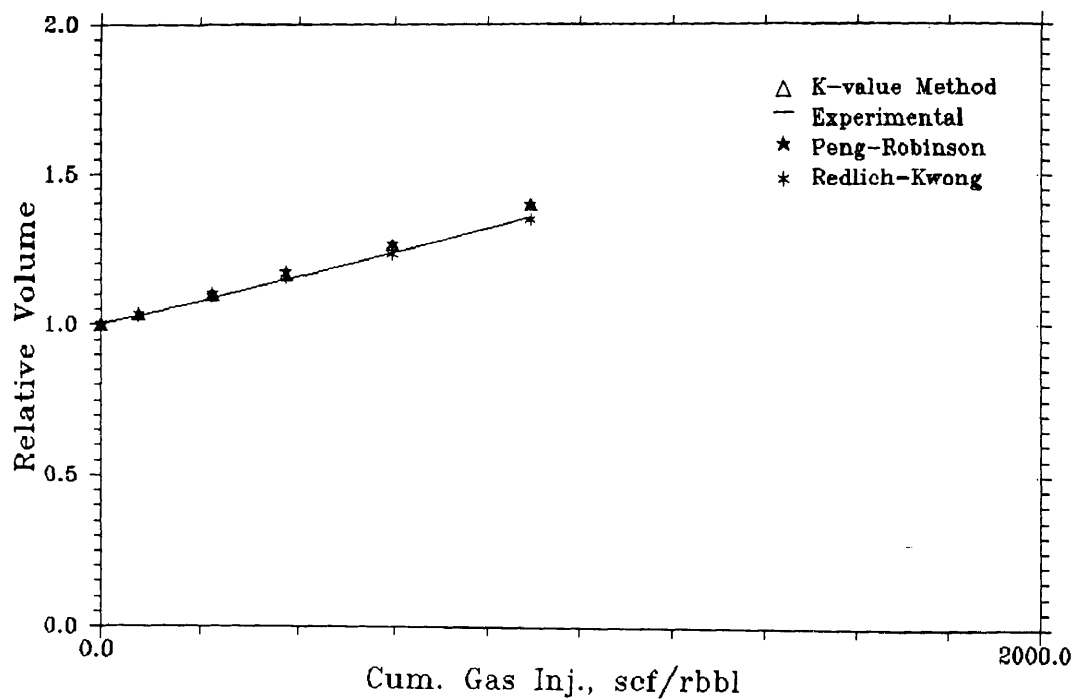


Fig. 31 - Solubility and Swelling of Case 5:
Relative Volume vs. Cum. CO₂ Injected,
The K-value Method against Eqns. of State.

Case 5

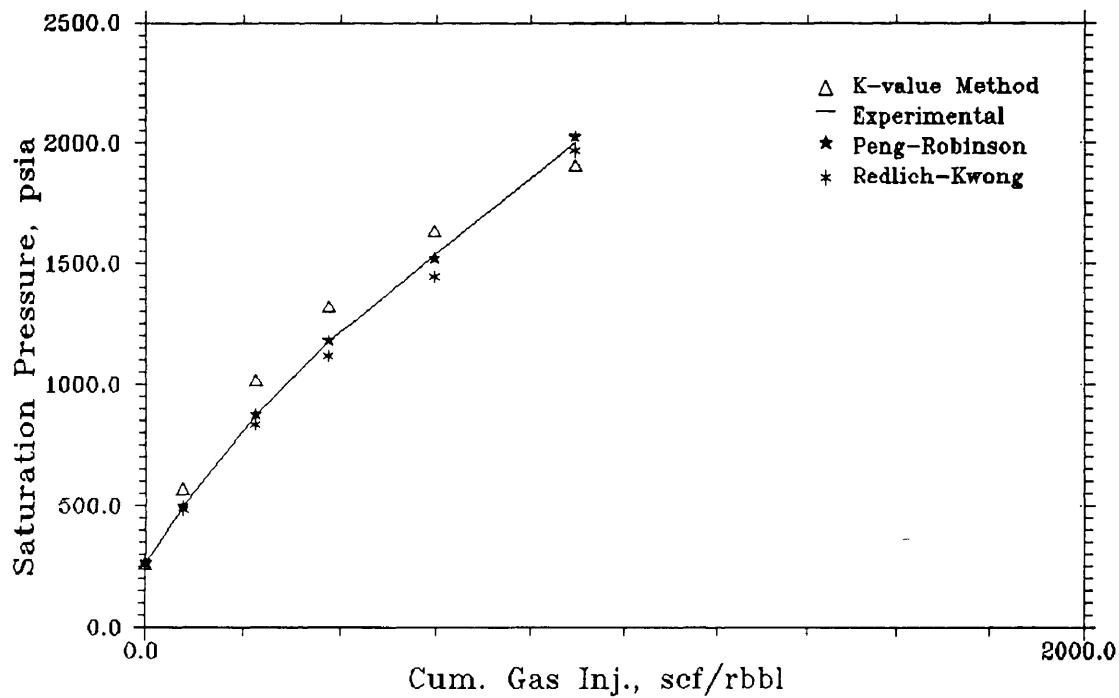


Fig. 32 - Solubility and Swelling of Case 5:
 Sat. Press. vs. Cum. CO₂ Injected,
 The K-value Method against Eqns. of State.

Case No. 6

The sixth fluid sample is oil. This sample has a convergence pressure of 10,860 psia, reservoir temperature of 155 °F and bubble point pressure of 250 psig. Constant composition expansion and solubility and swelling tests were simulated. The data are available in Tables C-18 through C-20. The simulation study included the solubility and swelling test for pure carbon dioxide.

The simulation results obtained are graphically represented as comparisons between the K-value method and the equations of state in Figs. 33 through 35. The matching parameters are summarized in Table 3. The average deviations between the experimental and calculated results are summarized in Table 4 in next section.

Case 6

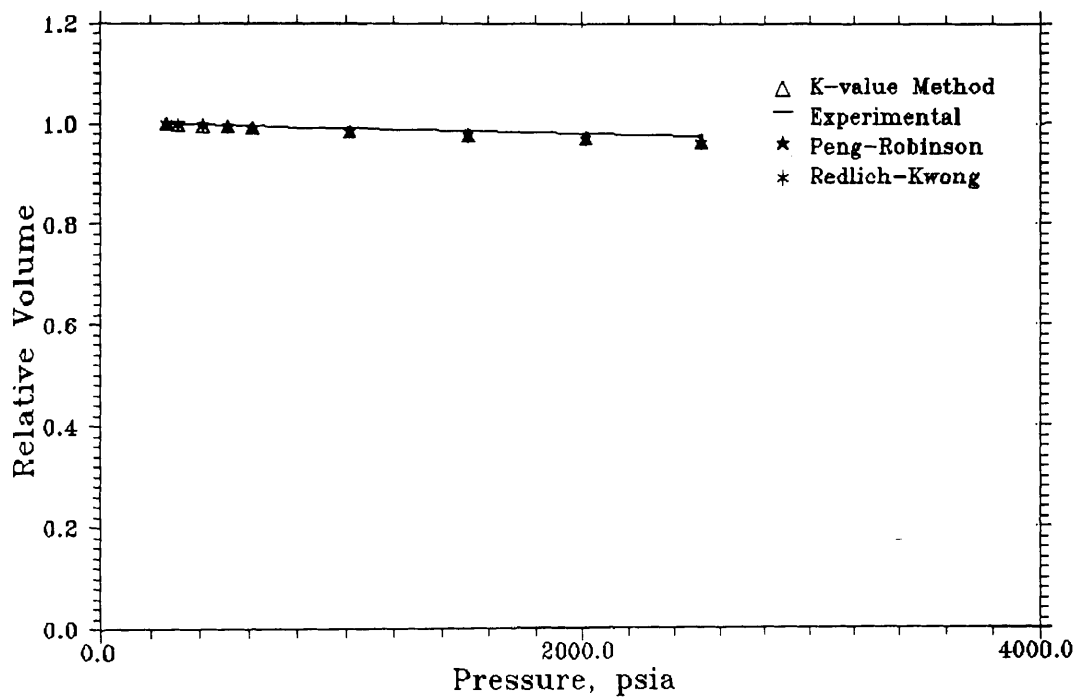


Fig. 33 - Constant Composition Expansion of Case 6:
Relative Volume vs. Pressure,
The K-value Method against Eqns. of State.

Case 6

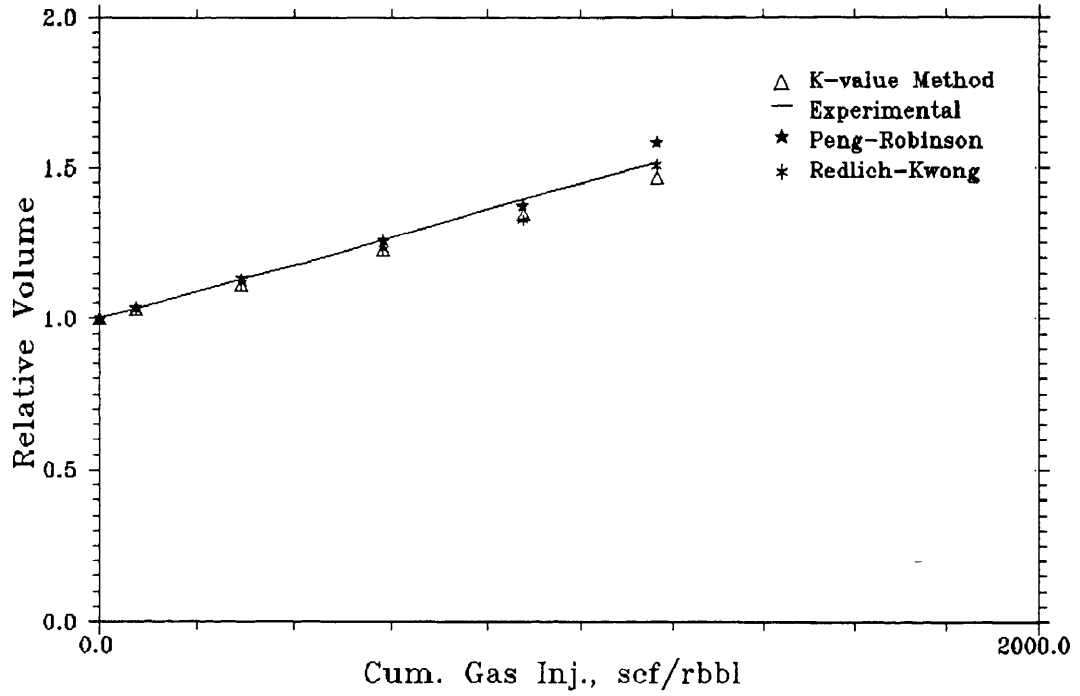


Fig. 34 - Solubility and Swelling of Case 6:
 Relative Volume vs. Cum. CO₂ Injected,
 The K-value Method against Eqns. of State.

Case 6

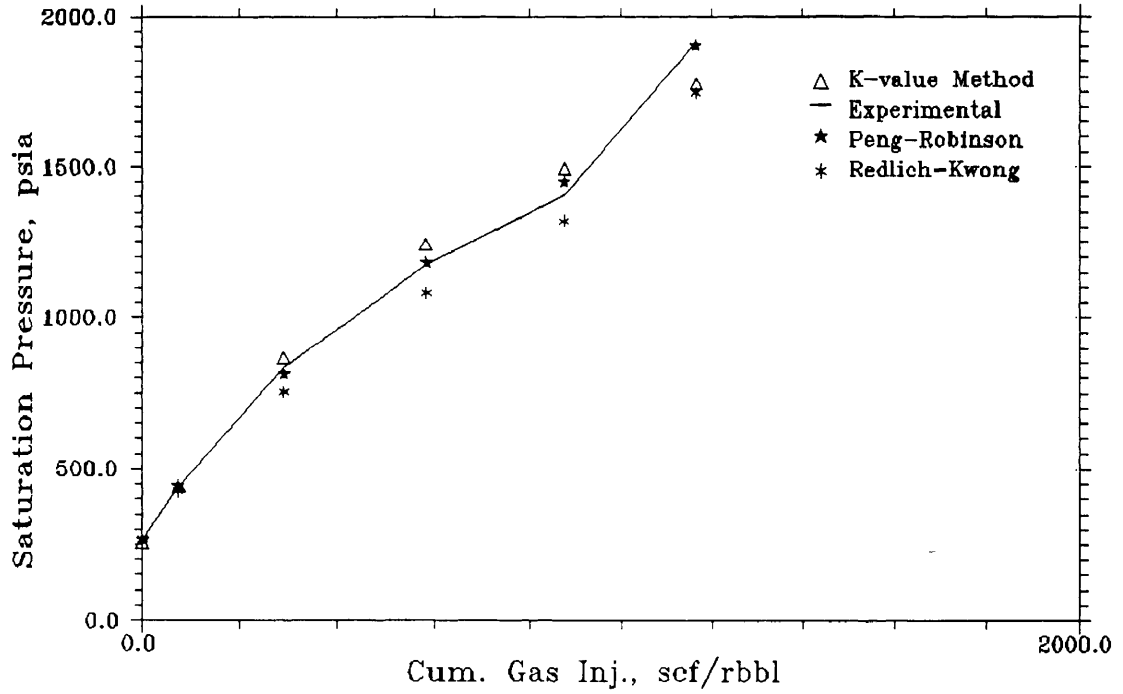


Fig. 35 - Solubility and Swelling of Case 6:
 Sat. Press. vs. Cum. CO₂ Injected,
 The K-value Method against Eqns. of State.

Case No. 7

The seventh fluid sample is gas condensate. This sample has a convergence pressure of 8,800 psia, reservoir temperature of 193 °F and dew point pressure of 4,450 psig. Constant composition expansion and constant volume depletion were simulated. The data are available in Tables C-21 through C-23.

The simulation results obtained are graphically represented as comparisons between the K-value method and the equations of state in Figs. 36 through 38. The matching parameters are summarized in Table 3. The average deviations between the experimental and calculated results are summarized in Table 4 in next section.

Case 7

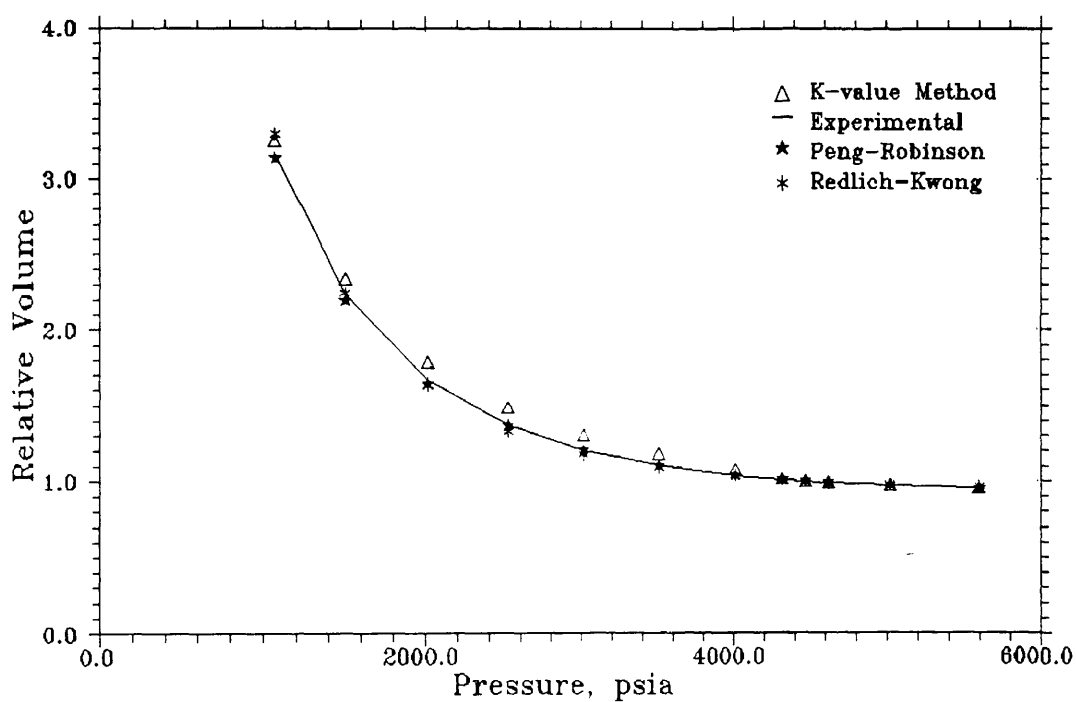


Fig. 36 - Constant Composition Expansion of Case 7:
Relative Volume vs. Pressure,
The K-value Method against Eqns. of State.

Case 7

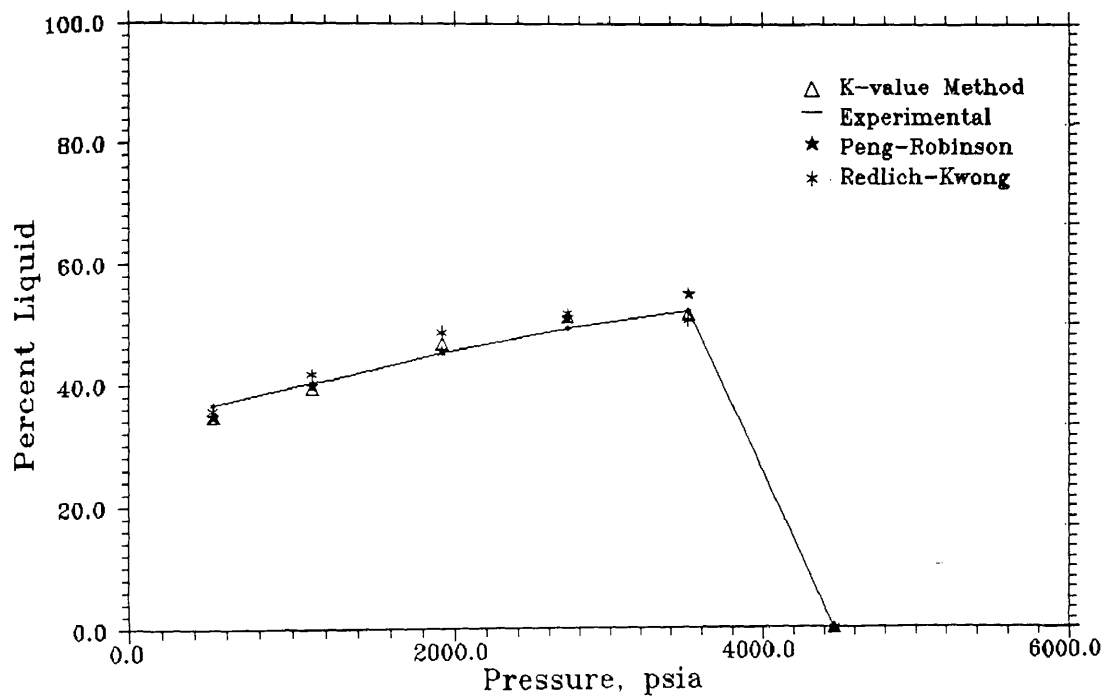


Fig. 37 - Constant Volume Depletion of Case 7:
Percent Liquid vs. Pressure,
The K-value Method against Eqns. of State.

Case 7

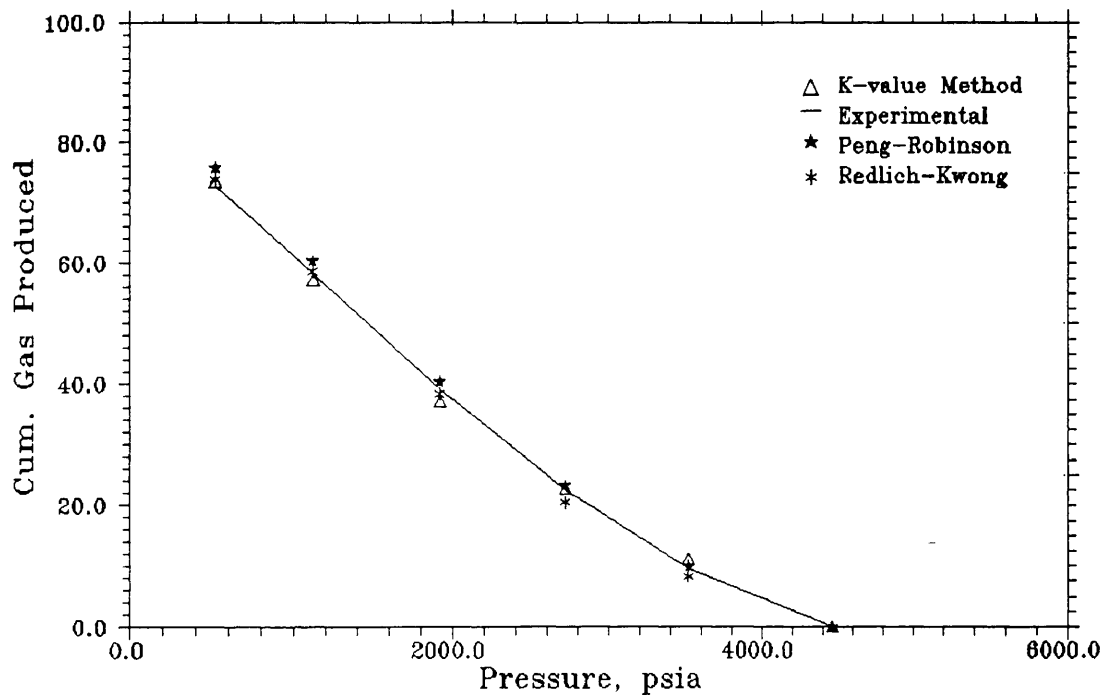


Fig. 38 - Constant Volume Depletion of Case 7:
 Cum. Gas Produced vs. Pressure,
 The K-value Method against Eqns. of State.

Case No. 8

The eighth fluid sample is gas condensate. This sample has a convergence pressure of 5,800 psia, reservoir temperature of 267 °F and dew point pressure of 4,842 psig. Constant composition expansion and constant volume depletion were simulated. The data are available in Tables C-24 through C-26.

The simulation results obtained are graphically represented as comparisons between the K-value method and the equations of state in Figs. 39 through 41. The matching parameters are summarized in Table 3. The average deviations between the experimental and calculated results are summarized in Table 4 in next section.

Case 8

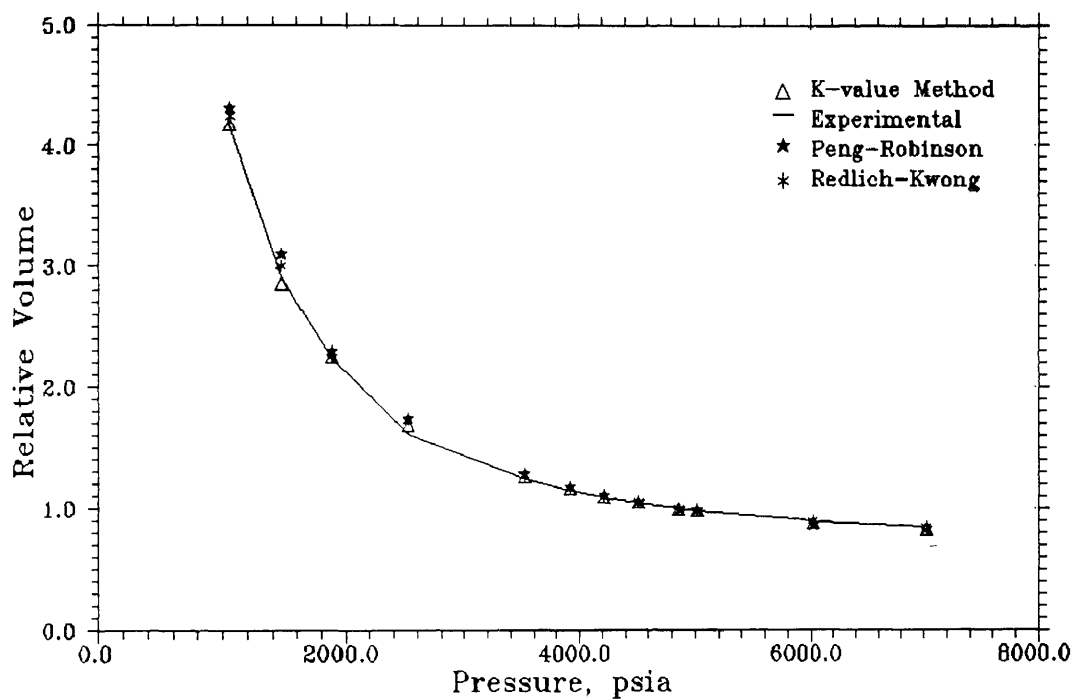


Fig. 39 - Constant Composition Expansion of Case 8:
Relative Volume vs. Pressure,
The K-value Method against Eqns. of State.

Case 8

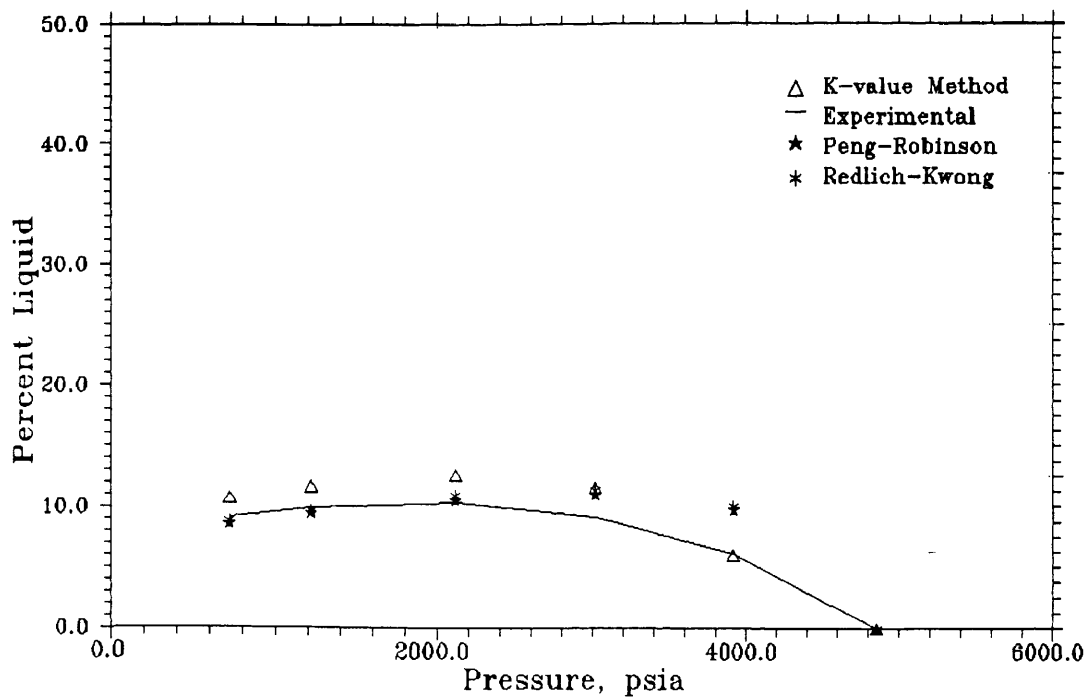


Fig. 40 - Constant Volume Depletion of Case 8:
Percent Liquid vs. Pressure,
The K-value Method against Eqns. of State.

Case 8

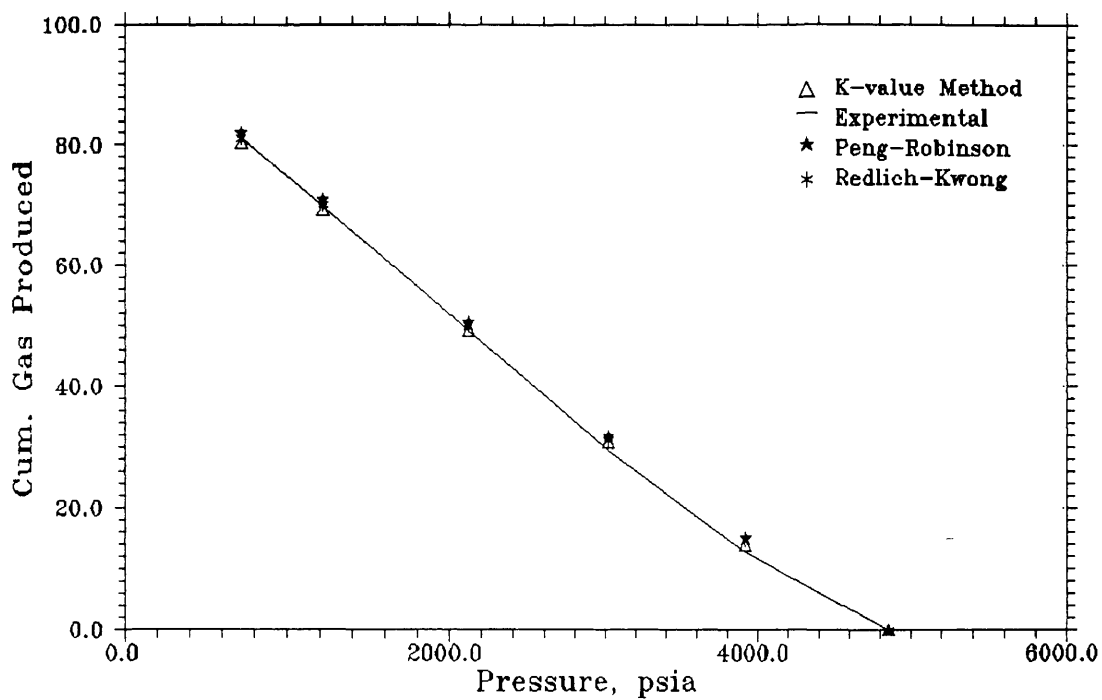


Fig. 41 - Constant Volume Depletion of Case 8:
Cum. Gas Produced vs. Pressure,
The K-value Method against Eqns. of State.

Case No. 9

The ninth fluid sample is gas condensate. This sample has a convergence pressure of 6,180 psia, reservoir temperature of 176 °F and bubble point pressure of 4,460 psig. Constant composition expansion and constant volume depletion were simulated. The data are available in Tables C-27 through C-29.

The simulation results obtained are graphically represented as comparisons between the K-value method and the equations of state in Figs. 42 and 43. The matching parameters are summarized in Table 3. The average deviations between the experimental and calculated results are summarized in Table 4 in next section.

Case 9

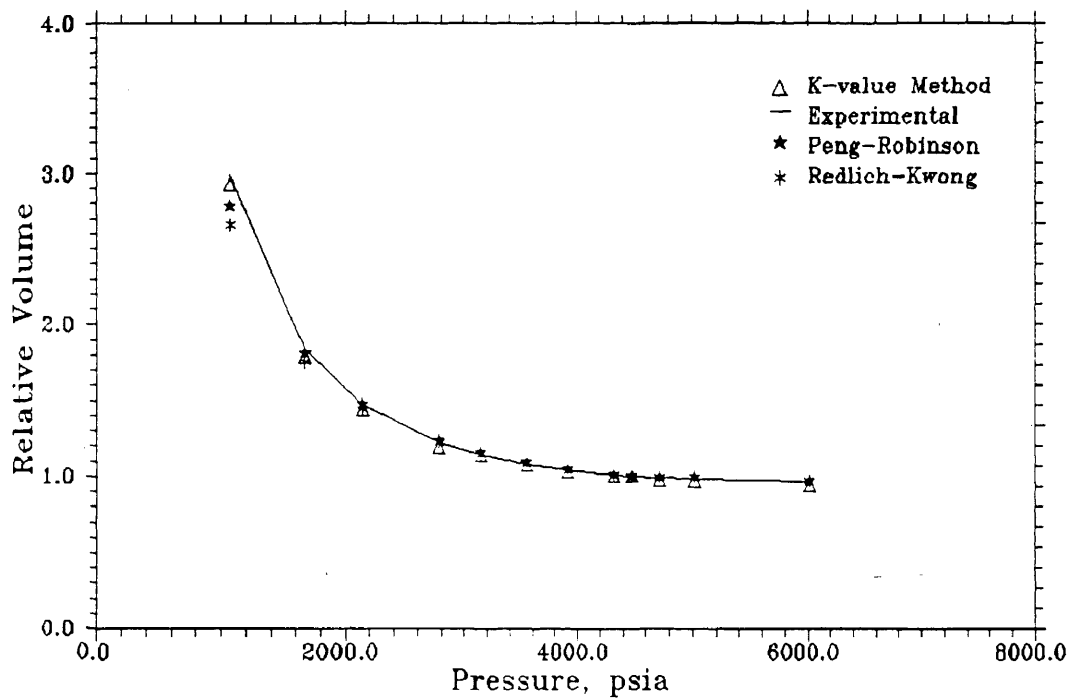


Fig. 42 - Constant Composition Expansion of Case 9:
Relative Volume vs. Pressure,
The K-value Method against Eqns. of State.

Case 9

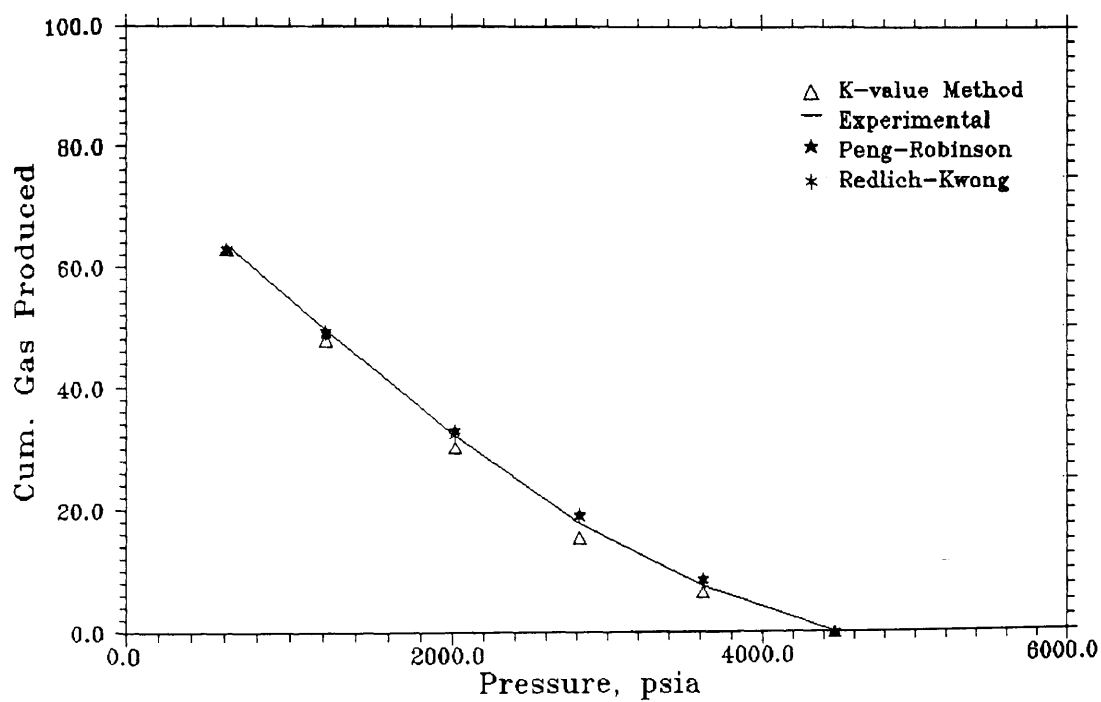


Fig. 43 - Constant Volume Depletion of Case 9:
Cum. Gas Produced vs. Pressure,
The K-value Method against Eqns. of State.

DISCUSSION OF RESULTS

The PVT program developed in this work was run using both the K-value method and the three equations of state capabilities. In addition, Nolen's commercial PVT package⁷⁴ was used to run the same test cases to verify the developed model and validate the K-value method. The results obtained from the nine sets of hydrocarbon mixtures are shown in the previous section.

In each case of this simulation study, the least squares-linear programming (LSLP) model was used to estimate the matching parameters for the mathematical expression of the K-value method such that an acceptable match with the experimental data was obtained. The LSLP technique was originally developed by Coats *et al*⁴⁰, and was used in petroleum reservoir history matching^{40,91}, and was also used in phase behavior matching by Coats *et al*¹ and Obut *et al*^{8,67}. This technique was extended by Coats *et al*¹ to a nonlinear programming by iterating on the constraints. This procedure can be summarized in the following (details of this technique are available in Appendix B):

- 1) Several computer runs are performed using the PVT model, each run using a different set of parameters for the K-value expression.
- 2) By the end of each run, the difference between the computed and the experimental performance variables is calculated.

3) After completing a number of runs (at least one more than the number of parameters), the LSLP model is used to manipulate the data and as a result a set of parameters for the K-value expression is obtained.

4) This set of parameters is then used in the PVT program to compute the K-values. If the match of the experimental data with the calculated is not satisfactory, another iteration is performed with a modified set of constraints starting with step number 1.

At each iteration of the regression, a local subregion of the global parameter space is selected by moving the boundaries on the constraints.

In addition to the saturation pressures, the performance variables selected for the matching process were percent liquid and cumulative gas produced as functions of pressure for the constant volume depletion test, relative volumes of oil as function of pressure for the constant composition expansion test, and relative swollen volumes and saturation pressures as functions of cumulative gas volumes injected for the solubility and swelling test. In the LSLP model, the differences between the computed and the experimental saturation pressures were normalized by dividing each value by the original saturation pressure of the fluid sample, and for the other performance variables the differences were computed as percentages.

Nolen's commercial PVT package used in this study for the comparative analysis, has an iterative nonlinear regression

capability which automatically adjusts the properties of the hydrocarbon components to match the experimental data.

A summary of the measured and computed saturation pressures by the K-value method and the equations of state is shown in Table 1. The constraints imposed on the K-value method parameters and used by the optimization model are tabulated in Table 2. Also, a summary of the K-value method parameters calculated by the optimization model are tabulated in Table 3. It is worth mentioning that the theoretical value of the constant a_0 ($a_0 = 1$) was used, and that the constant b_0 was considered equal to zero assuming that the convergence pressure was adjusted in the input data. The average deviations between the experimental and calculated results is calculated using the formula:

$$\epsilon = \sum_{j=1}^{NJ} | (d_j^e - d_j^c) / d_j^e | \quad \dots\dots\dots(121)$$

The calculated average deviations for each case are summarized in Table 4.

Verification of The K-value Method

A verification of the K-value method was performed including the following points:

1 - **Comparison with Experimental K-values Data:** To verify the K-values calculated by this method, a comparison was conducted with the experimentally determined K-values of two fluid systems reported by Brinkmann and Sicking²⁸.

TABLE 1 - A Summary of Saturation Pressures for the Test Cases.

| Case | Saturation Pressure, psig | | | |
|------|---------------------------|--------|--------|----------------|
| | Measured | RK | PR | K-value Method |
| 1 | 3428.0 | 3435.8 | 3427.5 | 3428.2 |
| 2 | 6750.0 | 6747.6 | 6746.3 | 6751.1 |
| 3 | 1500.0 | 1505.9 | 1500.4 | 1496.0 |
| 4 | 215.0 | 215.3 | 215.0 | 209.0 |
| 5 | 249.0 | 250.0 | 248.9 | 251.8 |
| 6 | 250.0 | 252.6 | 249.8 | 253.6 |
| 7 | 4450.0 | 4441.7 | 4435.7 | 4449.0 |
| 8 | 4842.0 | 4852.2 | 4833.5 | 4840.3 |
| 9 | 4460.0 | 4465.7 | 4460.4 | 4462.3 |

TABLE 2 - A Summary of of The Parameters' Constraints
of The K-value Method for The Test Cases.

| Case | Test | Parameters | | | | | | | Bound |
|------|------|----------------|----------------|----------------|----------------|----------------|----------------|----------------|-------|
| | | a ₁ | a ₂ | a ₃ | a ₄ | b ₁ | b ₂ | b ₃ | |
| 1 | CCX | -.9900 | -.0100 | -.0010 | -.0030 | -10.00 | -100.0 | -100.0 | lower |
| | | -1.500 | -.6000 | -.4000 | -.1000 | 10.00 | 100.0 | 100.0 | upper |
| | CVD | -.9900 | -.0100 | -.0010 | -.0030 | -10.00 | -100.0 | -100.0 | lower |
| | | -1.500 | -.6000 | -.4000 | -.1000 | 10.00 | 100.0 | 100.0 | upper |
| 2 | CVD | -.8000 | -.0200 | -.0010 | -.0030 | -10.00 | -100.0 | -100.0 | lower |
| | | -1.550 | -.8000 | -.4000 | -.1000 | 10.00 | 100.0 | 100.0 | upper |
| 3 | CCX | -.8000 | -.0200 | -.0010 | -.0300 | -10.00 | -100.0 | -100.0 | lower |
| | | -1.500 | -.6000 | -.4000 | -.1000 | 10.00 | 100.0 | 100.0 | upper |
| | SWL1 | -.0200 | -.0300 | -.0050 | -.0001 | -10.00 | -100.0 | -100.0 | lower |
| | | -.1400 | -.8500 | -.0400 | -.2000 | 10.00 | 100.0 | 100.0 | upper |
| | SWL2 | -.0000 | -.0300 | -.0050 | -.0000 | -10.00 | -100.0 | -100.0 | lower |
| | | -1.400 | -.8500 | -.0400 | -.2000 | 10.00 | 100.0 | 100.0 | upper |
| 4 | CCX | -.0100 | -.0020 | -.0050 | -.0001 | -10.00 | -100.0 | -100.0 | lower |
| | | -1.400 | -.8500 | -.0400 | -.2000 | 10.00 | 100.0 | 100.0 | upper |
| | SWL1 | -.0200 | -.0300 | -.0050 | -.0001 | -10.00 | -100.0 | -100.0 | lower |
| | | -1.400 | -.8500 | -.0400 | -.2000 | 10.00 | 100.0 | 100.0 | upper |
| 5 | CCX | -.0100 | -.0020 | -.0050 | -.0001 | -10.00 | -100.0 | -100.0 | lower |
| | | -1.400 | -.8500 | -.0400 | -.2000 | 10.00 | 100.0 | 100.0 | upper |
| | SWL1 | -.0200 | -.0300 | -.0050 | -.0001 | -10.00 | -100.0 | -100.0 | lower |
| | | -1.400 | -.8500 | -.0400 | -.2000 | 10.00 | 100.0 | 100.0 | upper |
| 6 | CCX | -.9000 | -.0100 | -.0010 | -.0300 | -10.00 | -100.0 | -100.0 | lower |
| | | -1.500 | -.5600 | -.4000 | -.1000 | 10.00 | 100.0 | 100.0 | upper |
| | SWL1 | -.1000 | -.0100 | -.0010 | -.0300 | -100.0 | -200.0 | -300.0 | lower |
| | | -1.500 | -.6500 | -.4000 | -.6000 | 100.0 | 200.0 | 300.0 | upper |
| 7 | CCX | -.0200 | -.0100 | -.0010 | -.0300 | -10.00 | -100.0 | -600.0 | lower |
| | | -1.400 | -.3000 | -.1000 | -.8000 | 10.00 | 100.0 | 600.0 | upper |
| | CVD | -.0200 | -.0100 | -.0010 | -.0300 | -100.0 | -100.0 | -600.0 | lower |
| | | -1.400 | -.3000 | -.1000 | -.8000 | 100.0 | 100.0 | 600.0 | upper |

TABLE 2 - Continued

| Case | Test | Parameters | | | | | | | Bound |
|------|------|----------------|----------------|----------------|----------------|----------------|----------------|----------------|-------|
| | | a ₁ | a ₂ | a ₃ | a ₄ | b ₁ | b ₂ | b ₃ | |
| 8 | CCX | -.0200 | -.0100 | -.0010 | -.0300 | -10.00 | -100.0 | -100.0 | lower |
| | | -1.500 | -.4000 | -.3000 | -.1000 | 10.00 | 100.0 | 100.0 | upper |
| | CVD | -.0200 | -.0100 | -.0010 | -.0300 | -10.00 | -100.0 | -100.0 | lower |
| | | -1.500 | -.4000 | -.3000 | -.1000 | 10.00 | 100.0 | 100.0 | upper |
| 9 | CCX | -.7000 | -.0100 | -.0010 | -.0300 | -10.00 | -100.0 | -100.0 | lower |
| | | -1.500 | -.5200 | -.5400 | -1.140 | 10.00 | 100.0 | 100.0 | upper |
| | CVD | -.0200 | -.0100 | -.0010 | -.0300 | -50.00 | -100.0 | -300.0 | lower |
| | | -1.500 | -.8000 | -.4000 | -1.440 | 50.00 | 100.0 | 300.0 | upper |

Where:

- CCX = Constant Composition Expansion.
- CVD = Constant Volume Depletion.
- SWL1 = Solubility & Swelling with CO₂ Injection.
- SWL2 = Solubility & Swelling with N₂+CO₂ Injection.
- a₁-a₄ = Parameters of the slope polynomial, a₀ = 1.
- b₁-b₃ = Parameters of the p_k polynomial, b₀ = 0.

TABLE 3 - A Summary of The K-value Method Parameters,
and Convergence Pressures for the Test Cases.

| Case | Test | Parameters | | | | | | | P _k psia |
|------|------|----------------|----------------|----------------|----------------|----------------|----------------|----------------|------------------------|
| | | a ₁ | a ₂ | a ₃ | a ₄ | b ₁ | b ₂ | b ₃ | |
| 1 | CCX | -.9900 | -.0100 | -.4000 | -.0542 | -0.000 | 0.000 | 0.000 | 5500.0 |
| | CVD | -1.027 | -.1299 | -.4000 | -.0461 | -1.545 | 0.000 | 0.000 | |
| 2 | CVD | -.8107 | -.1628 | -.0010 | -.0891 | -0.000 | 0.000 | -61.05 | 8180.0 |
| 3 | CCX | -.8000 | -.0200 | -.0010 | -.0300 | 0.000 | 0.000 | 0.000 | 9500.0 |
| | SWL1 | -.0200 | -.3087 | -.0400 | -.0001 | -.0300 | 0.000 | 0.000 | |
| | SWL2 | 0.000 | -.8500 | -.0400 | 0.000 | 0.000 | 0.000 | 0.000 | |
| 4 | CCX | -.0199 | -.0299 | -.0400 | -.2000 | 0.000 | 0.000 | 0.000 | 13560.0 |
| | SWL1 | -.0871 | 0.000 | -.0400 | -.0307 | -.0300 | 5.000 | 0.000 | |
| 5 | CCX | -.0168 | -.0268 | -.0400 | -.2000 | 0.000 | 0.000 | 0.000 | 11820.0 |
| | SWL1 | -.2325 | -.3300 | -.0400 | -.2000 | -.0300 | 0.000 | 0.000 | |
| 6 | CCX | -.9900 | -.0174 | -.0505 | -.0300 | 0.000 | 0.000 | 0.000 | 10860.0 |
| | SWL1 | -.1000 | -.6500 | -3.300 | -5.080 | -52.73 | 101.8 | -253.4 | |
| 7 | CCX | -1.400 | -.2900 | -.1000 | -.8000 | 0.000 | 0.000 | 0.000 | 8800.0 |
| | CVD | -1.400 | -.2900 | -.1000 | -.8000 | -61.71 | 73.04 | -504.1 | |
| 8 | CCX | -.4862 | -.4000 | -.0848 | -.0852 | 0.000 | 0.000 | 0.000 | 5800.0 |
| | CVD | -1.140 | -.2445 | -.2389 | -.0300 | -2.648 | 17.88 | -23.19 | |
| 9 | CCX | -.7000 | -.5200 | -.5400 | -1.140 | 0.000 | 0.000 | 0.000 | 6180.0 |
| | CVD | -.6058 | -.7055 | -.4000 | -1.440 | -37.43 | 94.21 | -290.9 | |

Where:

- CCX = Constant Composition Expansion.
- CVD = Constant Volume Depletion.
- SWL1 = Solubility & Swelling with CO₂ Injection.
- SWL2 = Solubility & Swelling with N₂+CO₂ Injection.
- a₁-a₄ = Parameters of the slope polynomial, a₀ = 1.
- b₁-b₃ = Parameters of the p_k polynomial, b₀ = 0.

TABLE 4 - A Summary of Average Deviations, (%).

| Case | Test | Relationship | K-value | PR | RK |
|------|------|--------------------|---------|--------|--------|
| 1 | CCX | Rel.Vol.- Pressure | 5.099 | 1.628 | 1.849 |
| | CVD | Liq. % - Pressure | 3.834 | 6.163 | 5.714 |
| | CVD | Gp - Pressure | 5.637 | 1.811 | 2.012 |
| 2 | CVD | Liq. % - Pressure | 3.785 | 12.255 | 12.001 |
| | CVD | Gp - Pressure | 5.029 | 5.421 | 5.617 |
| 3 | CCX | Rel.Vol.- Pressure | 0.655 | 0.632 | 0.435 |
| | SWL1 | Rel.Vol.- Gas Inj. | 1.312 | 0.633 | 1.045 |
| | SWL1 | Psat - Gas Inj. | 3.859 | 1.211 | 3.259 |
| | SWL2 | Rel.Vol.- Gas Inj. | 0.854 | 3.401 | 3.203 |
| | SWL2 | Psat - Gas Inj. | 2.503 | 1.187 | 4.319 |
| 4 | CCX | Rel.Vol.- Pressure | 0.011 | 0.416 | 0.421 |
| | SWL1 | Rel.Vol.- Gas Inj. | 0.587 | 3.497 | 2.965 |
| | SWL1 | Psat - Gas Inj. | 6.659 | 1.140 | 2.191 |
| 5 | CCX | Rel.Vol.- Pressure | 0.328 | 0.485 | 0.414 |
| | SWL1 | Rel.Vol.- Gas Inj. | 1.268 | 1.577 | 2.961 |
| | SWL1 | Psat - Gas Inj. | 5.236 | 0.481 | 3.412 |
| 6 | CCX | Rel.Vol.- Pressure | 0.754 | 0.798 | 0.905 |
| | SWL1 | Rel.Vol.- Gas Inj. | 2.022 | 1.132 | 1.643 |
| | SWL1 | Psat - Gas Inj. | 6.354 | 1.287 | 6.176 |
| 7 | CCX | Rel.Vol.- Pressure | 3.342 | 0.534 | 1.736 |
| | CVD | Liq. % - Pressure | 2.685 | 2.673 | 3.615 |
| | CVD | Gp - Pressure | 6.681 | 3.077 | 4.431 |
| 8 | CCX | Rel.Vol.- Pressure | 2.574 | 4.495 | 2.331 |
| | CVD | Liq. % - Pressure | 14.125 | 15.489 | 16.411 |
| | CVD | Gp - Pressure | 2.741 | 5.174 | 3.683 |
| 9 | CCX | Rel.Vol.- Pressure | 1.177 | 1.142 | 2.098 |
| | CVD | Gp - Pressure | 6.573 | 4.608 | 3.650 |

The first system was a gas condensate exhibiting a dew point pressure of 5,500 psia at reservoir temperature of 187 °F and its composition is shown in Table 5. The plot of $\log(K)$ vs. $\log(p)$ comparing the calculated and the experimentally determined K-values is shown in Fig. 44. From this figure, it can be seen that the calculated K-values are smooth and are in reasonable agreement with the experimental values. The second fluid system is a volatile oil exhibiting a bubble point pressure of 4,000 psia at reservoir temperature of 234 °F and its composition is shown in Table 6. Fig. 45 depicts the plot of $\log(K)$ vs. $\log(p)$ comparing the calculated and the experimentally determined K-values. From this figure, it can be seen that the calculated K-values are smooth and are in reasonable agreement with the experimental values.

2 - Effect of Varying the Convergence Pressure on the K-values:

The data of test cases 1 and 2 were used as examples to show the effect of varying the convergence pressure p_k on the calculated K-values by the K-value method. The plots of $\log(k)$ vs. $\log(p)$ are shown in Figs. 46 and 47. For case 1, the K-values were calculated at two convergence pressures of 5,500 and 6,000 psia. Fig. 46 shows the two sets of K-values as solid lines and dashed lines. For case 2, the K-values were calculated at two convergence pressures of 7,500 and 8,180 psia. Fig. 47 shows the two sets of K-values as solid lines and dashed lines.

TABLE 5 - Composition of Brinkmann's Gas Condensate System

| Component | Mole % |
|---------------|--------------------|
| Methane | 85.85 |
| Ethane | 6.95 |
| Propane | 2.60 |
| Butanes | 1.31 |
| Pentanes | 0.60 |
| Hexanes | 0.39 |
| Heptanes plus | 2.30 |
| | <hr/> 100.00 <hr/> |

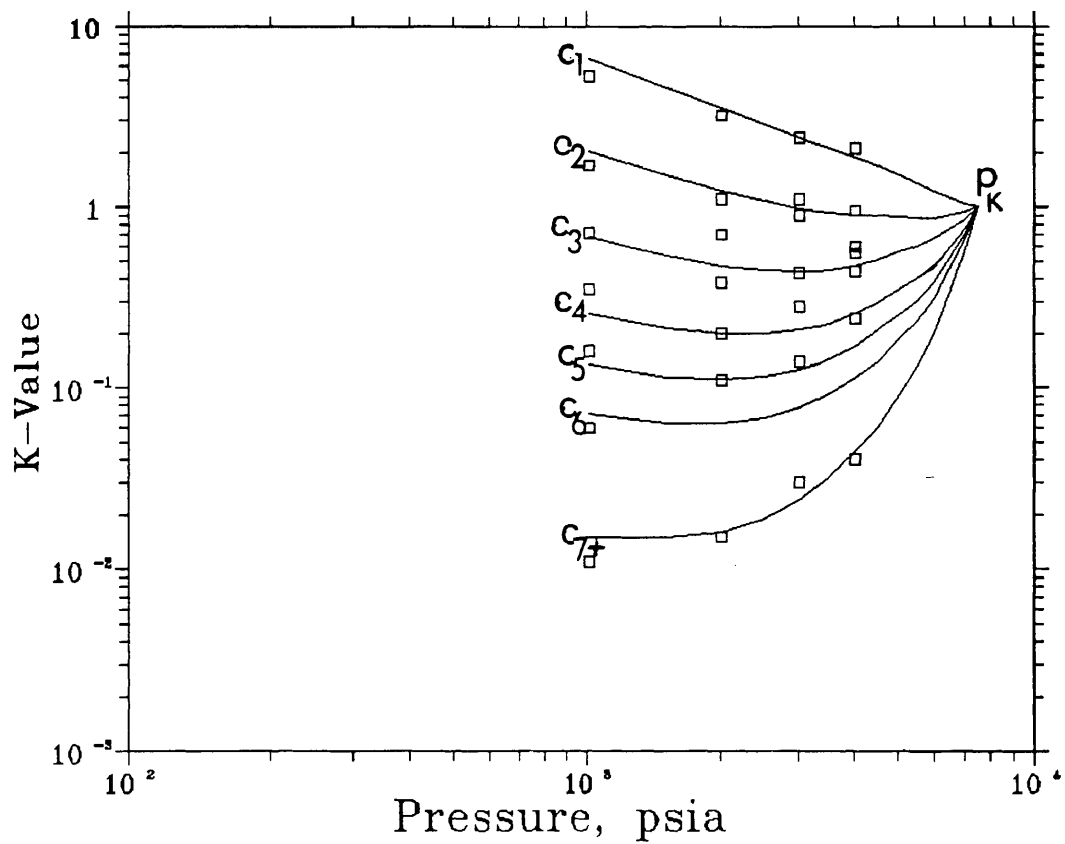


Fig. 44 - Comparison of Calculated and Experimental K-values of Brinkmann's Gas Condensate System.

TABLE 6 - Composition of Brinkmann's Crude Oil System

| Component | Mole % |
|----------------|--------------|
| Methane | 49.74 |
| Ethane | 8.60 |
| Propane | 8.98 |
| Butanes | 5.84 |
| Pentanes | 3.37 |
| Hexanes | 2.33 |
| Heptanes plus | 21.10 |
| Carbon Dioxide | 0.04 |
| | <hr/> 100.00 |

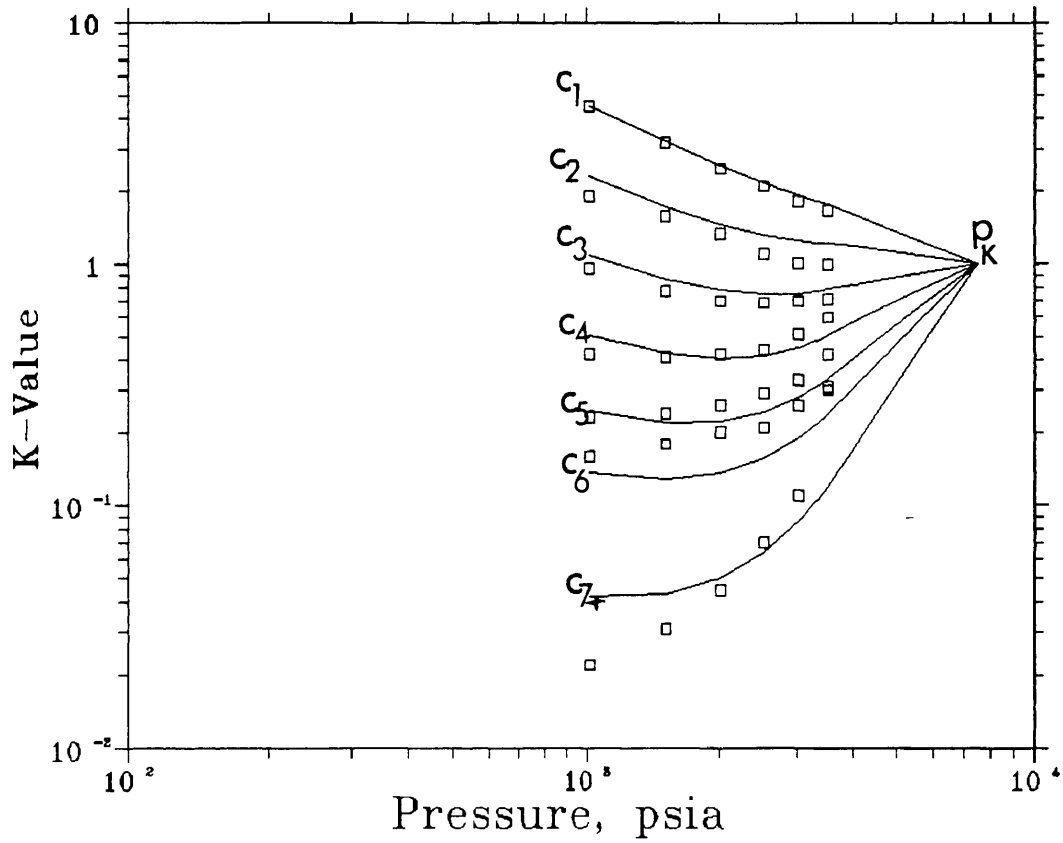


Fig. 45 - Comparison of Calculated and Experimental K-values of Brinkmann's Crude Oil System.

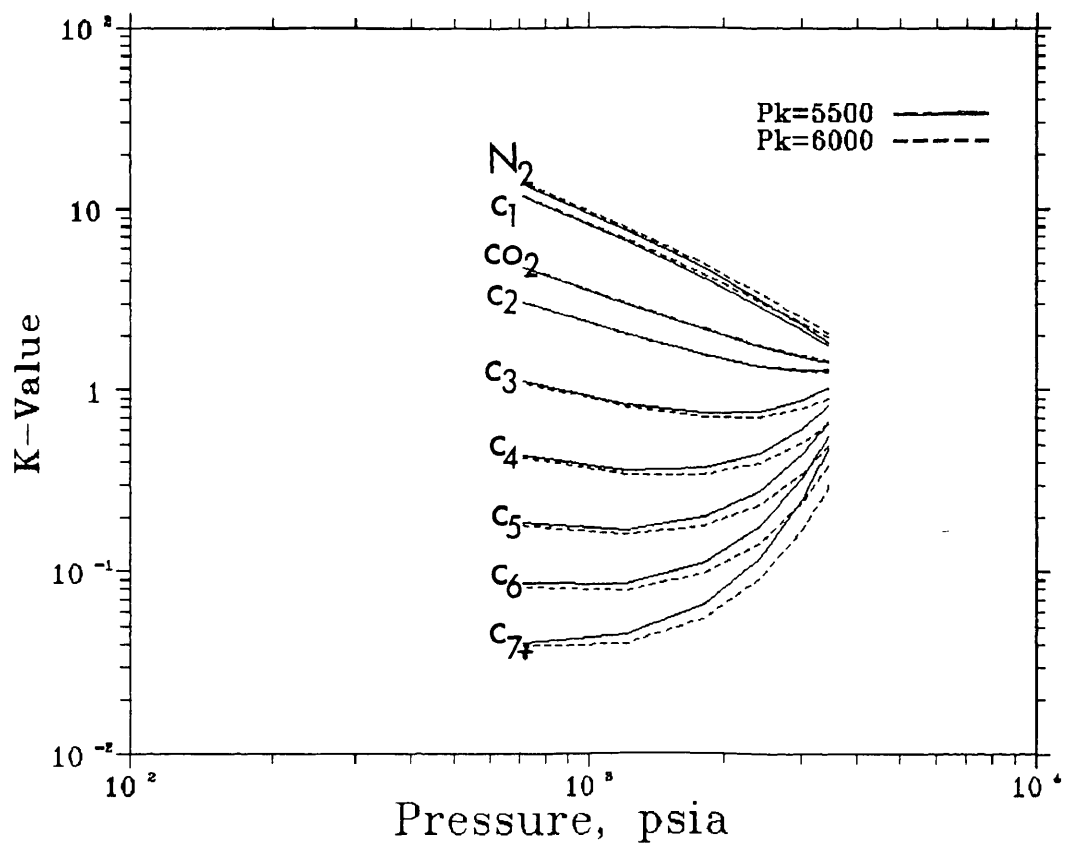


Fig. 46 - K-values of Case 1 at Different P_k .

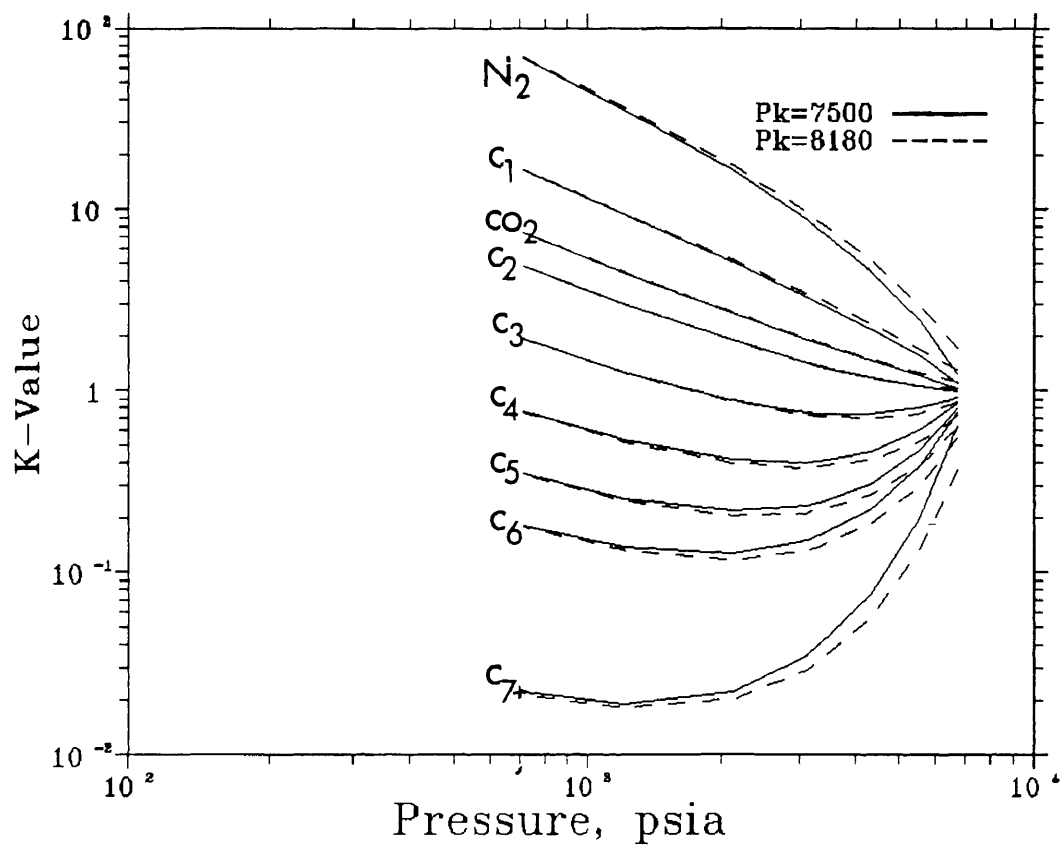


Fig. 47 - K-values of Case 2 at Different P_k .

3 - Possible Oscillations Between Matched Points: Since the slope of the K-value equation was expressed as a polynomial of the ratio of (p/p_k) , possible oscillations between the matched points due to using the polynomial form were verified. Therefore, the slope of the K-value equation was plotted vs. pressure for each of the cases of this study (cases 1 through 9), using data of Table 4, to show if any oscillations exist between the matched points. From the plots, it was concluded that no oscillations exist on any of them, and that the slopes change smoothly with pressure.

Also, since the change of convergence pressure as a function of the change of mole fraction of the intermediate hydrocarbons was expressed in the form of polynomial, possible oscillations due to using the polynomial form were verified. The change of convergence pressure as a function of the change of mole fraction of the intermediate hydrocarbons was plotted for each of the cases. From these plots, no oscillations could be observed on any of these plots.

Analyses of the results of each case simulated in this work are covered in the following:

Case No. 1

The fluid sample of the SPE comparative study is gas condensate. This sample has a dew point pressure of 3,428 psig at reservoir temperature of 200 °F. The convergence pressure calculated by eq. 2 was 4,129.95 psia, and that was adjusted to 5,500 psia to match the

experimental data. The simulation results, Figs. 12 through 17, show the match between the computed and the experimental data. Figs. 12 through 14 depict comparisons between the K-value method and the equations of state of Nolen's model. Since the characterization factor, which is function of the boiling temperature of the component, has a direct effect on the calculated K-values by the K-value method, it was thought that adjusting the boiling temperature for the key components would improve the match. To be able to match the dew point pressure of the sample, the boiling temperature of methane was adjusted from its tabulated value to -262 °F. Table 4 summarizes the average deviation for each plot. From Fig. 12, the K-value method shows an average deviation of 5.1% compared to 1.6% by PR and 1.8% by RK. From Fig. 13, the K-value method shows an average deviation of 3.8% compared to 6.2% by PR and 5.7% by RK. From Fig. 14, the K-value method shows an average deviation of 5.6% compared to 1.8% by PR and 2.0% by RK. Although the average deviation varies from one method to the other, the overall matching is acceptable. Figs. 15 through 17 depict comparisons between the equations of state of Nolen's model and the PVT program of this work. From these figures, a good agreement between the two models can be observed.

Figs. 18 and 19 show the published results of the SPE third comparative solution project. From those figures, we can see the variations between the results obtained from different companies. These differences could be due to selecting different number of hydrocarbon components or pseudocomponents to characterize the fluid sample and probably due to using different models. The results are in

reasonable agreement with both the K-value method and the equations of state.

A speed test between the K-value method and the equations of state was performed on a desktop 286 PC (clock speed = 8 MHz), using the data of case 1 for the constant volume depletion test and the constant volume expansion test. A summary of the average CPU times per run, in seconds, and the average number of iterations in K-value calculations are tabulated in Table 7. The speed test results show that the K-value method takes less CPU time than any of the equations of state. In the first test, the K-value method took 6.49 seconds to complete the test compared to 147.21 seconds by PR equation, 46.87 by SRK equation and, 121.52 by SW equation. The K-value method computed the K-values in one iteration per pressure increment compared to an average of 20.06 by PR equation, 17.71 by SRK equation, and 17.58 by SW equation. In the second test, the K-value method took 7.92 seconds to complete the test compared to 65.23 seconds by PR equation, 62.06 by SRK equation, and 163.12 by SW equation. The K-value method computed the K-values in one iteration per pressure increment compared to an average of 17.61 by PR equation, 17.61 by SRK equation, and 17.54 by SW equation.

TABLE 7 - A Summary of Speed Tests between
The K-value Method and The Equations of State.

| | K-value Method | PR | RK | SW |
|--|----------------|--------|-------|--------|
| <u>Constant Volume Depletion:</u> | | | | |
| Avg. CPU Time, sec. | 6.49 | 147.21 | 46.87 | 121.52 |
| Avg. Number of Iterations | 1.00 | 20.06 | 17.71 | 17.58 |
| <u>Constant Composition Expansion:</u> | | | | |
| Avg. CPU Time, sec. | 7.92 | 65.23 | 62.06 | 163.12 |
| Avg. Number of Iterations | 1.00 | 17.61 | 17.61 | 17.54 |

Case No. 2

The North Sea sample is a rich gas condensate. This sample exhibits a dew point pressure of 6,750 psig at a reservoir temperature of 280 °F. The convergence pressure calculated by eq. 2 was 3,986.22 psia, and it was adjusted to 8,180 psia (compared to 8,000 psia used by Whitson) to match the experimental data. The simulation results, Figs. 20 and 21, show the match between the computed and the experimental data. These Figures depict comparisons between the K-value method and the equations of state of Nolen's model. To be able to match the dew point pressure of the sample, the boiling temperature of methane was adjusted from its tabulated value to -261 °F. Table 4 summarizes the average deviation for each plot. From Fig. 20, the K-value method shows an average deviation in the liquid dropout calculation of 3.8% compared to 12.3% by PR and 12.0% by RK. From Fig. 21, the K-value method shows an average deviation in the cumulative gas volume produced of 5.0% compared to 5.4% by PR and 5.6% by RK. Although the average deviation varies from one method to the other, the overall matching is acceptable.

Case No. 3

The third fluid sample is oil. This sample exhibits a bubble point pressure of 1,500 psig at reservoir temperature of 225 °F. The convergence pressure calculated by eq. 1 was 9,600 psia, and it was adjusted to 9,500 psia to match the experimental data. The simulation

study on this oil sample included the solubility and swelling test for two types of injection gases. The first was pure carbon dioxide, and the second was a mixture of 50% carbon dioxide and 50% nitrogen.

The simulation results, Figs. 22 through 26, show the match between the computed and the experimental data. These Figures depict comparisons between the K-value method and the equations of state of Nolen's model. Since the characterization factor, which is function of the boiling temperature of the component, has a direct effect on the calculated K-values by the K-value method, it was thought that adjusting the boiling temperature for the key components would improve the match. To be able to match the original bubble point pressure of the sample, the boiling temperature of methane was adjusted from its tabulated value to -249 °F. Also to match the saturation pressures after each injection of CO_2 or CO_2+N_2 slug, the boiling temperatures of CO_2 and N_2 were adjusted from the tabulated values. The boiling temperatures were adjusted to -129.3 °F for CO_2 , and to -330.4 °F for N_2 . Table 4 summarizes the average deviation for each plot. From Fig. 22, the K-value method shows an average deviation in the relative liquid volume calculation of 0.66% compared to 0.63% by PR and 0.44% by RK. Fig. 23 depicts the relative swollen volume vs. cumulative CO_2 volume injected. In this figure, the K-value method shows an average deviation of 1.31% compared to 0.63% by PR and 1.05% by RK. Fig. 24 depicts the saturation pressures vs. the cumulative CO_2 volume injected. In this figure, the K-value method shows an average deviation of 3.86% compared to 1.21% by PR and 3.26% by RK. Fig. 25 depicts the relative swollen volume vs. cumulative N_2+CO_2 volume

injected. In this figure, the K-value method shows an average deviation of 0.85% compared to 3.40% by PR and 3.20% by RK. Fig. 26 depicts the saturation pressures vs. the cumulative N_2+CO_2 volume injected. In this figure, the K-value method shows an average deviation of 2.50% compared to 1.19% by PR and 4.32% by RK. Although the average deviation varies from one method to the other, the overall matches are reasonable.

Case No. 4

The fourth fluid sample is oil. This sample exhibits a bubble point pressure of 215 psig at reservoir temperature of 110 °F. The convergence pressure calculated by eq. 1 was 13,500 psia, and that was adjusted to 13,560 psia to match the experimental data. The simulation study included the solubility and swelling test for pure carbon dioxide injection.

The simulation results, Figs. 27 through 29, show the match between the computed and the experimental data. These Figures depict comparisons between the K-value method and the equations of state of Nolen's model. To be able to match the original bubble point pressure of the sample, the boiling temperature of methane was adjusted from its tabulated value to -252 °F. Also to match the saturation pressures after each injection of CO_2 slug, using the K-value method, the boiling temperature of CO_2 was adjusted from its tabulated value to 130.3 °F. Table 4 summarizes the average deviation for each plot. From Fig. 27, the K-value method shows an average deviation in the

relative liquid volume calculation of 0.01% compared to 0.42% by PR and 0.42% by RK. Fig. 28 depicts the relative swollen volume vs. cumulative CO₂ injected. In this figure, the K-value method shows an average deviation of 0.59% compared to 3.50% by PR and 2.97% by RK. Fig. 29 depicts the saturation pressures vs. the cumulative CO₂ injected. In this figure, the K-value method shows an average deviation of 6.66% compared to 1.14% by PR and 2.19% by RK. Although the average deviation varies from one method to the other, the overall matches are reasonable.

Case No. 5

The fifth fluid sample is oil. This sample has a bubble point pressure of 249 psig at reservoir temperature of 155 °F. The convergence pressure calculated by eq. 1 was 11,700 psia, and that was adjusted to 11,820 psia to match the experimental data. The simulation study included the solubility and swelling test for pure carbon dioxide injection.

The simulation results, Figs. 30 through 32, show the match between the computed and the experimental data. These Figures depict comparisons between the K-value method and the equations of state of Nolen's model. To be able to match the original bubble point pressure of the sample, the boiling temperature of methane was adjusted from its tabulated value to -247 °F. Also to match the saturation pressures after each injection of CO₂ slug, using the K-value method, the boiling temperature of CO₂ was adjusted from its tabulated value to-

132.3 °F. Table 4 summarizes the average deviation for each plot. From Fig. 30, the K-value method shows an average deviation in the relative liquid volume calculation of 0.33% compared to 0.49% by PR and 0.42% by RK. Fig. 31 depicts the relative swollen volume vs. cumulative CO₂ injected. In this figure, the K-value method shows an average deviation of 1.27% compared to 1.58% by PR and 2.96% by RK. Fig. 32 depicts the saturation pressures vs. the cumulative CO₂ injected. In this figure, the K-value method shows an average deviation of 5.24% compared to 0.48% by PR and 3.41% by RK. Although the average deviation varies from one method to the other, the overall matches are reasonable.

Case No. 6

The sixth fluid sample is oil which has a bubble point pressure of 250 psig at reservoir temperature of 155 °F. The convergence pressure calculated by eq. 1 was 10,900 psia, and that was adjusted to 10,860 psia to match the experimental data. The simulation study included the solubility and swelling test for pure carbon dioxide injection.

The simulation results, Figs. 33 through 35, show the match between the computed and the experimental data. These Figures depict comparisons between the K-value method and the equations of state of Nolen's model. To be able to match the original bubble point pressure of the sample, the boiling temperature of methane was adjusted from its tabulated value to -249 °F. Also to match the saturation pressures

after each injection of CO₂ slug, using the K-value method, the boiling temperature of CO₂ was adjusted from its tabulated value to 134.3 °F. Table 4 summarizes the average deviation for each plot. From Fig. 33, the K-value method shows an average deviation in the relative liquid volume calculation of 0.75% compared to 0.80% by PR and 0.91% by RK. Fig. 34 depicts the relative swollen volume vs. cumulative CO₂ injected. In this figure, the K-value method shows an average deviation of 2.02% compared to 1.13% by PR and 1.64% by RK. Fig. 35 depicts the saturation pressures vs. the cumulative CO₂ injected. In this figure, the K-value method shows an average deviation of 6.35% compared to 1.29% by PR and 6.18% by RK. Although the average deviation varies from one method to the other, the overall matches are reasonable. At the critical point, (the last point on the graph at p=1914.7 psia), PR equation was more accurate than RK and the K-value method. This could be due to uncertainty in the measured data as reported in the laboratory report.

Case No. 7

Coats' gas condensate # 2 is a fluid virtually at its critical point. This sample exhibits a dewpoint pressure of 4,465 psia, at a reservoir temperature of 190 °F. The convergence pressure calculated by eq. 2 was 2,118.42 psia, and that was adjusted to 8,800 psia to match the experimental data. The simulation results, Figs. 36 through 38, show the match between the computed and the experimental data. These Figures depict comparisons between the K-value method and the

equations of state of Nolen's model. To be able to match the dew point pressure of the sample, the boiling temperature of methane was adjusted from its tabulated value to -245 °F. Table 4 summarizes the average deviation for each plot. From Fig. 36, the K-value method shows an average deviation in the relative liquid volume calculation of 3.34% compared to 0.53% by PR and 1.74% by RK. Fig. 37 depicts the liquid dropout vs. pressure. In this figure, the K-value method shows an average deviation of 2.69% compared to 2.67% by PR and 3.62% by RK. Fig. 38 depicts the cumulative gas produced vs. pressure. In this figure, the K-value method shows an average deviation of 6.68% compared to 3.08% by PR and 4.43% by RK. Although the average deviation varies from one method to the other, the overall matches are reasonable. Fig. 36 shows the change in relative volume as a function of pressure, the K-value method deviates slightly from the measured data and PR and RK equations show slightly better match.

Case No. 8

Coats' gas condensate # 5 exhibits a dewpoint pressure of 4,856.7 psia at 267 °F. The convergence pressure calculated by eq. 2 was 4,826.18 psia, and that was adjusted to 5,800 psia to match the experimental data. The simulation results, Figs. 39 through 41, show the match between the computed and the experimental data. These Figures depict comparisons between the K-value method and the equations of state of Nolen's model. To be able to match the dew point pressure of the sample, the boiling temperature of methane was

adjusted from its tabulated value to -242 °F. Table 4 summarizes the average deviation for each plot. From Fig. 39, the K-value method shows an average deviation in the relative liquid volume calculation of 2.57% compared to 4.50% by PR and 2.33 by RK. Fig. 40 depicts the liquid dropout vs. pressure. In this figure, the K-value method shows an average deviation of 14.13% compared to 15.49% by PR and 16.41% by RK. Fig. 41 depicts the cumulative gas produced vs. pressure. In this figure, the K-value method shows an average deviation of 2.74% compared to 5.17% by PR and 3.68% by RK. Although the average deviation varies from one method to the other, the overall matches are reasonable.

Case No. 9

Coats' oil # 2 is very volatile at a bubble point pressure of 4,475 psia and temperature of 176 °F. The convergence pressure calculated by eq. 1 was 6,200 psia, and that was adjusted to 6,180 psia to match the experimental data. The simulation results, Figs. 42 and 43, show the match between the computed and the experimental data. These Figures depict comparisons between the K-value method and the equations of state of Nolen's model. To be able to match the bubble point pressure of the sample, the boiling temperature of methane was adjusted from its tabulated value to -240 °F. Table 4 summarizes the average deviation for each plot. From Fig. 42, the K-value method shows an average deviation in the relative liquid volume calculation of 1.18% compared to 1.14% by PR and 2.10% by RK. Fig. 43 depicts the

cumulative gas produced vs. pressure. In this figure, the K-value method shows an average deviation of 6.57% compared to 4.61% by PR and 3.65% by RK. Although the average deviation varies from one method to the other, the overall matches are reasonable.

As concluding remarks on matching the PVT data, it is worth mentioning that, it was noted that some key parameters have direct effect on computed saturation pressure and phase equilibrium as follows:

- 1 - The critical properties of the heavy fractions play a fundamental role in matching the saturation pressure.
- 2 - The convergence pressures computed by Standing's equation for oils and Besserer's equation for condensates usually need more adjustments to improve the match. It is recommended to use those equations for initial estimates only.
- 3 - The boiling point of methane controls the computed saturation pressure by the K-value method, since it has direct effect on the values of the characterization factor and the computed K-values in turn. Therefore, slight adjustments to its value may improve the match.
- 4 - The boiling points of the injected gases control the computed saturation pressure by the K-value method, in particular CO₂ and N₂. Therefore, slight adjustments to those values may improve the match.

- 5 - In selecting the upper and lower bounds for the K-values equation parameters, for the LSLP model, it is recommended that different values be tried to get the best match.
- 6 - The fluid components to be selected into the compositional dependence of convergence pressure equation, in the K-value method, are usually intermediate hydrocarbons from ethane to hexanes.

CONCLUSIONS

The nine reservoir fluid samples simulated in this study, four retrograde gas condensate and five oil samples, included constant composition expansion, constant volume depletion, and solubility and swelling tests. Based on the simulation study, the following conclusions were reached:

- 1 - The K-value method developed in this work has shown good match with the experimental data for all mixtures, including crude oil-carbon dioxide mixtures. Comparing the results to those obtained by using the equations of state, the K-value method has shown the same level of accuracy as the equations of state. The K-value method was faster than the equations of state by a factor of seven to twenty. In addition, it required less computer memory, less input data and fewer parameters to adjust than the equations of state.
- 2 - The K-value method, despite the fact that it cannot be used for density calculations, worked well compared to the equations of state for matching the saturation pressures and the swollen volumes of four cases of CO₂ and N₂ injections into crude oil systems. The compositional data were not included in these tests. One of the four cases was a near critical point miscibility.

- 3 - The characterization factors of methane or the injection gases (CO_2 and N_2) were key factors in estimating the saturation pressures by the K-value method, since they had a direct effect on the computed K-values. Therefore, slight adjusting of the characterization factors may improve the match, by adjusting the boiling points of methane or the injection gases. In addition, the convergence pressure of each fluid system was adjusted from its theoretical value to improve the matching.
- 4 - The LSLP model was used to estimate the matching parameters for the K-value equation. The values of the upper and lower constraints for the K-value equation parameters were successively modified until the most acceptable match was obtained.
- 5 - An approach for characterizing the heavy hydrocarbon fractions was developed in this study as a combination of Ahmed's method, Whitson's method and Kay's mixing rules. It was successfully used to split the heptanes-plus into pseudo components and estimate their properties.

NOMENCLATURE

- a,b - constants in van der Waals' equation.
- A,B - constants of the cubic equations of state.
- C₇₊ - heptane plus pseudocomponent.
- C_n - carbon number.
- f_i - fugacity of component i.
- F_i - Hoffmann characterization factor of component i.
- F_k - characterization factor at p_k.
- g - function of liquid fractions.
- G_i^o - standard Gibbs free energy of component i.
- H_m - latent heat of vaporization.
- K_i - vapor-liquid equilibrium ratio of component i.
- L - number of moles in liquid phase, mole.
- MW - molecular weight, lb/mole.
- n_{ij} - number of moles of component i in phase j.
- N - total number of moles in a mixture, mole.
- N_c - total number of components in a mixture.
- N_g - number of multiple carbon number (MCN) groups.
- NI - number of observations (experimental data points).
- NJ - number of influence parameters.
- NR - number of runs.
- p - pressure, psia.
- P_i^o - vapor pressure of component i, psia.

| | | |
|--------|---|---|
| p_c | - | critical pressure, psia. |
| p_i | - | partial pressure of component i, psia. |
| p_k | - | convergence pressure, psia. |
| p_r | - | reduced pressure. |
| P | - | total pressure of a mixture, psia. |
| R | - | universal gas constant, per mole. |
| R_i | - | fugacity ratio of component i. |
| R_n | - | random number at run n. |
| T | - | temperature, °F(°R). |
| T_b | - | normal boiling temperature, °F(°R). |
| T_c | - | critical temperature, °F(°R). |
| T_r | - | reduced temperature. |
| v | - | volume, cu. ft. |
| V | - | number of moles in vapor phase, mole. |
| V_c | - | critical volume, cu. ft. |
| x_i | - | liquid mole fraction of component i in a mixture. |
| X_j | - | influence parameter j. |
| XL_j | - | lower bound of influence parameter j. |
| XU_j | - | upper bound of influence parameter j. |
| y_i | - | vapor mole fraction of component i in a mixture. |
| z_i | - | mole fraction of component i in total mixture. |
| Z | - | compressibility factor. |
| Z_c | - | compressibility factor at the critical point. |
| Z_n | - | mole fraction of carbon number fraction C_n . |

Greek

- γ - specific gravity.
 δ_{ij} - binary interaction parameter for hydrocarbons.
 ϵ - error norm (tolerance).
 ζ_{ij} - binary interaction parameter for hydrocarbon-carbon dioxide system.
 ω - Pitzer acentric factor.
 Ω_a, Ω_b - equations of state empirical constants.
 Φ_i - fugacity coefficient of component i.

Subscripts

- b - bubble point.
c - critical.
d - dew point.
g - MCN group.
i - component i.
I - pseudocomponent I.
j - component j, or phase j.
k - convergence.
r - reduced.
1,2 - intended to indicate different conditions of pressure and temperature.

Superscripts

- cal - calculated value.
exp - experimental value.

- j - iteration number.
- r - run number r.
- ° - degree.
- 0 - standard values.

Abbreviations

- Exp - exponential.
- °F - degree Fahrenheit.
- °R - degree Rankin.
- ln - logarithm (natural).
- log - logarithm.
- psia - pounds per square inch absolute.
- psig - pounds per square inch gauge.
- rbbl - reservoir barrels.
- scf - standard cubic feet.
- vs - versus.

REFERENCES

1. Coats, K. H. and Smart, G. T.: "Application of a Regression-Based EOS PVT Program to Laboratory Data," SPE Reservoir Eng., (May 1986) 277-299.
2. Stalkup, F.I.: "Status of Miscible Displacement," JPT, (April 1983) 815-826.
3. Turek, E. A., Metcalfe, R. S., Yarborough, L., and Robinson Jr., R. L.: "Phase Equilibria in Carbon Dioxide-Multicomponent Hydrocarbon Systems: Experimental Data and an Improved Prediction Technique," SPE Paper 9231, presented at the 55th Annual Technical Conference and Exhibition, Dallas, Tx, Sept. 21-24, 1980.
4. Moses, P. L.: "Engineering Applications of Phase Behavior of Crude Oil and condensate Systems," JPT, (July 1986) 715-723.
5. Simon, R. , Rosman, A., and Zana, E.: "Phase Behavior Properties of CO₂-Reservoir Oil Systems," SPE Paper 6387, presented at the Permian Basin Oil and Gas Recovery Conference, Midland, TX, March 10-11, 1977.
6. Besserer, G. J., Serra, J. W., and Best, D. D.: "An Efficient Phase behavior Package for Use in Compositional Reservoir Simulation Studies," SPE Paper 8288, presented the 54th Annual Technical Conference and Exhibition, Las Vegas, NV, Sept. 23-25, 1979.
7. Stalkup, F. I.: "Miscible Displacement", Monograph Series, SPE Dallas (1983), 8.
8. Obut, S. T., Ertkin, T., and Geisbrecht, R. A.: "A Versatile Phase Equilibrium Package for Compositional Simulation," SPE Paper 15083, presented at the 56th California Regional Meeting, Oakland, CA, April 2-4, 1986.
9. Risnes, R., Dalen, V., and Jensen, J. I.: "Phase Equilibrium Calculations in the Near-Critical Region," Proceedings, 1981 European Symposium on EOR, Elsevier Sequoia S. A., Lausanne, Sept. 21-23, 1981.

10. Varotsis, N., Todd, A. C., and Stewart, G.: "An Iterative Method for Phase Equilibria Calculations with Particular Application to Multicomponent Miscible Systems," Proceedings, 1981 European Symposium on EOR, Elsevier Sequoia S. A., Lausanne, Sept. 21-23, 1981.
11. Mehra, R. K., Heidmann, R. A., and Aziz, K.: "Computation of Multiphase Equilibrium for Compositional Simulation," SPEJ, (February 1982), 61-68.
12. Grigg, R. B. and Lingane, P. J.: "Predicting Phase Behavior of Mixtures of Reservoir Fluids with Carbon Dioxide," SPE Paper 11960, presented at the 58th Annual Conference and Exhibition, San Francisco, CA, Oct. 5-8, 1983.
13. Bashbush, J. L.: "A Method to Determine K-Values From Laboratory Data and its Applications," SPE Paper 10127, presented at the 56th Annual Technical Conference and Exhibition, San Antonio, TX, Oct. 5-7, 1981.
14. Rzasa, M. J., Glass, E. D., and Opfell, J. B.: "Prediction of Critical Properties and Equilibrium Vaporization Constants for Complex Hydrocarbon Systems," Chem. Eng. Progr. Symp. Series No. 2 (1952) 48, 28-37.
15. Engineering Data Book, 7th Edition, Natural Gas Processors and Suppliers Assoc., Tulsa, Oklahoma (1957) 162-174, K-1 - K-132.
16. Norman, R. L., and Williams, B.: "Presentation of NGPA Equilibrium Ratio Data for Machine Computation," Proc., 37th Annual Conv., Natural Gasoline Assoc. of America (1958), 61-64.
17. Engineering Data Book, 8th Edition, Natural Gas Processors and Suppliers Assoc., Tulsa, Oklahoma (1966) 216-293.
18. Cajander, B. C., Hipkin, H.G., and Lenior, J. M.: "Prediction of Equilibrium Ratios From Nomograms of Improved Accuracy," J. Chem. Eng. Data, (July 1960) 5, 251-259.
19. Woertz, B. B.: "Vapor-Liquid Equilibrium Ratios (K-Values) of Light Hydrocarbons at Reservoir Conditions," SPEJ (June 1971) 11, 176-184; Trans. AIME, 251.
20. Canfield, F. G.: "Estimate K-Values with Computer," Hydrocarbon Proc. (April 1971) 50, 137-138.
21. MacDonald, R. C.: "Reservoir Simulation with Interphase Mass Transfer," Report No. UT 71-2, Texas Petroleum Research Committee, The University of Texas at Austin (Dec. 15, 1971).

22. Vadiei, A.: "Correlation of Vapor-Liquid Equilibrium Ratios for Light Normal Paraffin Hydrocarbons," Report No. UT 72-5, Texas Petroleum Research Committee, The University of Texas at Austin (July 31, 1972).
23. Lawal, A. S., and Silberberg, I. H.: "A New Correlation of Vapor-Liquid Equilibrium Ratios Internally Consistent With Critical Behavior," SPE Paper 10287, presented at the 56th Annual Technical Conference and Exhibition, San Antonio, TX, Oct. 5-7, 1981.
24. Galimberti, M., and Campbell, J. M.: "New Method Helps Correlate K-Values for Behavior of Paraffin Hydrocarbons," the Oil & Gas Journal, (November 3rd, 1969) 64-67.
25. Wilson, G. M.: "A Modified Redlich-Kwong Equation of State, Application to General Physical Data Calculations," paper presented at the 65th National AIChE Meeting, Cleveland, OH, 1969.
26. Whitson, C. H., and Torp, S. B.: "Evaluating Constant Volume Depletion Data," JPT (March 1983), 610-620.
27. Hoffmann, A. E., Crump, J. S. and Hocott, C. R.: "Equilibrium Constants for a Gas-Condensate System," Trans., AIME (1953) 198, 1-10.
28. Brinkmann, F. H. and Sicking, J. N.: "Equilibrium Ratios for Reservoir Studies," Trans., AIME (1960) 219, 313-319.
29. Dykstra, H. and Mueller, T. D.: "Calculation of Phase Compositions and Properties for Lean- or Enriched-Gas Drive," paper SPE Paper 1019, presented at SPE California Regional Meeting, Los Angeles, CA, Nov. 5-6, 1964.
30. Soave, G.: "Equilibrium Constants From a Modified Redlich-Kwong Equation of State," Chem. Engineers Science (1972) 27, No. 6, 1197-1203.
31. Peng, D. Y. and Robinson, D. B.: "A New Two-Constant Equation of State," I. & E. C. Fundamentals (1976) 15, No. 1, 59-64.
32. Schmidt, G. and Wenzel, H.: "A Modified Van der Waals' Type Equation of state," Chem. Eng. Science, Vol. 135, 1503-1512, 1980.
33. Whitson, C. H.: "Effect of C₇₊ Properties on Equation-of-State Predictions," SPEJ, (December 1984) 685-696.

34. Van Ness, H. C. and Abbott, M. M., Classical Thermodynamics of Nonelectrolyte Solutions, 1st edition, 1982, McGraw-Hill, New York, 423-430.
35. Ahmed, T. H., Cady, G. V., and Story, A. L.: "A Generalized Correlation for Characterizing the Hydrocarbon Heavy Fractions," SPE Paper 14266, presented at the 60th Annual Conference and Exhibition, Las Vegas, NV, Sept. 22-25, 1985.
36. Katz, D. L. and Firozabadi, A.: "Predicting Phase Behavior of Condensate-Crude Oil Systems Using Methane Interaction Coefficients," SPE Paper 6721, presented at the 52nd Annual Conference and Exhibition, Denver, Colorado, Oct. 9-12, 1977.
37. Orr Jr, F. M. and Jensen, C. M.: "Interpretation of Pressure-Composition Phase Diagrams for CO₂/Crude-Oil Systems," SPEJ, (October 1984), 485-497.
38. Kenyon, D. E. and Behie, A.: "Third SPE Comparative Solution Project: Gas Cycling of Retrograde Condensate Reservoirs," SPE Paper 12278, presented at the Reservoir Simulation Symposium, San Francisco, CA, Nov. 15-18, 1983.
39. Ahmed, T. A.: "Comparative Study of Eight Equations of State for Predicting Hydrocarbon Volumetric Phase Behavior," SPE Paper 15673, presented at the 61th Annual Technical Conference and Exhibition, New Orleans, LA, Oct. 5-8, 1986.
40. Coats, K. H., Dempsey, J. R. and Henderson, J. H.: "A New Technique for Determining Reservoir Description from Field Performance Data," SPEJ (March 1970), 66-74.
- 41 - Metcalfe, R. S., and Yarborough, L.: "Effect of Phase Equilibria on the CO₂ Displacement Mechanism," SPEJ (August 1979) 242-252.
42. Engineering Data Book, 9th Edition, Natural Gas Processors and Suppliers Assoc., Tulsa, Oklahoma (1972) 18-1 - 18-111.
43. Hadden, S. T.: "Convergence Pressure in Hydrocarbon Vapor-Liquid Equilibria," AICHE Progress Series, No. 7, (1953) 53.
44. Kesler, M. G., Lee, B. I., Benzing, D. W., and Cruz, A.: "Method Improves Convergence Pressure Predictions," Hydrocarbon Process, (June 1977) 56, No. 6, 177-179.
45. Rowe, A. M.: "Internally Consistent Correlation for Predicting Phase Composition for Use in Reservoir Composition Simulators," paper SPE Paper 7475 presented at 53rd Annual Fall Meeting, Houston, Texas, (Oct. 1978).

46. Standing, M. B.: "Volumetric and Phase Behavior of Oil Field Hydrocarbon Systems," Published by SPE/AIME, Dallas, Texas, (1977).
- 47 - Abel, W., Jackson, R. F., and Wattenbarger, R.A.: "Simulation of a Partial Pressure Maintenance Gas Cycling Project with a Compositional Model, Carson Creek Field, Alberta," SPE Paper 2580, presented at the 44th Annual Conference and Exhibition, Denver, Colorado, Sept. 28 - Oct.1, 1969.
- 48 - Van der Waals, J. D.: Doctoral Dissertation, Leiden, Holland, 1873.
- 49 - Redlich, O., and Kwong, J. N. S.: "On the Thermodynamics of Solutions. V: An Equation of State. Fugacities of Gaseous Solutions," Chem. Reviews (1948) 44, 233-244.
- 50 - Martin, J. J.: "Equations of State," Applied Thermodynamics Symposium (1967) 59, 12, 34-52.
- 51 - Usdin, E., and McAuliffe, J. C.: "A One Parameter Family of Equations of State," Chem. Eng. Sci. (1976) 31, 1077-1084.
- 52 - Baker, L. E., Pierce, A. C., and Kramer, D. L.: "Gibbs Energy Analysis of Phase Equilibria," SPE/DOE 9806, presented at SPE/DOE 2nd joint Symposium on EOR, Tulsa, PK, April 5-8, 1981.
- 53 - Watson, K. M. and Nelson, E. F.: "Improved Methods for Approximating Critical and Thermal Properties of Petroleum Fraction," Ind. Eng. Chem. (August 1933) 880-887.
- 54 - Watson, K. M., Nelson, E. F., and Murphy, G. B.: "Characterization of Petroleum Fractions," Ind. Eng. Chem. (December 1935) 1460-1464.
- 55 - Edmister, W. C.: "Improved Integral Technique for Petroleum Distillation Calculations," AIChE J. (September 1955) 1685-1690.
- 56 - Taylor, D. L. and Edmister, W. C.: Proceedings of the International Symposium on Distillation, Inst. Chem. Engrs., London, 1969, p.5.
- 57 - Taylor, D. L. and Edmister, W. C.: "Solutions for Distillation Processes Treating Petroleum Fractions," AIChE J. (November 1971) 1324-1329.
- 58 - Lee, S. T., Jacoby, R. H., Chen, W. H., and Culham, W. E.: "Experimental and Theoretical Studies on the Fluid Properties Required for Simulation of Thermal Processes," SPEJ (October 1981) 535-550.

- 59 - Whitson, C. H.: "Characterizing Hydrocarbon Plus Fractions," SPEJ (August 1983) 683-694.
- 60 - Mehra, R. K., Heidmann, R. A., Aziz, K., and Donnelly, J. K.: "A Statistical Approach for Combining Reservoir Fluids into Pseudo-Components for Compositional Model Studies," SPE Paper 11201, presented at the SPE Annual Fall Technical Conference and Exhibition held in New Orleans, September 26-29, 1982.
- 61 - Kesler, M. G. and Lee, B. I.: "Improved Predictions of Enthalpy of Fractions," Hydrocarbon Processing (March 1976) 153-158.
- 62 - Hong, K. C.: "Lumped-Component Characterization of Crude Oils for Compositional Simulation," SPE/DOE Paper 10691 presented at the SPE/DOE Third Joint Symposium on Enhanced Oil Recovery held in Tulsa, April 4-7, 1982.
- 63 - Schlijper, A. G.: "Simulation of Compositional Processes: The Use of Pseudo-Components in Equation-of-State Calculations," SPE Reservoir Engineering (September 1986) 441-452.
- 64 - Montel, F. and Gouel, P. L.: "A New Lumping Scheme of Analytical Data for Compositional Studies," SPE Paper 13119 presented at the SPE Annual Technical Conference and Exhibition held in Houston, September 16-19, 1984.
- 65 - Ahmed, T. H., Cady, G. V., and Story, A. L.: "A Generalized Correlation for Characterizing the Hydrocarbon Heavy Fractions," SPE Paper 14266 presented at the SPE Annual Technical Conference and Exhibition held in Las Vegas, September 22-25, 1985.
- 66 - Behrens, R. A. and Sandler, S. I.: "The Use of Semicontinuous Description to Model the C₇₊ Fraction in Equation of State Calculation," SPE/DOE Paper 14925 presented at the SPE/DOE Fifth Joint Symposium on Enhanced Oil Recovery held in Tulsa, April 20- 23, 1986.
- 67 - Obut, S. T. and Ertekin, T.: "Determination of Interaction Coefficients and Critical Properties of Heavy Fractions for Equation of State Computations: An Automated Algorithmic Approach," SPE Paper 16940 presented at the Annual Technical Conference and Exhibition held in Dallas, September 27-30, 1987.
- 68 - Kay, W. B.: "Density of Hydrocarbon Gases and Vapors at High Temperature and Pressure," Ind. and Eng. Chem. (1936) 28, 1014-1019.

- 69 - Lohrenz, J., Bray, B. G., and Clark, C. R.: "Calculating Viscosities of Reservoir Fluids from their Compositions," JPT (October 1984) 1171-1176.
- 70 - Pedersen, K. S., Thomassen, P., and Fredenslund, A.: "Phase Envelope Calculations Using the SRK equation of State, I," SPE Paper 8204, presented the 54th Annual Technical Conference and Exhibition, Las Vegas, NV, Sept. 23-25, 1979.
- 71 - Pedersen, K. S., Thomassen, P., and Fredenslund, A.: "Flash and PVT Calculations Using the SRK equation of State, II," SPE Paper 8207, presented the 54th Annual Technical Conference and Exhibition, Las Vegas, NV, Sept. 23-25, 1979.
- 72 - Ahmed, T. H., Cady, G. V., and Story, A. L.: "An Accurate Method for Extending the Analysis of C₇₊," SPE Paper 12916 presented at the 1984 Rocky Mountain Regional Meeting held in Casper, NY, May 21-23, 1984.
- 73 - Documentation of SSC N-Comp Simulation Package, Scientific Software, Houston, Texas, 1971.
- 74 - Documentation of Nolen's Compositional Simulation Package, Nolen's & Associates, Houston, Texas, 1987.
- 75 - Rachford, Jr., H. H. and Rice, J. D.: "Procedure for Use of Electronic Digital Computers in Calculating Flash Vaporization Hydrocarbon Equilibrium," JPT, (October 1952) sec.1/19-sec.2/3.
- 76 - Mehra, R. K., Heidmann, R. A., and Aziz, K.: "The Computation of Multi-phase Equilibrium in Compositional Reservoir Studies" Ph.D. Dissertation, University of Calgary, (1981).
- 77 - Callen, H. B.: "Thermodynamics," Wiley, New York, (1960).
- 78 - Trangenstein, J. A.: "Minimization of Gibbs Free Energy in Compositional Reservoir Simulation," SPE Paper 13520, presented at the Reservoir Simulation Symposium, Dallas, TX, Feb. 10-13, 1985.
- 79 - Heidemann, R. A.: "Three-Phase Equilibria Using Equations of State," AIChE Journal, 20, 5, (Sept. 1974) 847-855.
- 80 - Fussell, L. T. and Fussell, D. D.: "An Iterative Sequence for Compositional Reservoir Models Incorporating the Redlich-Kwong Equation of State," SPE 6891, presented at the 52nd Annual Conference and Exhibition, Denver, Colorado, Oct. 9-12, 1977.
- 81 - Fussell, D. D. and Yanosik, J. L.: "An Iterative Sequence for Phase-Equilibria Calculations Incorporating the Redlich-Kwong Equation of State," SPEJ (June 1978), 173-182.

- 82 - Williams, C. A., Zana, E. N., and Humphrys, G. E.: "Use of the Peng-Robinson Equation of State to Predict Hydrocarbon Phase Behavior and Miscibility for Fluid Displacement," SPE 8817, presented at the First Joint SPE/DOE Symposim on EOR, Tulsa, OK, April 20-23, 1980.
- 83 - Heidemann, R. A. and Khalil, A. M.: "The Calculation of Critical Points," AIChE Journal, 26, 5, (Sept. 1980) 769-779.
- 84 - Risnes, R., and Dalen, V.: "Equilibrium Calculations for Coexisting Liquid Phases," SPEJ (February 1984) 87-96.
- 85 - Nghiem, L. X. and Heidmann, R. A.: "General Acceleration Procedure for Multiphase Flash Calculation with Application to Oil-Gas-Water Systems," Proceedings, 1982 European Symposium on EOR, Paris, France, Nov.8-10, 1982.
- 86 - Mehra, R. K., Heidmann, R. A., and Aziz, K.: "An Accelerated Successive Substitution Algorithm," the Canadian Journal of Chem. Eng. (August 1983) 590-596.
- 87 - Nghiem, L. X. and Li, Y. K.: "Approximate Flash Calculations for Equation-of-State Compositional Models," SPE 13517, presented at the Reservoir Simulation Symposium, Dallas , TX, Feb. 10-13, 1985.
- 88 - Enick, R. M., Holder, G. D., Grenko, J. A., and Brainard, A. J.: "Four-Phase Flash Equilibrium Calculations for Multicomponent Systems Containing Water," American Chemical Society, Chapter 24, 494-518, 1986.
- 89 - Enick, R. M., Holder, G. D. and Mohamed, R. S.: "Four-Phase Flash Equilibrium Calculations Using the Peng-Robinson Equation of State and a Mixing Rule for Asymmetric Systems," SPE 14148, presented at the 60th Annual Technical Conference and Exhibition, Las Vegas, NV, Sept. 22-25, 1985.
- 90 - Kossack, C. A., Hagen, S., and Munkerud, P. K.: "Phase Behavior Calculations Near the Critical Point," SPE 15402, presented at the 61st Annual Technical Conference and Exhibition, New Orleans, LA, Oct. 5-8, 1986.
- 91 - Mohammed, S. A.: "Simulation As A Petroleum Engineering Tool for Predicting the Performance of Oil Reservoirs Under Varying Conditions" M.Sc. Thesis, Cairo University, Egypt, (1982).
- 92 - Taha, H. A.: "Operations Research - An Introduction" 4th edition, McMillan Publishing Co., Inc., (1987).

- 93 - Special PVT Routine Laboratory data Report, Private communication, 1987.
- 94 - McCain, W. D. Jr.: "The Properties of Petroleum Fluids", PennWell Publishing Co., Tulsa, Oklahoma, (1973).

APPENDIX A

FLASH CALCULATIONS

The most common procedure for flash calculations is the method of successive substitution.⁷⁵ This method is used in this study, along with the modifications introduced to accelerate and stabilize this technique. The modified method is known as the accelerated and stabilized successive substitution method.

Some highlights on the backgrounds of the phase equilibria of hydrocarbon systems and their thermodynamics, and the details of the flash calculation process, are introduced in the following.

EQUILIBRIUM CONDITIONS FOR MULTIPHASE SYSTEMS

The criterion of equilibrium for a system which is isolated from all external influences may be expressed in any of the following entirely equivalent forms:⁷⁶⁻⁷⁸

(1) For the equilibrium of any isolated system it is necessary and sufficient that in all possible variations of the state of the system which do not alter its energy, the variation of its entropy shall either vanish or be negative. Therefore, in mathematical terms, the condition is expressed as:

$$(\delta S)_U \leq 0 \quad \dots\dots\dots(A-1)$$

(2) For the equilibrium of any isolated system it is necessary and sufficient that in all possible variations of the state of the

system which do not alter its entropy, the variation of its energy shall either vanish or be positive, Thus:

$$(\delta U)_S \geq 0 \quad \dots\dots\dots(A-2)$$

(3) In a state of thermodynamic equilibrium, the Gibbs free energy of the system is minimum over the manifold of states of constant temperature and pressure. Thus:

$$(\delta G)_{T,p} \leq 0 \quad \dots\dots\dots(A-3)$$

For the case of multiphase systems, Callen (1960)⁷⁷ described the equilibrium state as the state which produces a minimum on the free energy surface. Therefore, the equilibrium problem is to minimize:

$$G = R T \sum_{j=1}^{\pi} \sum_{i=1}^{Nc} n_{ij} \mu_{ij} + \sum_{i=1}^{Nc} n_i^0 G_i^0 \quad \dots\dots\dots(A-4)$$

Subject to the mass balance constraints:

$$\sum_{j=1}^{\pi} n_{ij} = n_i^0 \quad i = 1, 2, \dots, Nc \quad \dots\dots\dots(A-5)$$

and $n_{ij} > 0$

$$i = 1, 2, \dots, Nc$$

$$j = 1, 2, \dots, \pi$$

.....(A-6)

where:

- G_i^0 : Standard Gibbs free energy of component i.
 n_{ij} : Number of moles of component i in phase j.
 μ_{ij} : Chemical potential of component i in phase j.
 N_c : Number of components in the system.
 π : Number of phases.

TWO PHASE FLASH CALCULATIONS

To perform the two-phase flash calculations in this study, the systematic approach of addition of phases introduced by Risnes *et al*⁹ is implemented. The basis of this approach for a two-phase flash problem is the successive substitution method, which consists of the following four basic steps:⁷⁹⁻⁹⁰

- (1) assumption of starting k-values,
- (2) calculation of vapor and liquid phases mole fractions and compositions that correspond to the assumed k-values,
- (3) calculation of component fugacities in each phase and checking for the equality criterion, and
- (4) correcting the assumed k-values on the basis of fugacities, if the equality criterion is not satisfied.

Repetition of steps 2 - 4 is continued until convergence is observed. Simultaneous handling of phases is the most efficient method as long as the initial k-values estimates are sufficiently good.

For two phase systems, considering N moles of feed mixture, having composition z_i , which separates into L moles of liquid, of composition x_i , and V moles of vapor, of composition y_i , we would have an overall material balance and a component balance equation for each component as:

$$L + V = N \quad \dots\dots\dots(A-7)$$

$$L x_i + V y_i = N z_i \quad \dots\dots\dots(A-8)$$

As the compositions are given in mole fractions, we can impose the following constraints:

$$\sum_{i=1}^{Nc} z_i = 1.0$$

$$\sum_{i=1}^{Nc} x_i = 1.0$$

$$\sum_{i=1}^{Nc} y_i = 1.0 \quad \dots\dots\dots(A-9)$$

Eqs. A-7, A-8, and A-9 constitute a system of $Nc+2$ equations in the $2Nc+2$ unknowns; namely: L , V , x_i and y_i . From the thermodynamic equilibrium of the system, the fugacities in the liquid and the vapor phase of each component must be equal, and that will provide additional Nc equations.

$$f_{iL} = f_{iV} \dots\dots\dots(A-10)$$

Now, the $2N_c+2$ equations define the two phase equilibrium problem completely.

In an equation of state approach, the fugacities can be directly calculated from the equation of state. The fugacity then will depend on the temperature, pressure, composition, and type of phase considered, i.e.:

$$f_i = F(T, p, x_i, \text{phase}(L, V)) \dots\dots\dots(A-11)$$

For a cubic equation of state, the same equation is used both for the liquid and the vapor phases.

Basic Successive Substitution Method

The basic successive substitution method is based on the concept of equilibrium ratios K_i defined by:

$$K_i = y_i / x_i \dots\dots\dots(A-12)$$

Introducing the fugacity coefficient ψ_i , the fugacities can be written as:

$$f_{iL} = x_i \psi_{iL} P \quad \dots\dots\dots(A-13)$$

$$f_{iV} = y_i \psi_{iV} P \quad \dots\dots\dots(A-14)$$

In equilibrium, the fugacities are equal and hence the equilibrium ratios are given by:

$$K_i = \psi_{iL} / \psi_{iV} \quad \dots\dots\dots(A-15)$$

This is an important relation since it allows the definition of K-values outside the two-phase region. During the iteration process when the fugacities are not yet equal, the improved K-value estimates are obtained by:

$$\begin{aligned} K_i^{j+1} &= \psi_{iL} / \psi_{iV} \\ &= K_i^j R_i^j \quad \dots\dots\dots(A-16) \end{aligned}$$

where:

j : iteration number

R_i : fugacity ratio = f_{iL} / f_{iV}

The criterion for acceptance of a solution is based on the fugacity ratio. To comply with the other solution methods, the following error norm is used in this work:

$$\rho = \sum_{i=1}^{Nc} (R_i - 1.0)^2 < \epsilon \quad \dots\dots\dots(A-17)$$

Typically, this error norm, $\epsilon = 10^{-12}$.

When the equilibrium ratios are given, the system of flash Eqs. A-7 - A-10, and A-12 can be solved using the $g(V)$ function. Considering one mole of feed, $N = 1.0$, and eliminating L in Eq. A-8, we get:

$$\sum_{i=1}^{Nc} x_i + V \sum_{i=1}^{Nc} (y_i - x_i) = 1.0 \quad \dots\dots\dots(A-18)$$

The $g(V)$ function is defined by:

$$\begin{aligned} g(V) &= \sum_{i=1}^{Nc} (y_i - x_i) \\ &= \sum_{i=1}^{Nc} (K_i - 1.0) z_i / (1.0 + V (K_i - 1.0)) \\ &= 0.0 \quad \dots\dots\dots(A-19) \end{aligned}$$

From Eq. A-19, the vapor mole fraction V can be readily determined as the root of this equation. Looking at this equation, we notice that:

$$\begin{aligned} g(0) &= \sum_{i=1}^{Nc} z_i K_i - 1.0 \\ &= 0.0 \quad \dots\dots\dots(A-20) \end{aligned}$$

$$\begin{aligned}
 g(1) &= 1.0 - \sum_{i=1}^{Nc} (z_i / K_i) \\
 &= 0.0 \quad \dots\dots\dots(A-21)
 \end{aligned}$$

This function is characterized by the following:

- (1) It is monotonic in V as its slope (the first derivative) is always negative;

$$g'(V) = - \sum_{i=1}^{Nc} z_i (K_i - 1.0)^2 / (1.0 + V (K_i - 1.0))^2 \quad \dots\dots\dots(A-22)$$

- (2) When $g(0) \geq 0.0$ and $g(1) = 0.0$, the mixture is at its dew point (saturated vapor).
- (3) When $g(0) = 0.0$ and $g(1) \leq 0.0$, the mixture is at its bubble point (saturated liquid).
- (4) When $g(0) > 0.0$ and $g(1) < 0.0$, two phases, liquid and vapor, are present.
- (5) When $g(0) \geq 0.0$ and $g(1) \geq 0.0$, single vapor phase exists.
- (6) When $g(0) \leq 0.0$ and $g(1) \leq 0.0$, single liquid phase exists.

Eq. A-19 can be readily solved by the Newton-Raphson method. As the $g(V)$ function has always a negative slope, there will only be one root of interest. When the value of V is determined, the compositions can be calculated in a straight forward manner. When

the root of Eq. A-19 gets outside the interval [0.0 , 1.0], this indicates a single-phase state. Then, the non-existing phase is calculated as if the system were at the saturation pressure.

If $V < 0.0$, this means single liquid phase exists, then set:

$$V = 0.0$$

$$x_i = z_i$$

$$y_i = K_i x_i / \sum_{i=1}^{Nc} (K_i x_i) \dots\dots\dots(A-23)$$

If $V > 1.0$, this means single vapor phase exists, then set:

$$V = 1.0$$

$$y_i = z_i$$

$$x_i = (y_i / K_i) / \sum_{i=1}^{Nc} (y_i / K_i) \dots\dots\dots(A-24)$$

The normalization is necessary as this is not automatically assured outside the two-phase region. A common factor in the K-values has no effect on the composition of the non-existing phase; and when the K-values are corrected according to the fugacity ratios, the compositions are corrected only to the extent that the

fugacity ratios deviate from the average value. The system will converge to a definite composition, and the fugacity ratios will converge to a common constant value. This limiting value will be different from unity unless the system is at the saturation pressure.

K-values Estimation

To start the iteration procedure of the flash calculations, a set of initial K-values should be estimated as a starting point. There are three conditions which these estimates should meet:

- (1) The estimates should be as close as possible to the expected values in order to obtain a rapid solution.
- (2) The estimates should assure that the flash calculations start in the two-phase region in order to avoid false single-phase solutions.
- (3) The estimates should have sufficient spread to avoid false solutions where all K-values become equal to one.

It was found that Wilson's empirical Eq. A-25, having the form:

$$K_i = (1.0 / P_{ri}) \exp[5.3727 (1.0 + \omega_i) (1.0 - 1.0 / T_{ri})] \dots\dots\dots(A-25-a)$$

sufficiently meets all the previously mentioned conditions.

Eq. A-25-a was latter modified by Whitson²⁶ to consider the convergence pressure to properly estimate K-values near the critical

region, normally at pressures above 500 psia. The new form of this correlation is:

$$K_i = (P_{ci}/P_k)^{(A-1)} (1/P_{ri}) \exp[5.3727 (1 + \omega_i) (1 - 1/T_{ri})] \dots\dots\dots(A-25-b)$$

where:

A : slope of $\log(K_i p)$ vs. $\log(F_i)$

The Acceleration Procedure

When the system is near the critical point, the rate of convergence may become very slow. An equation similar to Aitken's accelerating formula can then be used to speed up the convergence rate. 9,84-86

The equilibrium constants can be regarded as long products, starting with initial estimate K_i^0 and then multiplied by the fugacity ratios R_i which approaches unity as the number of iterations increases. This can be written as:

$$K_i = K_i^0 * R_i^1 * R_i^2 * R_i^3 * \dots\dots * R_i^j \dots\dots\dots(A-26)$$

Taking the logarithm of both sides, we obtain:

$$\begin{aligned} \log(K_i) = & \log(K_i^0) + \log(R_i^1) + \log(R_i^2) + \dots \\ & \dots + \log(R_i^j) \\ & \dots \dots \dots (A-27) \end{aligned}$$

Since in the first part of an equilibrium calculation the fugacity ratios may change from values smaller than one to values greater than one, the signs in the series in Eq. A-27 will alternate. Usually after 20 - 50 iterations, the situation is characterized by a monotone and a steady approach towards the solution. Therefore, after doing 50 - 60 iterations or more, the process can be accelerated by replacing the remaining part of the series by a geometric series where Q is the ratio between any two consecutive terms. Then, we get:

$$\begin{aligned} \log(K_i^{j+1}) = & \log(K_i^j) + \log(R_i^j) * (1.0 + Q + Q^2 + \dots) \\ & \dots \dots \dots (A-28) \end{aligned}$$

$$\begin{aligned} = & \log(K_i^j) + \log(R_i^j) * 1.0 / (1.0 - Q) \\ & \dots \dots \dots (A-29) \end{aligned}$$

where:

$$\begin{aligned} Q = & \log(R_i^{j+1}) / \log(R_i^j) \\ = & \log(R_i^j) / \log(R_i^{j-1}) \\ \approx & (R_i^j - 1.0) / (R_i^{j-1} - 1.0) \\ & \dots \dots \dots (A-30) \end{aligned}$$

The resulting acceleration formula is:

$$K_i^{j+1} = K_i^j \cdot [R_i^j]^{(1.0 / (1.0 - Q))} \dots\dots\dots(A-31)$$

A common practice, in doing this acceleration procedure, is to do a single step calculation between each accelerated step in order to determine the value of Q in the exponent in Eq. A-31.

The Bring - Back Procedure

When the system is in a single-phase state, the composition of the non-existing phase is calculated by Eq. A-23:^{9,84}

$$y_i = x_i K_i / \sum_{i=1}^{Nc} (x_i K_i) \dots\dots\dots(A-23)$$

or by Eq. A-24:

$$x_i = (y_i / K_i) / \sum_{i=1}^{Nc} (y_i / K_i) \dots\dots\dots(A-24)$$

Since a common factor in the set of equilibrium ratios has no effect on the composition of the non-existing phase, this gives the possibility to adjust the K-values to make the g(V) function equals zero, or in other words, to keep the non-existing phase at the edge of the two-phase region while testing for its existence.

In the first case of a single-phase liquid, V equals zero, and the multiplication factor β can be determined from the relation:

$$\sum_{i=1}^{Nc} (\beta K_i - 1.0) z_i = 0.0 \quad \dots\dots\dots(A-32)$$

i.e.:

$$\beta = \frac{\sum_{i=1}^{Nc} z_i}{\sum_{i=1}^{Nc} (K_i z_i)} \quad \dots\dots\dots(A-33)$$

which gives a new set of equilibrium ratios as:

$$\begin{aligned} K_i^{\text{new}} &= \beta K_i \\ &= K_i / \sum_{i=1}^{Nc} (K_i z_i) \quad \dots\dots\dots(A-34) \end{aligned}$$

on which we apply the normal correction factors as the fugacity ratios (f_{iL} / f_{iV}).

As explained by Risnes *et al*⁹, from a physical point of view, this corresponds to creating a nucleus gas bubble and see if it will grow or disappear. A gas bubble will grow spontaneously if the fugacity is lower in the gas phase than in the liquid phase. This corresponds to having correction factors (f_{iL} / f_{iV}) mostly greater than one. The K -values will then be further increased and the system will return to the two phase state.

On the other hand, if the fugacities are higher in the gas phase than in the liquid phase, the bubble will disappear spontaneously. When the correction factors (f_{iL} / f_{iV}) are mostly less than one, the K-values are reduced bringing the system back to the single liquid phase state.

In the second case, when the single-phase is gas, V equals one, and the multiplication factor β is then determined from the relation:

$$\sum_{i=1}^{Nc} (1.0 - (1.0 / \beta K_i)) z_i = 0.0 \quad \dots\dots\dots(A-35)$$

i.e.:

$$\beta = \frac{\sum_{i=1}^{Nc} (z_i / K_i)}{\sum_{i=1}^{Nc} z_i} \quad \dots\dots\dots(A-36)$$

which gives a new set of equilibrium ratios as:

$$\begin{aligned} K_i^{\text{new}} &= \beta K_i \\ &= K_i / \sum_{i=1}^{Nc} (K_i / z_i) \quad \dots\dots\dots(A-37) \end{aligned}$$

on which the normal correction factors (f_{iL} / f_{iV}) are applied.

Similarly, this can be interpreted as it corresponds to creating a small droplet of liquid and see if it will grow or vanish. A liquid droplet will grow spontaneously if the fugacity is

lower in the liquid phase than in the gas phase. This corresponds to having correction factors (f_{iL} / f_{iV}) mostly less than one. The K-values will then be further decreased and the system will return to the two-phase state.

On the other hand, if the fugacities are higher in the liquid phase than in the gas phase, the liquid droplet will spontaneously vanish. When the correction factors (f_{iL} / f_{iV}) are mostly greater than one, the K-values are then increased bringing the system back to the single gas phase state.

APPENDIX B
LEAST SQUARES LINEAR PROGRAMMING
AS AN OPTIMIZATION TECHNIQUE

The least squares-linear programming technique, introduced by Coats *et al*⁴⁰, is employed in this study as an optimization tool for:

- 1 - tuning the binary interaction parameters of the equations of state.
- 2 - adjusting the critical properties of the heavy fractions of the hydrocarbon systems.
- 3 - correlating the parameters of the new equilibrium ratios equation.

This technique requires a number of runs using the PVT analysis simulator; each run using a set of binary interaction coefficients, critical properties, or the correlating parameters. These are randomly selected within limits specified from the experimental data. Then, the second phase of the phase behavior model (LSLP model), utilizes the least squares-linear programming algorithm to process the output results of the PVT model runs, and then produces the optimal parameters.

In the least squares-linear programming approach, we use the least squares method to generate the constraints (as linear

relationships) which are subsequently used in a two-phase minimization algorithm to obtain the optimal parameters using the linear programming technique.^{40,91}

FORMULATION OF THE OPTIMIZATION MODEL

In this model, the experimental test data are available as input data, and the binary interaction coefficients, the critical properties, or the K-value correlation parameters are considered unknowns.

The experimental performance data (observations) are the percent liquid, relative volumes, cumulative gas produced, and/or saturation pressures at different pressures or volumes of cumulative gas injected. The influence parameters are the binary interaction coefficients, critical properties, or the K-value correlation parameters. Restrictions on the experimental performance data and the influence parameters are that the number of observations must exceed the number of the influence parameters; i.e.: $N_I > N_J$. In addition, each parameter value (X_j) should have some effect on the calculated value of at least one of the experimental data points (observations). Also, the number of runs needed to perform the optimization study should be at least equal one plus the number of influence parameters and not exceed twice as much; i.e.: $N_J < N_R < 2 N_J$. If the error surface ϵ_i was truly linear, then, we would require exactly $N_J + 1$ simulation runs to determine the surface ϵ_i .

For every single simulation run using a random set of the influence parameters (X_j), a number of calculated points (V_i^{cal}) are obtained, and an error set (ϵ_i) is then calculated as:

$$\epsilon_i = (V_i^{exp} - V_i^{cal})$$

$$i = 1, 2, \dots, NI \quad \dots\dots\dots(B-1)$$

Now, the objective is to assign values to the influence parameters (X_j) in such a way that the calculated points match as closely as possible the actual experimental values.

For each influence parameter (X_j), upper and lower bounds are imposed. In each simulation run, the influence parameters are calculated as:

$$X_j^r = XL_j + R (XU_j - XL_j)$$

$$\dots\dots\dots(B-2)$$

where:

X_j^r : Assigned influence parameter at run r.

XL_j : Lower bound of influence parameter.

XU_j : Upper bound of influence parameter.

R : A normalized random number, such that

$$0.0 \leq R \leq 1.0$$

This random number is generated, each run, using the formula:

$$R_n = \text{Fraction} [(R_{n-1} + \pi)^8]$$

.....(B-3)

where:

R_n : New random number.

R_{n-1} : Old random number.

The Least Squares Scheme

The sets of errors can be linearly correlated with the influence parameters using the least squares technique. The procedure, then, can be presented in the following manner:

The error in the i^{th} observation is defined as:

$$\begin{aligned} \epsilon_i^r &= V_i^{\text{exp}} - V_i^{\text{cal}}(r) \\ i &= 1, 2, \dots, NI \\ r &= 1, 2, \dots, NR \end{aligned} \quad \text{.....(B-4)}$$

Since these errors are single valued functions of the influence parameters (X_j), the error in the i^{th} observation can be assumed to be a linear combination of the influence parameters, i.e.:

$$\begin{aligned} \epsilon_i &= a_{i,0} + a_{i,1} X_1 + a_{i,2} X_2 + \dots \\ &\quad \dots + a_{i,NJ} X_{NJ} \\ &= \sum_{j=0}^{NJ} (a_{ij} X_j) \end{aligned} \quad \text{.....(B-5)}$$

where:

$$X_0 = 1.0$$

a_{ij} : coefficients to be determined by least squares.

X_j : j^{th} influence parameter.

This linear dependence is an approximation imposed into surfaces, $\epsilon_i(X_1, \dots, X_j)$, which are in fact curvilinear. This approximation will be justified in proportion to the extent of success of this following technique, which is based upon that approximation, in backing out the correct influence parameters from the given behavior.⁴⁰

Since the calculated error matrix ϵ_i^r :

$$\epsilon_i^r = \{ \epsilon(i,r) \}$$

$$i = 1, 2, \dots, NI$$

$$r = 1, 2, \dots, NR \dots \dots \dots (B-6)$$

is available from the NR sets of simulation runs; then, we can define the deviation (D_i^r) between the calculated error and the correlated error by the linear function as:

$$D_i^r = \epsilon_i^r - \sum_{j=0}^{NJ} (a_{ij} X_j)$$

$$i = 1, 2, \dots, NI$$

$$r = 1, 2, \dots, NR \quad \dots \dots \dots (B-7)$$

Now, we want to select the coefficients a_{ij} in such a way to minimize the sum for the i^{th} observation as:

$$S_i = \sum_{r=1}^{NR} [D_i^r]^2 \quad \dots \dots \dots (B-8)$$

Substituting Eq. B-7 into Eq. B-8, and expanding, we get:

$$S_i = \sum_{r=1}^{NR} [\epsilon_i^r - \sum_{j=0}^{NJ} (a_{ij} X_j^r)]^2$$

$$= \sum_{r=1}^{NR} [(\epsilon_i^r)^2 - 2 \epsilon_i^r \sum_{j=0}^{NJ} (a_{ij} X_j^r) + (\sum_{j=0}^{NJ} a_{ij} X_j^r)^2]$$

$$= \sum_{r=1}^{NR} (\epsilon_i^r)^2 - 2 \sum_{r=1}^{NR} \epsilon_i^r \sum_{j=0}^{NJ} a_{ij} X_j^r + \sum_{r=1}^{NR} (\sum_{j=0}^{NJ} a_{ij} X_j^r)^2$$

$$\dots \dots \dots (B-9)$$

Based on the least squares method, the following condition should be satisfied:

$$\partial(S_i) / \partial(a_{iL}) = 0.0$$

$$L = 0,1,2, \dots , NJ \dots\dots\dots(B-10)$$

Then, differentiating Eq. B-9 w.r.t. a_{iL} , we get:

$$\begin{aligned} \partial(S_i) / \partial(a_{iL}) = 0.0 & - 2 \sum_{r=1}^{NR} \partial \left(\sum_{j=0}^{NJ} a_{ij} \epsilon_i^r X_j^r \right) / \partial(a_{iL}) \\ & + \sum_{r=1}^{NR} \left[2 \left(\sum_{j=0}^{NJ} a_{ij} X_j^r \right) \partial \left(\sum_{j=0}^{NJ} a_{ij} X_j^r \right) \right. \\ & \left. / \partial(a_{iL}) \right] \dots\dots\dots(B-11) \end{aligned}$$

Considering that:

$$\begin{aligned} \partial \left(\sum_{j=0}^{NJ} a_{ij} X_j^r \right) / \partial(a_{iL}) & = \partial \left(a_{iL} X_L^r + \sum_{j=0}^{NJ} a_{ij} X_j^r \right. \\ & \left. - a_{iL} X_L^r \right) / \partial(a_{iL}) \\ & = X_L^r \dots\dots\dots(B-12) \end{aligned}$$

Similarly:

$$\partial \left(\sum_{j=0}^{NJ} a_{ij} \epsilon_j^r X_j^r \right) / \partial(a_{iL}) = \epsilon_i^r X_L^r \dots\dots\dots(B-13)$$

Substituting Eq. B-12 and A-13 into Eq. B-11, we get:

$$\begin{aligned} - 2 \sum_{r=1}^{NR} \epsilon_i^r X_L^r + \sum_{r=1}^{NR} 2 \left(\sum_{j=0}^{NJ} a_{ij} X_j^r \right) X_L^r & = 0.0 \\ i = 1,2,3, \dots , NI \\ L = 0,1,2, \dots , NJ \dots\dots\dots(B-14) \end{aligned}$$

Rearranging this equation, we get:

$$\sum_{j=0}^{NJ} \left(\sum_{r=1}^{NR} X_L^r X_j^r \right) a_{ij} = \sum_{r=1}^{NR} \epsilon_i^r X_L^r$$

$i = 1, 2, 3, \dots, NI$
 $L = 0, 1, 2, \dots, NJ \dots \dots \dots (B-15)$

Now, if we define:

$$A(j, i) = a_{ij} \dots \dots \dots (B-16)$$

$$B(L, j) = \sum_{r=1}^{NR} X_L^r X_j^r \dots \dots \dots (B-17)$$

such that:

$$X_0^r = 1.0 \dots \dots \dots (B-18)$$

then:

$$B(0, 0) = \sum_{r=1}^{NR} 1.0$$

$$= NR \dots \dots \dots (B-19)$$

$$B(0, j) = \sum_{r=1}^{NR} X_j^r \dots \dots \dots (B-20)$$

and defining:

$$C(L, i) = \sum_{r=1}^{NR} \epsilon_i^r X_L^r \dots \dots \dots (B-21)$$

Then Eq. B-15 becomes:

$$\sum_{j=0}^{NJ} B(L,j) * A(j,i) = C(L,i)$$

$$i = 1,2,3, \dots , NI$$

$$L = 0,1,2, \dots , NJ \dots \dots \dots (B-22)$$

For the i^{th} observation, one obtains the following matrix form:

$$B * \begin{bmatrix} A(0,i) \\ A(1,i) \\ A(2,i) \\ \dots \\ A(NJ,i) \end{bmatrix} = \begin{bmatrix} C(0,i) \\ C(1,i) \\ C(2,i) \\ \dots \\ C(NJ,i) \end{bmatrix}$$

.....(B-23)

where:

$$B = B(L,j)$$

$$L = 0,1,2, \dots , NJ$$

$$j = 0,1,2, \dots , NJ$$

Thus, we end up with the matrix equation (the normal equation):

$$B * A = C \dots \dots \dots (B-24)$$

where:

$$B = \begin{bmatrix} B(0, 0) & \dots & B(0,NJ) \\ \dots & \dots & \dots \\ B(NJ, 0) & \dots & B(NJ,NJ) \end{bmatrix}$$

.....(B-25)

$$A = \begin{bmatrix} A(0, 1) & \dots & A(0, NI) \\ \dots & \dots & \dots \\ A(NJ, 1) & \dots & A(NJ, NI) \end{bmatrix} \dots \dots \dots (B-26)$$

$$C = \begin{bmatrix} C(0, 1) & \dots & C(0, NI) \\ \dots & \dots & \dots \\ C(NJ, 1) & \dots & C(NJ, NI) \end{bmatrix} \dots \dots \dots (B-27)$$

Thus, the coefficients a_{ij} ($a_{ij} = A(j,i)$) can be simultaneously obtained by solving Eq. B-24 in the unknown matrix of coefficients A, as:

$$A = B^{-1} * C \dots \dots \dots (B-28)$$

Finally, after solving this system of equations, we get the required linear correlation for the error sets defined earlier in Eq. B-5.

The Linear Programming Formulation

In this linear programming problem, the following are provided as given data:

- The coefficients a_{ij} of the linear function of errors.
- The upper and lower limits of the influence parameters X_j .

and we want to select the parameters X_j in such a way to minimize the error. In other words, the objective is:

$$\text{Minimize } Z : \sum_{i=1}^{NI} |\epsilon_i| = \sum_{i=1}^{NI} \left| \left(\sum_{j=0}^{NJ} a_{ij} X_j \right) \right| \dots\dots\dots(B-29)$$

The error ϵ_i can be expressed by slack variables as:

$$\epsilon_i = X_{NJ+NI+i} - X_{NJ+i} \quad i = 1, 2, \dots, NI \quad \dots\dots\dots(B-30)$$

Since,

$$\text{Min. } |\epsilon_i| = |X_{NJ+NI+i} - X_{NJ+i}| \quad \dots\dots\dots(B-31)$$

is exactly equivalent to minimizing the term:

$$X_{NJ+NI+i} + X_{NJ+i} \quad \dots\dots\dots(B-32)$$

which is a more demanding objective.

Thus, the objective function could be expressed as:

$$\text{Min. } Z : \sum_{i=1}^{NI} (X_{NJ+NI+i} + X_{NJ+i}) \dots\dots\dots(B-33)$$

This objective function is subject to the following constraints:

$$\sum_{j=0}^{NJ} a_{ij} X_j - X_{NJ+NI+i} + X_{NJ+i} = 0.0$$

$i = 1, 2, \dots, NI \dots\dots\dots(B-34)$

In addition, there are some other conditions which should be fulfilled; these are:

$$XL_j \leq X_j \leq XU_j \dots\dots\dots(B-35)$$

this simply means;

$$X_j - XU_j \leq 0.0 \dots\dots\dots(B-36)$$

and,

$$X_j - XL_j \geq 0.0 \dots\dots\dots(B-37)$$

These inequality conditions, Eqs. B-36 and B-37, could be expressed more explicitly by the aid of some slack variables as:

$$X_j - XL_j - X_{NJ+2NI+j} = 0.0 \dots\dots\dots(B-38)$$

and similarly,

$$X_j - XU_j + X_{2NJ+2NI+j} = 0.0 \dots\dots\dots(B-39)$$

Finally, this linear programming problem can be summarized as follows:

$$\text{Min. } Z : \sum_{i=1}^{NI} (X_{NJ+NI+i} + X_{NJ+i}) \dots\dots\dots(B-40)$$

Subject to:

$$(a) \sum_{j=0}^{NJ} a_{ij} X_j - X_{NJ+NI+i} + X_{NJ+i} = 0.0 \\ i = 1, 2, \dots, NI \dots\dots\dots(B-34)$$

$$(b) X_j - XL_j - X_{NJ+2NI+j} = 0.0 \\ j = 1, 2, \dots, NJ \dots\dots\dots(B-38)$$

$$(c) X_j - XU_j + X_{2NJ+2NI+j} = 0.0 \\ j = 1, 2, \dots, NJ \dots\dots\dots(B-39)$$

This is a two phase linear programming problem, which can be readily solved for the optimal parameters by using the *SIMPLEX* method.⁹²

APPENDIX C**TEST CASES**

Three basic routine laboratory tests are simulated in this work. For each PVT laboratory test special experimental data are needed to compare the simulated results with the experimental measurements. The test cases data considered in this study were mostly collected from the literature. These test cases are listed in Table C-1.

TABLE C-1 - A Summary of Test Cases.

| Sample | Original Fluid | Tests | | |
|-------------------------|----------------|---------------------|---------------------|--|
| | | Constant Comp. Exp. | Constant Vol. Depl. | Sol. & Swelling |
| 1. SPE 3rd. Comp. Study | Gas Cond. | X | X | Methane |
| 2. Whitson's Data | Gas Cond. | --- | X | --- |
| 3. Special Data PVT # 2 | Oil | Oil phase | --- | CO ₂ CO ₂ +N ₂ |
| 4. Special Data PVT # 3 | Oil | Oil phase | --- | CO ₂ |
| 5. Special Data PVT # 5 | Oil | Oil phase | --- | CO ₂ |
| 6. Special Data PVT # 6 | Oil | Oil phase | --- | CO ₂ |
| 7. Coats' Data Gas # 2 | Gas Cond. | X | X | --- |
| 8. Coats' Data Gas # 5 | Gas Cond. | X | X | --- |
| 9. Coats' Data Oil # 2 | Oil | X | X | --- |

CASE # 1: SPE THIRD COMPARATIVE SOLUTION PROJECT DATA.³⁸

In this case study, three test data are available. The system considered is a gas condensate with the following overall composition:

TABLE C-2 - Fluid Composition (Case 1).

| Component | Well stream composition Mole Percent |
|------------------|---|
| CO ₂ | 1.21 |
| N ₂ | 1.94 |
| C ₁ | 65.99 |
| C ₂ | 8.69 |
| C ₃ | 5.91 |
| C _{4-i} | 2.39 |
| C _{4-n} | 2.78 |
| C _{5-i} | 1.57 |
| C _{5-n} | 1.12 |
| C ₆ | 1.81 |
| C ₇₊ | 6.59 |
| | 100.00 |

Reservoir Temperature = 200.0 deg. F.

Properties of C₇₊ are:

Specific gravity = 0.774

Molecular weight = 140.0

TABLE C-3 - Constant Composition Expansion Test (Case 1).

| Pressure, psig | Relative Volume |
|----------------|----------------------------------|
| 6000.0 | 0.8045 |
| 5500.0 | 0.8268 |
| 5000.0 | 0.8530 |
| 4500.0 | 0.8856 |
| 4000.0 | 0.9284 |
| 3600.0 | 0.9745 |
| 3428.0 | <u>Dew Point Pressure</u> 1.0000 |
| 3400.0 | 1.0043 |
| 3350.0 | 1.0142 |
| 3200.0 | 1.0468 |
| 3000.0 | 1.0997 |
| 2800.0 | 1.1644 |
| 2400.0 | 1.3412 |
| 2000.0 | 1.6113 |
| 1600.0 | 2.0412 |
| 1300.0 | 2.5542 |
| 1030.0 | 3.2925 |
| 826.0 | 4.1393 |

TABLE C-4 - Constant Volume Depletion Test (Case 1).

Depletion Study:

| Comp | Pressures, psig | | | | | |
|-----------------------------------|-----------------|--------------|--------------|--------------|--------------|--------------|
| | 3428 | 3000 | 2400 | 1800 | 1200 | 700 |
| CO ₂ | 1.21 | 1.24 | 1.27 | 1.31 | 1.33 | 1.32 |
| N ₂ | 1.94 | 2.13 | 2.24 | 2.27 | 2.20 | 2.03 |
| C ₁ | 65.99 | 69.78 | 72.72 | 73.98 | 73.68 | 71.36 |
| C ₂ | 8.69 | 8.66 | 8.63 | 8.79 | 9.12 | 9.66 |
| C ₃ | 5.91 | 5.67 | 5.46 | 5.38 | 5.61 | 6.27 |
| C _{4-i} | 2.39 | 2.20 | 2.01 | 1.93 | 2.01 | 2.40 |
| C _{4-n} | 2.78 | 2.54 | 2.31 | 2.18 | 2.27 | 2.60 |
| C _{5-i} | 1.57 | 1.39 | 1.20 | 1.09 | 1.09 | 1.23 |
| C _{5-n} | 1.12 | 0.96 | 0.82 | 0.73 | 0.72 | 0.84 |
| C ₆ | 1.81 | 1.43 | 1.08 | 0.88 | 0.83 | 1.02 |
| C ₇₊ | 6.59 | 4.00 | 2.26 | 1.46 | 1.14 | 1.27 |
| | <u>100.0</u> | <u>100.0</u> | <u>100.0</u> | <u>100.0</u> | <u>100.0</u> | <u>100.0</u> |
| <u>C₇₊ Properties:</u> | | | | | | |
| MW | 140 | 127 | 118 | 111 | 106 | 105 |
| Sp. Gr. | 0.774 | 0.761 | 0.752 | 0.745 | 0.740 | 0.739 |
| <u>Cum. Gas Prod., %:</u> | | | | | | |
| | 0.000 | 9.095 | 24.702 | 42.026 | 59.687 | 74.019 |
| <u>Liquid Volume, %:</u> | | | | | | |
| | 0.0 | 15.00 | 19.90 | 19.20 | 17.10 | 15.20 |

TABLE C-5 - Solubility and Swelling Test (Case 1).
(Injection Gas = 95% Methane + 5% Ethane)

| Mixture No. | Cum. Gas Injected scf/rbbl | Dew Pt. Swollen Volume | Dew Pt. Press. psig |
|-------------|-------------------------------|---------------------------|------------------------|
| 0 | 0.00 | 1.0000 | 3428.00 |
| 1 | 190.00 | 1.1224 | 3635.00 |
| 2 | 572.00 | 1.3542 | 4015.00 |
| 3 | 1523.00 | 1.9248 | 4610.00 |
| 4 | 2467.00 | 2.5043 | 4880.00 |

CASE # 2: Whitson *et al*'s DATA (NS1):²⁶

In this case study, only the constant volume depletion test data are available. The system considered is a rich gas condensate with the following overall composition:

TABLE C-6 - Fluid Composition (Case 2).

| Component | Well stream composition Mole Percent |
|------------------|---|
| CO ₂ | 2.37 |
| N ₂ | 0.31 |
| C ₁ | 73.19 |
| C ₂ | 7.80 |
| C ₃ | 3.55 |
| C _{4-i} | 0.71 |
| C _{4-n} | 1.45 |
| C _{5-i} | 0.64 |
| C _{5-n} | 0.68 |
| C ₆ | 1.09 |
| C ₇₊ | 8.21 |
| | 100.00 |

Reservoir Temperature = 280.0 deg. F.

Properties of C₇₊ are:

Specific gravity = 0.816

Molecular weight = 184.0

TABLE C-7 - Constant Volume Depletion Test (Case 2).

Depletion Study:

| Comp | <u>Pressures, psig</u> | | | | | | |
|-----------------------------------|------------------------|--------------|--------------|--------------|--------------|--------------|--------------|
| | 6750 | 5500 | 4300 | 3100 | 2100 | 1200 | 700 |
| CO ₂ | 2.37 | 2.40 | 2.45 | 2.50 | 2.53 | 2.57 | 2.60 |
| N ₂ | 0.31 | 0.32 | 0.33 | 0.34 | 0.34 | 0.34 | 0.33 |
| C ₁ | 73.19 | 75.56 | 77.89 | 79.33 | 79.62 | 78.90 | 77.80 |
| C ₂ | 7.80 | 7.83 | 7.87 | 7.92 | 8.04 | 8.40 | 8.70 |
| C ₃ | 3.55 | 3.47 | 3.40 | 3.41 | 3.53 | 3.74 | 3.91 |
| C _{4-i} | 0.71 | 0.67 | 0.65 | 0.64 | 0.66 | 0.72 | 0.78 |
| C _{4-n} | 1.45 | 1.37 | 1.31 | 1.30 | 1.33 | 1.44 | 1.56 |
| C _{5-i} | 0.64 | 0.59 | 0.55 | 0.53 | 0.54 | 0.59 | 0.64 |
| C _{5-n} | 0.68 | 0.62 | 0.58 | 0.56 | 0.57 | 0.61 | 0.66 |
| C ₆ | 1.09 | 0.97 | 0.88 | 0.83 | 0.82 | 0.85 | 0.90 |
| C ₇₊ | 8.21 | 6.20 | 4.09 | 2.64 | 2.02 | 1.84 | 2.12 |
| | <u>100.0</u> | <u>100.0</u> | <u>100.0</u> | <u>100.0</u> | <u>100.0</u> | <u>100.0</u> | <u>100.0</u> |
| <u>C₇₊ Properties:</u> | | | | | | | |
| MW | 184 | 160 | 142 | 127 | 119 | 115 | 114 |
| Sp Gr | 0.816 | 0.799 | 0.783 | 0.770 | 0.762 | 0.758 | 0.757 |
| <u>Cum. Gas Prod., %:</u> | | | | | | | |
| | 0.000 | 9.024 | 21.744 | 38.674 | 55.686 | 72.146 | 81.301 |
| <u>Liquid Volume, %:</u> | | | | | | | |
| | 0.0 | 14.10 | 19.70 | 21.60 | 21.30 | 20.20 | 19.30 |

CASE # 3: SPECIAL DATA (PVT # 2):⁹³

In this case study, three test data are available. The system considered is an oil with the following overall composition:

TABLE C-8 - Fluid Composition (Case 3).

| Component | Well stream composition Mole Percent |
|----------------------------------|---|
| CO ₂ | 0.91 |
| N ₂ +H ₂ S | 1.43 |
| C ₁ | 21.40 |
| C ₂ | 9.23 |
| C ₃ | 5.64 |
| C ₄ -i | 0.98 |
| C ₄ -n | 2.98 |
| C ₅ -i | 1.50 |
| C ₅ -n | 2.22 |
| C ₆ | 3.24 |
| C ₇ + | 50.47 |
| | 100.00 |

Reservoir Temperature = 225.0 deg. F.

Properties of C₇+ are:

Specific gravity = 0.8620

Molecular weight = 230.0

TABLE C-9 - Constant Composition Expansion Test (Case 3).

| Pressure, psig | Relative Volume |
|----------------|-----------------------------------|
| 5000.0 | 0.9643 |
| 4500.0 | 0.9685 |
| 4000.0 | 0.9729 |
| 3500.0 | 0.9776 |
| 3000.0 | 0.9827 |
| 2500.0 | 0.9880 |
| 2000.0 | 0.9937 |
| 1800.0 | 0.9962 |
| 1700.0 | 0.9974 |
| 1600.0 | 0.9986 |
| 1500.0 | <u>Bubble Pt. Pressure</u> 1.0000 |

TABLE C-10 - Solubility and Swelling Test (Case 3).
(Injection Gas - Pure Carbon Dioxide)

| Mixture No. | Cum. Gas Injected scf/rbbl | B.Pt. Swollen Volume | Bubble Pt. Press. psig |
|-------------|-------------------------------|-------------------------|---------------------------|
| 0 | 0.00 | 1.0000 | 1500.00 |
| 1 | 109.00 | 1.0434 | 1827.00 |
| 2 | 326.00 | 1.1406 | 2372.00 |
| 3 | 651.00 | 1.2861 | 2988.00 |
| 4 | 1194.00 | 1.5361 | 3725.00 |

TABLE C-11 - Solubility and Swelling Test (Case 3).
 (Injection Gas = 50% CO₂ + 50% N₂)

| Mixture No. | Cum. Gas Injected scf/rbbl | B.Pt. Swollen Volume | Bubble Pt. Press. psig |
|-------------|----------------------------|----------------------|------------------------|
| 0 | 0.00 | 1.0000 | 1500.00 |
| 1 | 85.00 | 1.0282 | 2425.00 |
| 2 | 171.00 | 1.0579 | 3321.00 |
| 3 | 256.00 | 1.0860 | 4151.00 |
| 4 | 290.00 | 1.0969 | 4477.00 |
| 5 | 380.00 | 1.1269 | 5236.00 |
| 6 | 518.00 | 1.1712 | 6343.00 |
| 7 | 606.00 | 1.2006 | 7030.00 |

CASE # 4: SPECIAL DATA (PVT # 3):⁹³

In this case study, two test data are available. The system considered is an oil with the following overall composition:

TABLE C-12 - Fluid Composition (Case 4).

| Component | Well stream composition Mole Percent |
|------------------|---|
| CO ₂ | 0.01 |
| N ₂ | 0.25 |
| C ₁ | 5.81 |
| C ₂ | 1.81 |
| C ₃ | 3.89 |
| C _{4-i} | 1.40 |
| C _{4-n} | 4.90 |
| C _{5-i} | 2.68 |
| C _{5-n} | 3.60 |
| C ₆ | 3.75 |
| C ₇₊ | 71.90 |
| | 100.00 |

Reservoir Temperature = 110.0 deg. F.

Properties of C₇₊ are:

Specific gravity = 0.8550

Molecular weight = 296.0

TABLE C-13 - Constant Composition Expansion Test (Case 4).

| Pressure, psig | Relative Volume |
|----------------|-----------------------------------|
| 2000.0 | 0.9895 |
| 1600.0 | 0.9917 |
| 1200.0 | 0.9940 |
| 800.0 | 0.9963 |
| 600.0 | 0.9975 |
| 500.0 | 0.9981 |
| 400.0 | 0.9988 |
| 300.0 | 0.9994 |
| 215.0 | <u>Bubble Pt. Pressure</u> 1.0000 |

TABLE C-14 - Solubility and Swelling Test (Case 4).
(Injection Gas = Pure Carbon Dioxide)

| Mixture No. | Cum. Gas Injected scf/rbbl | B.Pt. Swollen Volume | Bubble Pt. Press. psig |
|-------------|----------------------------|----------------------|------------------------|
| 0 | 0.00 | 1.0000 | 215.00 |
| 1 | 29.00 | 1.0106 | 293.00 |
| 2 | 109.00 | 1.0402 | 485.00 |
| 3 | 203.00 | 1.0754 | 675.00 |
| 4 | 327.00 | 1.1219 | 857.00 |
| 5 | 503.00 | 1.1867 | 1046.00 |
| 6 | 768.00 | 1.2893 | 1270.00 |
| 7 | 1121.00 | 1.4848 | 1300.00 |

CASE # 5: SPECIAL DATA (PVT # 5):⁹³

In this case study, two test data are available. The system considered is an oil with the following overall composition:

TABLE C-15 - Fluid Composition (Case 5).

| Component | Well stream composition Mole Percent |
|------------------|---|
| CO ₂ | 0.05 |
| N ₂ | 0.02 |
| C ₁ | 5.51 |
| C ₂ | 4.44 |
| C ₃ | 6.08 |
| C _{4-i} | 0.65 |
| C _{4-n} | 4.30 |
| C _{5-i} | 1.82 |
| C _{5-n} | 2.58 |
| C ₆ | 6.88 |
| C ₇₊ | 67.67 |
| | 100.00 |

Reservoir Temperature = 155.0 deg. F.

Properties of C₇₊ are:

Specific gravity = 0.8433

Molecular weight = 267.0

TABLE C-16 - Constant Composition Expansion Test (Case 5).

| Pressure, psig | Relative Volume |
|----------------|-----------------------------------|
| 2500.0 | 0.9847 |
| 2000.0 | 0.9878 |
| 1500.0 | 0.9911 |
| 1000.0 | 0.9944 |
| 600.0 | 0.9973 |
| 500.0 | 0.9981 |
| 400.0 | 0.9988 |
| 300.0 | 0.9996 |
| 249.0 | <u>Bubble Pt. Pressure</u> 1.0000 |

TABLE C-17 - Solubility and Swelling Test (Case 5).
(Injection Gas = Pure Carbon Dioxide)

| Mixture No. | Cum. Gas Injected scf/rbbl | B.Pt. Swollen Volume | Bubble Pt. Press. psig |
|-------------|----------------------------|----------------------|------------------------|
| 0 | 0.00 | 1.0000 | 249.00 |
| 1 | 74.00 | 1.0295 | 483.00 |
| 2 | 223.00 | 1.0884 | 862.00 |
| 3 | 372.00 | 1.1481 | 1163.00 |
| 4 | 594.00 | 1.2377 | 1520.00 |
| 5 | 892.00 | 1.3575 | 1987.00 |

CASE # 6: SPECIAL DATA (PVT # 6):⁹³

In this case study, two test data are available. The system considered is an oil with the following overall composition:

TABLE C-18 - Fluid Composition (Case 6).

| Component | Well stream composition Mole Percent |
|------------------|---|
| CO ₂ | 0.12 |
| N ₂ | 0.02 |
| C ₁ | 1.51 |
| C ₂ | 10.64 |
| C ₃ | 23.23 |
| C _{4-i} | 3.01 |
| C _{4-n} | 12.94 |
| C _{5-i} | 4.02 |
| C _{5-n} | 4.74 |
| C ₆ | 6.57 |
| C ₇₊ | 33.20 |
| | 100.00 |

Reservoir Temperature = 155.0 deg. F.

Properties of C₇₊ are:

Specific gravity = 0.8364

Molecular weight = 251.0

TABLE C-19 - Constant Composition Expansion Test (Case 6).

| Pressure, psig | Relative Volume |
|----------------|-----------------------------------|
| 2500.0 | 0.9756 |
| 2000.0 | 0.9804 |
| 1500.0 | 0.9855 |
| 1000.0 | 0.9909 |
| 600.0 | 0.9957 |
| 500.0 | 0.9968 |
| 400.0 | 0.9981 |
| 300.0 | 0.9993 |
| 250.0 | <u>Bubble Pt. Pressure</u> 1.0000 |

TABLE C-20 - Solubility and Swelling Test (Case 6).
(Injection Gas - Pure Carbon Dioxide)

| Mixture No. | Cum. Gas Injected scf/rbbl | B.Pt. Swollen Volume | Bubble Pt. Press. psig |
|-------------|----------------------------|----------------------|------------------------|
| 0 | 0.00 | 1.0000 | 250.00 |
| 1 | 73.00 | 1.0328 | 425.00 |
| 2 | 291.00 | 1.1300 | 818.00 |
| 3 | 582.00 | 1.2612 | 1160.00 |
| 4 | 873.00 | 1.3988 | 1394.00 |
| 5 | 1164.00 | 1.5175 | 1900.00 |

CASE # 7: COATS' DATA (GAS # 2):¹

In this case study, two test data are available. The system considered is a gas condensate with the following overall composition:

TABLE C-21 - Fluid Composition (Case 7).

| Component | Well stream composition Mole Percent |
|------------------|---|
| CO ₂ | 0.69 |
| H ₂ S | 0.04 |
| C ₁ | 58.32 |
| C ₂ | 13.55 |
| C ₃ | 7.61 |
| C ₄ | 4.03 |
| C ₅ | 2.41 |
| C ₆ | 1.90 |
| C ₇₊ | 11.45 |
| | 100.00 |

Reservoir Temperature = 190.0 deg. F.

Properties of C₇₊ are:

Specific gravity = 0.8135

Molecular weight = 193.0

TABLE C-22 - Constant Composition Expansion Test (Case 7).

| Pressure, psig | Relative Volume |
|----------------|--------------------------------|
| 5580.0 | 0.9525 |
| 5400.0 | 0.9589 |
| 5000.0 | 0.9737 |
| 4800.0 | 0.9819 |
| 4600.0 | 0.9916 |
| 4500.0 | 0.9972 |
| 4450.0 | <u>Dew Pt. Pressure</u> 1.0000 |
| 4440.0 | 1.0005 |
| 4420.0 | 1.0018 |
| 4388.0 | 1.0037 |
| 4339.0 | 1.0068 |
| 4300.0 | 1.0093 |
| 4180.0 | 1.0181 |
| 3993.0 | 1.0372 |
| 3780.0 | 1.0605 |
| 3490.0 | 1.1032 |
| 2998.0 | 1.2053 |
| 2505.0 | 1.3722 |
| 2000.0 | 1.6683 |
| 1485.0 | 2.2378 |
| 1058.0 | 3.1813 |

TABLE C-23 - Constant Volume Depletion Test (Case 7).

Depletion Study:

| Comp | <u>Pressures, psig</u> | | | | | | |
|-----------------------------------|------------------------|--------------|--------------|--------------|--------------|--------------|--------------|
| | 5580 | 4450 | 3500 | 2700 | 1900 | 1100 | 500 |
| CO ₂ +H ₂ S | 0.73 | 0.73 | 0.73 | 0.73 | 0.75 | 0.81 | 0.92 |
| C ₁ | 58.32 | 58.32 | 68.75 | 72.01 | 73.41 | 71.90 | 65.99 |
| C ₂ | 13.55 | 13.55 | 13.45 | 13.59 | 13.89 | 15.02 | 17.20 |
| C ₃ | 7.61 | 7.61 | 6.95 | 6.44 | 6.33 | 7.04 | 8.95 |
| C ₄ | 4.04 | 4.04 | 3.42 | 2.92 | 2.72 | 2.85 | 3.88 |
| C ₅ | 2.41 | 2.41 | 1.62 | 1.40 | 1.17 | 1.13 | 1.56 |
| C ₆ | 1.90 | 1.90 | 1.31 | 0.79 | 0.62 | 0.49 | 0.69 |
| C ₇₊ | 11.45 | 11.45 | 3.77 | 2.12 | 1.11 | 0.76 | 0.81 |
| | <u>100.0</u> | <u>100.0</u> | <u>100.0</u> | <u>100.0</u> | <u>100.0</u> | <u>100.0</u> | <u>100.0</u> |
| <u>C₇₊ Properties:</u> | | | | | | | |
| MW | 193 | 193 | 142 | 128 | 121 | 118 | 119 |
| <u>Cum. Gas Prod., %:</u> | | | | | | | |
| | 0.000 | 0.000 | 9.589 | 22.551 | 39.165 | 58.225 | 72.743 |
| <u>Liquid Volume, %:</u> | | | | | | | |
| | 0.000 | 0.000 | 52.310 | 49.400 | 45.330 | 40.510 | 36.820 |

CASE # 8: COATS' DATA (GAS # 5):¹

In this case study, three test data are available. The system considered is a gas condensate with the following overall composition:

TABLE C-24 - Fluid Composition (Case 8).

| Component | Well stream composition Mole Percent |
|-----------------|---|
| CO ₂ | 2.17 |
| N ₂ | 0.34 |
| C ₁ | 70.64 |
| C ₂ | 10.76 |
| C ₃ | 4.94 |
| C ₄ | 3.02 |
| C ₅ | 1.35 |
| C ₆ | 0.90 |
| C ₇₊ | 5.88 |
| | 100.00 |

Reservoir Temperature = 267.0 deg. F.

Properties of C₇₊ are:

Specific gravity = 0.8100

Molecular weight = 153.0

TABLE C-25 - Constant Composition Expansion Test (Case 8).

| Pressure, psig | Relative Volume |
|----------------|--------------------------------|
| 7000.0 | 0.8506 |
| 6500.0 | 0.8744 |
| 6000.0 | 0.9035 |
| 5500.0 | 0.9381 |
| 5300.0 | 0.9553 |
| 5100.0 | 0.9732 |
| 5000.0 | 0.9833 |
| 4900.0 | 0.9936 |
| 4842.0 | <u>Dew Pt. Pressure</u> 1.0000 |
| 4800.0 | 1.0046 |
| 4700.0 | 1.0161 |
| 4500.0 | 1.0429 |
| 4200.0 | 1.0906 |
| 3900.0 | 1.1468 |
| 3500.0 | 1.2444 |
| 3000.0 | 1.4147 |
| 2500.0 | 1.6129 |
| 2100.0 | 1.9851 |
| 1870.0 | 2.2376 |
| 1675.0 | 2.5062 |
| 1453.0 | 2.9132 |
| 1282.0 | 3.3338 |
| 1143.0 | 3.7547 |
| 1040.0 | 4.1757 |

TABLE C-26 - Constant Volume Depletion Test (Case 8).

Depletion Study:

| Comp | Pressures, psig | | | | | |
|-----------------------------------|-----------------|--------|--------|--------|--------|--------|
| | 4842 | 3900 | 3000 | 2100 | 1200 | 700 |
| CO ₂ | 2.17 | 2.17 | 2.20 | 2.23 | 2.28 | 2.33 |
| N ₂ | 0.34 | 0.36 | 0.38 | 0.38 | 0.36 | 0.34 |
| C ₁ | 70.64 | 72.05 | 73.65 | 74.57 | 74.42 | 73.38 |
| C ₂ | 10.76 | 10.78 | 10.87 | 10.99 | 11.13 | 11.34 |
| C ₃ | 4.94 | 4.90 | 4.85 | 4.85 | 4.97 | 5.18 |
| C ₄ | 3.02 | 2.93 | 2.83 | 2.79 | 2.92 | 3.13 |
| C ₅ | 1.35 | 1.25 | 1.18 | 1.15 | 1.21 | 1.35 |
| C ₆ | 0.90 | 0.80 | 0.72 | 0.68 | 0.71 | 0.81 |
| C ₇₊ | 5.88 | 4.76 | 3.32 | 2.36 | 2.00 | 2.14 |
| | 100.0 | 100.0 | 100.0 | 100.0 | 100.0 | 100.0 |
| <u>C₇₊ Properties:</u> | | | | | | |
| MW | 153 | 140 | 131 | 125 | 123 | 124 |
| <u>Cum. Gas Prod., %:</u> | | | | | | |
| | 0.000 | 12.812 | 29.341 | 49.110 | 69.907 | 81.220 |
| <u>Liquid Volume, %:</u> | | | | | | |
| | 0.000 | 6.100 | 9.100 | 10.400 | 9.900 | 9.100 |

CASE # 9: COATS' DATA (OIL # 2):¹

In this case study, two test data are available. The system considered is a volatile oil with the following overall composition:

TABLE C-27 - Fluid Composition (Case 9).

| Component | Well stream composition Mole Percent |
|-----------------|---|
| CO ₂ | 0.90 |
| N ₂ | 0.30 |
| C ₁ | 53.47 |
| C ₂ | 11.46 |
| C ₃ | 8.79 |
| C ₄ | 4.56 |
| C ₅ | 2.09 |
| C ₆ | 1.51 |
| C ₇₊ | 16.92 |
| | 100.00 |

Reservoir Temperature = 176.0 deg. F.

Properties of C₇₊ are:

Specific gravity = 0.8364

Molecular weight = 173.0

TABLE C-28 - Constant Composition Expansion Test (Case 9).

| Pressure, psig | Relative Volume |
|----------------|-----------------------------------|
| 6000.0 | 0.9589 |
| 5500.0 | 0.9700 |
| 5000.0 | 0.9827 |
| 4900.0 | 0.9856 |
| 4800.0 | 0.9883 |
| 4700.0 | 0.9919 |
| 4600.0 | 0.9951 |
| 4500.0 | 0.9984 |
| 4460.0 | <u>Bubble Pt. Pressure</u> 1.0000 |
| 4443.0 | 1.0009 |
| 4305.0 | 1.0097 |
| 3900.0 | 1.0412 |
| 3531.0 | 1.0812 |
| 3132.0 | 1.1425 |
| 2769.0 | 1.2232 |
| 2422.0 | 1.3356 |
| 2128.0 | 1.4738 |
| 1880.0 | 1.6384 |
| 1660.0 | 1.8415 |
| 1351.0 | 2.2768 |
| 1061.0 | 2.9892 |

TABLE C-29 - Constant Volume Depletion Test (Case 9).

Depletion Study:

| Comp | <u>Pressures, psig</u> | | | | | |
|-----------------------------------|------------------------|--------------|--------------|--------------|--------------|--------------|
| | 4460 | 3600 | 2800 | 2000 | 1200 | 600 |
| CO ₂ | 0.90 | 1.26 | 1.16 | 1.04 | 1.04 | 1.21 |
| N ₂ | 0.30 | 0.49 | 0.47 | 0.45 | 0.41 | 0.36 |
| C ₁ | 53.47 | 61.30 | 67.66 | 72.74 | 73.09 | 69.92 |
| C ₂ | 11.46 | 15.44 | 14.39 | 12.32 | 12.45 | 14.04 |
| C ₃ | 8.79 | 10.42 | 8.78 | 7.67 | 7.73 | 8.67 |
| C ₄ | 4.56 | 3.21 | 3.41 | 3.01 | 2.93 | 3.40 |
| C ₅ | 2.09 | 1.51 | 1.09 | 0.88 | 0.80 | 0.90 |
| C ₆ | 1.51 | 0.74 | 0.44 | 0.30 | 0.28 | 0.33 |
| C ₇₊ | 16.92 | 4.71 | 2.60 | 1.59 | 1.27 | 1.17 |
| | <u>100.0</u> | <u>100.0</u> | <u>100.0</u> | <u>100.0</u> | <u>100.0</u> | <u>100.0</u> |
| <u>C₇₊ Properties:</u> | | | | | | |
| MW | 173 | 117 | 108 | 103 | 100 | 102 |
| <u>Cum. Gas Prod., %:</u> | | | | | | |
| | 0.000 | 7.535 | 17.932 | 32.371 | 49.908 | 63.967 |

APPENDIX D
COMPONENTS' PROPERTIES DATA

TABLE D-1 - PURE COMPONENTS' PROPERTIES^{74,94}

| Comp | M.W. | <u>Critical Properties</u> | | T _b , °F | Acen. Fac. |
|------------------|--------|----------------------------|-----------------------|---------------------|------------|
| | | T _c , °F | P _c , psia | | |
| CO ₂ | 44.01 | 87.9 | 1071.0 | -109.3 | 0.2225 |
| H ₂ S | 34.08 | 212.6 | 1036.0 | - 76.6 | 0.0920 |
| N ₂ | 28.01 | -232.7 | 493.0 | -320.4 | 0.0372 |
| C ₁ | 16.04 | -116.7 | 667.8 | -258.7 | 0.0126 |
| C ₂ | 30.07 | 90.1 | 707.8 | -127.5 | 0.0978 |
| C ₃ | 44.10 | 206.0 | 616.3 | - 43.7 | 0.1541 |
| NC ₄ | 58.12 | 305.6 | 550.7 | 31.1 | 0.2015 |
| IC ₄ | 58.12 | 275.0 | 529.1 | 10.9 | 0.1840 |
| NC ₅ | 72.15 | 385.6 | 488.6 | 96.9 | 0.2524 |
| IC ₅ | 72.15 | 369.0 | 490.4 | 82.2 | 0.2286 |
| NC ₆ | 86.18 | 453.6 | 436.9 | 155.7 | 0.2998 |
| NC ₇ | 100.21 | 512.7 | 396.8 | 209.2 | 0.3498 |
| NC ₈ | 114.23 | 564.1 | 360.6 | 258.2 | 0.3981 |
| NC ₉ | 128.26 | 610.5 | 331.8 | 303.5 | 0.4452 |
| NC ₁₀ | 142.29 | 651.6 | 304.4 | 345.5 | 0.4904 |

TABLE D-2 - SMOOTHED HEAVY FRACTIONS' PROPERTIES.^{36,74}

| Comp | M.W. | Critical Properties | | T _b , °F | Acen. Fac. |
|-----------------|------|---------------------|-----------------------|---------------------|------------|
| | | T _c , °F | P _c , psia | | |
| C ₆ | 84 | 463 | 468.3 | 147.0 | 0.0298 |
| C ₇ | 96 | 525 | 449.4 | 197.5 | 0.0350 |
| C ₈ | 107 | 576 | 429.8 | 242.0 | 0.0381 |
| C ₉ | 121 | 625 | 402.0 | 282.0 | 0.0407 |
| C ₁₀ | 134 | 668 | 379.6 | 330.5 | 0.0427 |
| C ₁₁ | 147 | 706 | 359.3 | 369.0 | 0.0442 |
| C ₁₂ | 161 | 743 | 340.2 | 407.0 | 0.0458 |
| C ₁₃ | 175 | 776 | 323.9 | 441.0 | 0.0473 |
| C ₁₄ | 190 | 810 | 308.8 | 475.5 | 0.0488 |
| C ₁₅ | 206 | 844 | 294.3 | 511.0 | 0.0502 |
| C ₁₆ | 222 | 872 | 280.0 | 542.0 | 0.0512 |
| C ₁₇ | 237 | 900 | 269.3 | 572.0 | 0.0523 |
| C ₁₈ | 251 | 920 | 258.7 | 595.0 | 0.0530 |
| C ₁₉ | 263 | 940 | 251.3 | 617.0 | 0.0537 |
| C ₂₀ | 275 | 961 | 244.7 | 640.5 | 0.0544 |
| C ₂₁ | 291 | 982 | 235.4 | 664.0 | 0.0551 |
| C ₂₂ | 300 | 1001 | 232.1 | 686.0 | 0.0558 |
| C ₂₃ | 312 | 1020 | 226.9 | 707.0 | 0.0565 |
| C ₂₄ | 324 | 1037 | 221.6 | 727.0 | 0.0571 |
| C ₂₅ | 337 | 1055 | 216.2 | 747.0 | 0.0575 |
| C ₂₆ | 349 | 1071 | 211.5 | 766.0 | 0.0581 |
| C ₂₇ | 360 | 1087 | 207.8 | 784.0 | 0.0586 |
| C ₂₈ | 372 | 1102 | 203.4 | 802.0 | 0.0591 |
| C ₂₉ | 382 | 1114 | 200.0 | 817.0 | 0.0595 |
| C ₃₀ | 394 | 1129 | 196.2 | 834.0 | 0.0599 |
| C ₃₁ | 404 | 1143 | 193.7 | 850.0 | 0.0605 |
| C ₃₂ | 415 | 1156 | 190.5 | 866.0 | 0.0609 |
| C ₃₃ | 426 | 1169 | 187.5 | 881.0 | 0.0613 |
| C ₃₄ | 437 | 1180 | 184.2 | 895.0 | 0.0616 |
| C ₃₅ | 445 | 1191 | 182.5 | 908.0 | 0.0620 |
| C ₃₆ | 456 | 1202 | 179.5 | 922.0 | 0.0623 |
| C ₃₇ | 464 | 1213 | 178.1 | 934.0 | 0.0627 |
| C ₃₈ | 475 | 1223 | 175.2 | 947.0 | 0.0630 |
| C ₃₉ | 484 | 1233 | 173.2 | 959.0 | 0.0633 |
| C ₄₀ | 495 | 1243 | 170.6 | 972.0 | 0.0635 |
| C ₄₁ | 502 | 1252 | 169.4 | 982.0 | 0.0638 |
| C ₄₂ | 512 | 1260 | 166.9 | 993.0 | 0.0640 |
| C ₄₃ | 521 | 1269 | 165.2 | 1004.0 | 0.0642 |
| C ₄₄ | 531 | 1279 | 163.2 | 1017.0 | 0.0645 |
| C ₄₅ | 539 | 1287 | 161.8 | 1027.0 | 0.0648 |